NASA/TM-2003-212236/Vol.15

Topography Experiment (TOPEX) Software Document Series

Volume 15

TOPEX Radar Altimeter Engineering Assessment Report Update - Side B Turn-On to January 1, 2001

June 2001

D.W. Hancock III
G.S. Hayne
R.L. Brooks
D.W. Lockwood
D.C. Vandemark
N. Tran

TOPEX Contact:

David W. Hancock III
NASA/GSFC Wallops Flight Facility
Wallops Island, Virginia 23337

About the Series

The TOPEX Radar Altimeter Technical Memorandum Series is a collection of performance assessment documents produced by the NASA Goddard Space Flight Wallops Flight Facility over a period starting before the TOPEX launch in 1992 and continuing over greater than 10 year TOPEX lifetime. Because of the mission's success over this long period and because the data are being used internationally to redefine many aspects of ocean knowledge, it is important to make a permanent record of the TOPEX radar altimeter performance assessments which were originally provided to the TOPEX project in a series of internal reports over the life of the mission. The original reports are being printed in this series without change in order to make the information more publicly available as the original investigators become less available to explain the altimeter operation and details of the various data anomalies that have been resolved.

Foreword

The Engineering Assessment of the TOPEX Radar Altimeter is performed on a continuing basis by the TOPEX Altimeter Team at NASA / GSFC Wallops Flight Facility. The Assessment Team members are:

David W. Hancock III / NASA: TOPEX Altimeter Verification Manager / Team Leader
George S. Hayne / NASA: TOPEX Altimeter Verification Manager
Craig L. Purdy / NASA: TOPEX Altimeter Development Manager
Laurence C. Rossi / NASA: TOPEX Altimeter Manager
J. Barton Bull / NASA: TOPEX Altimeter System Engineer
Norman E. Schultz Jr. / NASA: TOPEX Altimeter System Engineer
Doug C. Vandemark / NASA
Lisa C. Brittingham / Raytheon ITSS
Ronald L. Brooks / Raytheon ITSS
Jeffrey E. Lee / Raytheon ITSS
Dennis W. Lockwood / Raytheon ITSS
Ngan Tran / Raytheon ITSS
Carol T. Purdy / Raytheon ITSS

For the latest updates on the performance of the TOPEX Radar Altimeter, and for accessing many of our reports, readers are encouraged to contact our WFF / TOPEX Home Page at http: / / topex.wff.nasa.gov.

For additional information on this topic, please contact the Team Leader, David W. Hancock III. He may be reached at 757-824-1238 (Voice), 757-824-1036 (FAX), or by e-mail at hancock@osb.wff.nasa.gov.

Table of Contents

List of Figures

List of Tables

Section 1

Introduction

1.1 Identification of Document

The initial TOPEX Radar Altimeter Engineering Assessment Report, in February 1994, presented performance results for the NASA Radar Altimeter on the TOPEX/POSEIDON spacecraft, from the time of its launch in August 1992 to February 1994. Since that initial report and prior to this report, there have been six interim supplemental Engineering Assessment Reports, issued in March 1995, May 1996, March 1997, June 1998, August 1999, and again in September 2000. The 1995-1998 reports updated the performance results to the end of calendar years 1994, 1995, 1996, and 1997, respectively. The 1999 report updated the performance to the time that TOPEX Side-A was turned off, on February 10, 1999; Side B was turned on the following day, marking the first time that Side B had been turned on since prior to launch.

The sixth supplement in September 2000 was the first assessment report that addressed Side-B performance, and presented the altimeter performance from the turn-on of Side-B until the end of calendar year 1999. This seventh interim report extends the performance assessment of Side B to the end of calendar year 2000.

Over the years since launch, we have performed a large variety of TOPEX performance studies; Appendix A provides an accumulative index of those studies. As the performance data base has expanded, and as analysis tools and techniques continue to evolve, the longer-term trends of the altimeter data have become more apparent. The updated findings are presented here.

Section 2

On-Orbit Instrument Performance (Cycles 236 through 305)

From the time of the initial turn-on of Side B on February 10, 1999, to the end of 2000, the NASA Radar Altimeter has been in TRACK mode for a total of approximately 15,000 hours. The altimeter has been in IDLE mode for an additional 1400 hours, generally due to the French Altimeter's being turned on. The altimeter has been OFF for a total of 51 hours, attributable to: a 16-hour spacecraft level safehold on August 31, 1999; a related 8-hour OFF status three days later to switch the spacecraft attitude control electronics; and a 27-hour spacecraft level safehold on November 24, 2000.

The succeeding sub-sections discuss:

- Side B internal calibration results
- Side B cycle-summary results
- Side B key events

2.1 Side B Internal Calibrations

The TOPEX altimeter's internal calibration mode has two submodes designated CAL-1 and CAL-2. In CAL-1 a portion of the transmitter output is fed back to the receiver through a digitally controlled calibration attenuator and delay line. The altimeter acquires and tracks this calibration signal for 10 seconds at each of 17 different preset calibration attenuator values; each calibration attenuator value is changed by 2 dB from its neighbor. The altimeter's CAL-1 has almost the same signal path as the normal fine-track mode, except that CAL-1 has a delay line, a different attenuator, and switches to select these components. The altimeter's automatic gain control (AGC) loop is active during each CAL-1 step, so changes in CAL-1 range and AGC should be directly relatable to changes in the altimeter's fine-track range and power estimation. The AGC level of CAL-1 Step 5 best represents the average level seen in normal over-ocean fine-tracking, so CAL-1 Step 5 data are used in the discussions of changes in calibration mode range and power estimates in this report.

When commanded to its calibration mode, the TOPEX altimeter first enters CAL-1 and then CAL-2. Each of the 17 steps within CAL-1 lasts about 10 seconds, and then CAL-2 lasts about a minute, so the entire calibration sequence lasts about 4 minutes. Internal altimeter calibrations are scheduled twice-per-day, over land areas, at approximately 0000 UTC and 1200 UTC. Internal calibrations are also performed whenever the NASA altimeter is commanded from TRACK to IDLE for a period of tracking by the French altimeter, or from IDLE back to TRACK when tracking resumes for the NASA altimeter. The calibrations prior to and after the French altimeter operations are not constrained to land areas, and usually occur over open ocean.

Our processing of the CAL-1 range data was modified in 1994, to remove the effect of the 7.3 mm quantization; the revised method is discussed in Section 2.1.1 (page 2) of the year 1994 supplement (published in March 1995). All the calibration data since launch have been processed using the revised method.

2.1.1 Range Calibrations

The change in Ku-Band range, from Side B turn-on on day 042 of 1999 to the end of 2000, is plotted in Figure 2-1 "Ku-Band Range CAL-1 Results" on page 2-3. CAL-1 steps 4 through 7 are shown in the figure. The Ku-Band delta range shown in Figure 2-1 (and in the succeeding calibration plots) is calculated based on the measurement minus a reference. This calibration range plot indicates that the Side B Ku-Band delta range has varied only about +1 mm from the time of its turn-on to the end of 2000.

The change in C-Band calibration range is depicted in Figure 2-2 "C-Band Range CAL-1 Results" on page 2-4. This plot indicates that, during the initial 200 days after turn-on, the Side B C-Band range negatively drifted (i.e., became shorter) by about 8 mm. Since that time, to the end of 2000, there has been no significant drift.

Range calibrations and their correction values are discussed in more detail in Section 3.1.

2.1.2 AGC Calibrations

2.1.2.1 CAL-1 and CAL-2

The change in Side B Ku-Band AGC since launch is shown in Figure 2-3 "Ku-Band AGC CAL-1 and CAL-2 Results" on page 2-5. CAL-1 steps 4 through 6, plus CAL-2, are depicted in the figure. At approximately 210 days after turn-on, there was an apparent step-function change as the Ku AGC increased approximately 0.2 dB. Since the time of that occurrence, the Ku AGC gradually increased another 0.1 dB. The step-function is discussed in more detail in Section 3.2.4.

The change in C-Band AGC since Side B turn-on is shown in Figure 2-4 "C-Band AGC CAL-1 and CAL-2 Results" on page 2-6. The Side B AGC has remained at essentially the same level (+0.1 dB) since turn-on.

A more in-depth analysis of the AGC calibrations is presented in Section 3.2.

2.2 Side B Cycle Summaries

The data in the Side B cycle summary plots which follow are extracted from the Geophysical Data Record (GDR) database at WFF. The criteria for TOPEX GDR measurements to be accepted for the WFF database are: 1) the data are classified as Deep Water, 2) the data are in normal Track Mode, and 3) selected data quality flags are not set.

For each measurement type, the plots contain one averaged measurement per cycle. The cycle average value is itself the mean of one-minute along-track boxcar averages, after editing. Data are excluded from the averaging process whenever the one-minute-averaged off-nadir angle exceeds 0.12 degree or the averaged Ku-Band

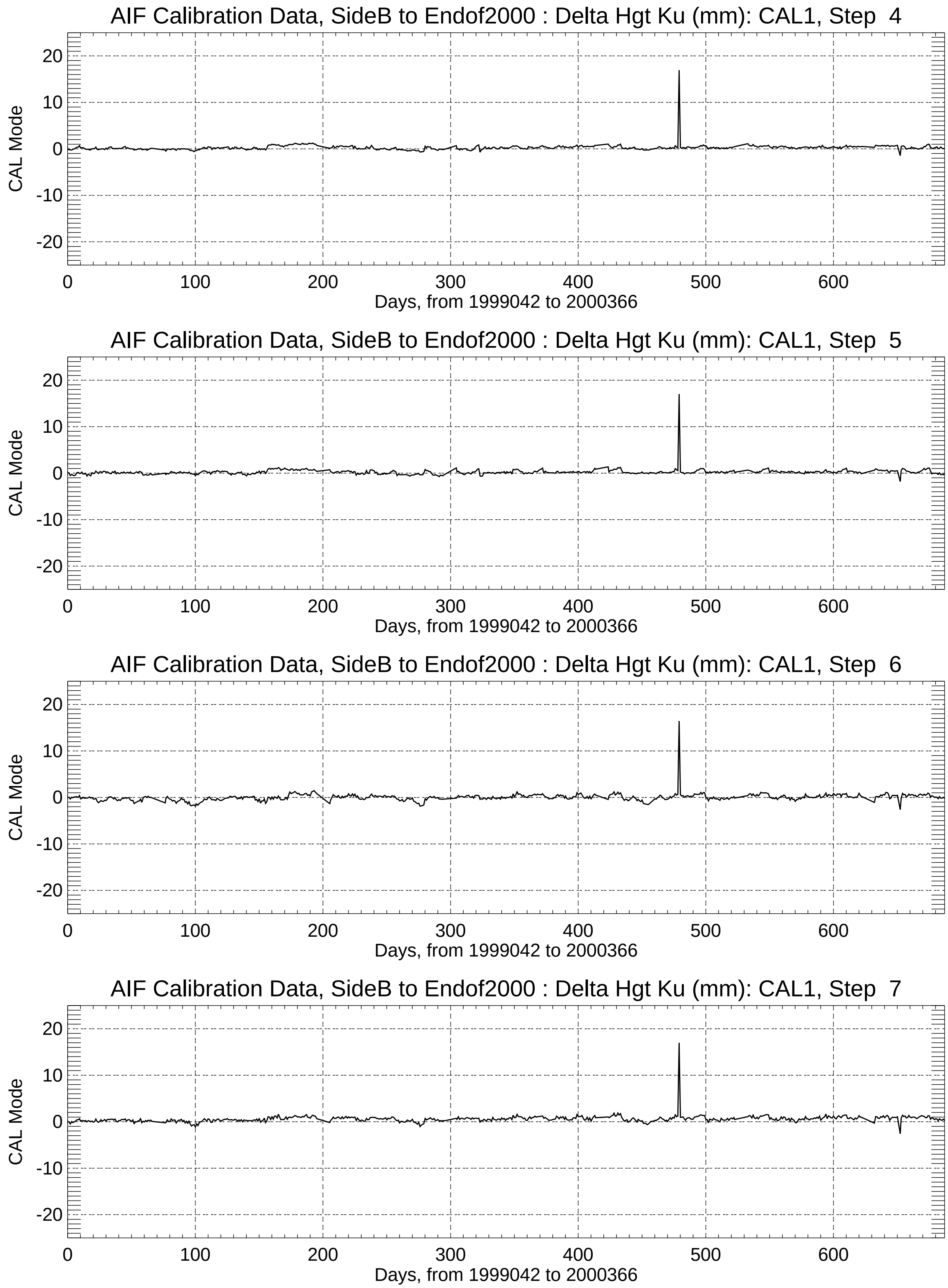

Figure 2-1 Ku-Band Range CAL-1 Results

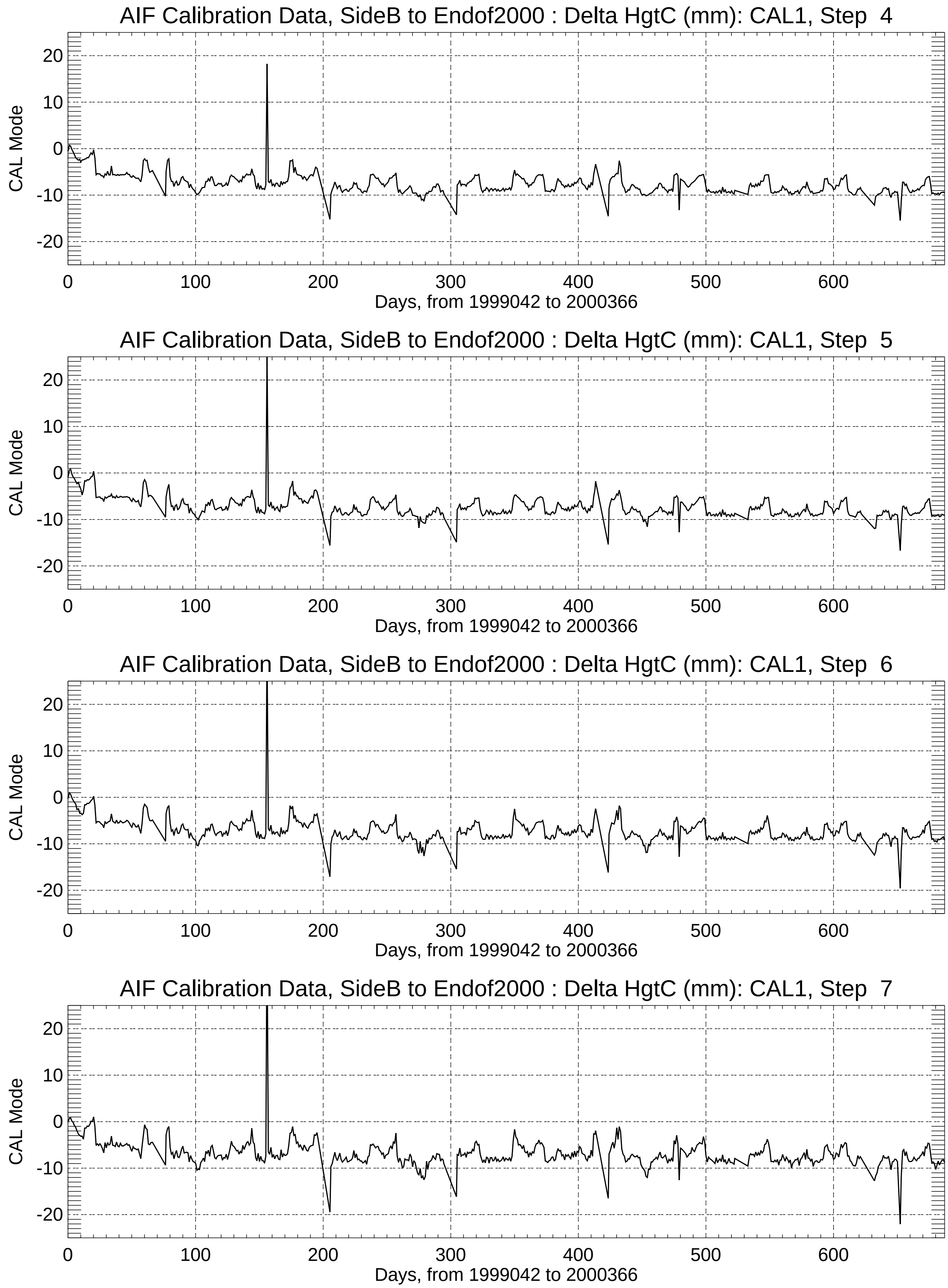

Figure 2-2 C-Band Range CAL-1 Results

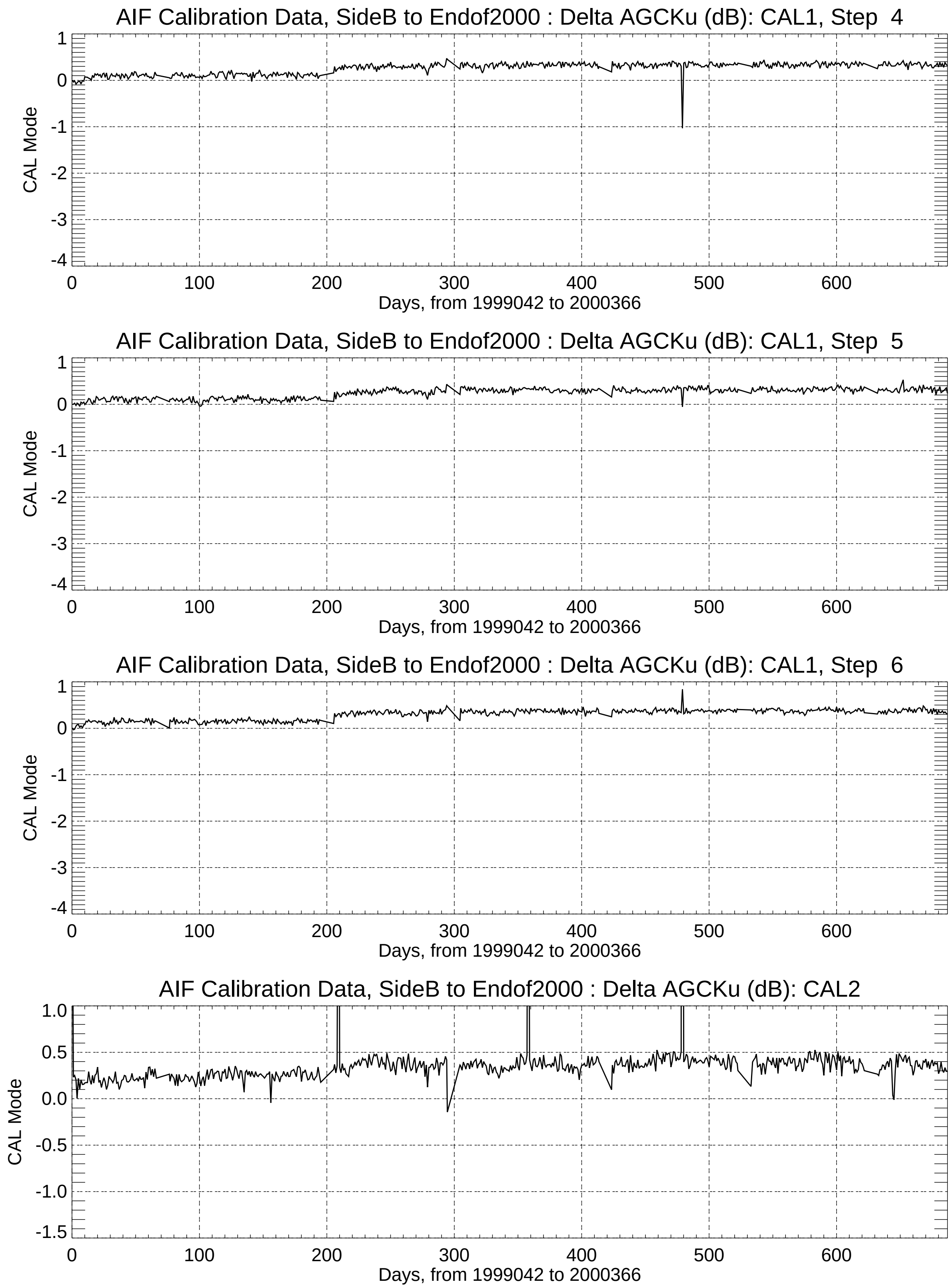

Figure 2-3 Ku-Band AGC CAL-1 and CAL-2 Results

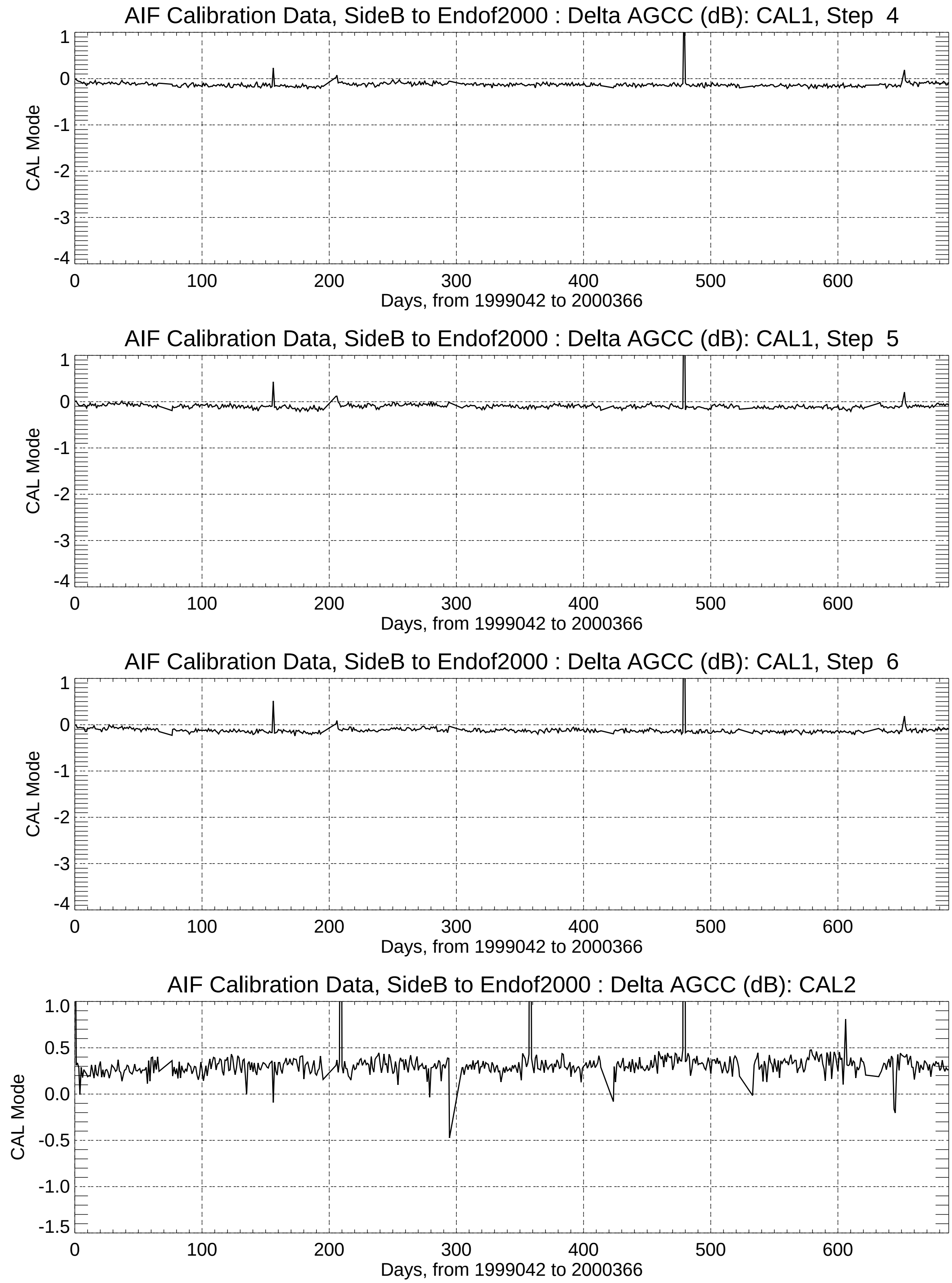

Figure 2-4 C-Band AGC CAL-1 and CAL-2 Results

sigma0 exceeds 16 dB or whenever the number of non-flagged frames within the one-minute interval is fewer than 45. These edit criteria primarily have to do with eliminating the effects of sigma0 blooms. As a result of this edit, approximately 15% of the database measurements are excluded from the averaging process. This tight editing is part of our effort to ensure that anomalous data are excluded from the performance assessment process.

2.2.1 Sea Surface Height

The sea surface heights (ssh) contained in the GDR files are based on combined heights. Cycle-average ssh are shown in Figure 2-5 "Cycle-Average Sea Surface Height in Meters". It is not possible to discern range drifts at the millimeter level from these data, but seasonal variations of global sea level are observable. [There are 36.8 cycles per year.].

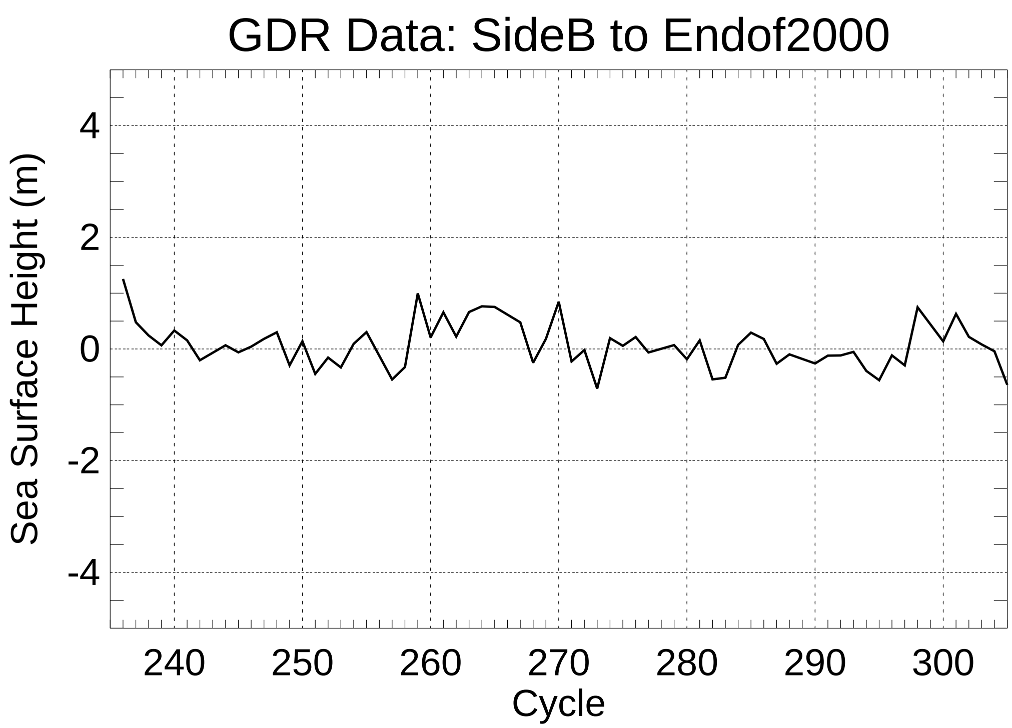

Figure 2-5 Cycle-Average Sea Surface Height in Meters

2.2.2 Sigma0

The sigma0 cycle-averages are plotted in Figure 2-6 "Cycle-Average Ku-Band Sigma0 in dB" and Figure 2-7 "Cycle-Average C-Band Sigma0 in dB" on page 2-8 for Ku-Band and C-Band, respectively. The Ku-Band sigma0 has generally remained in a band of 11.15±0.15 dB, while the C-Band has been in a band of 14.60±0.20 dB.

Sigma0 trends are discussed in more detail in Section 3.2.

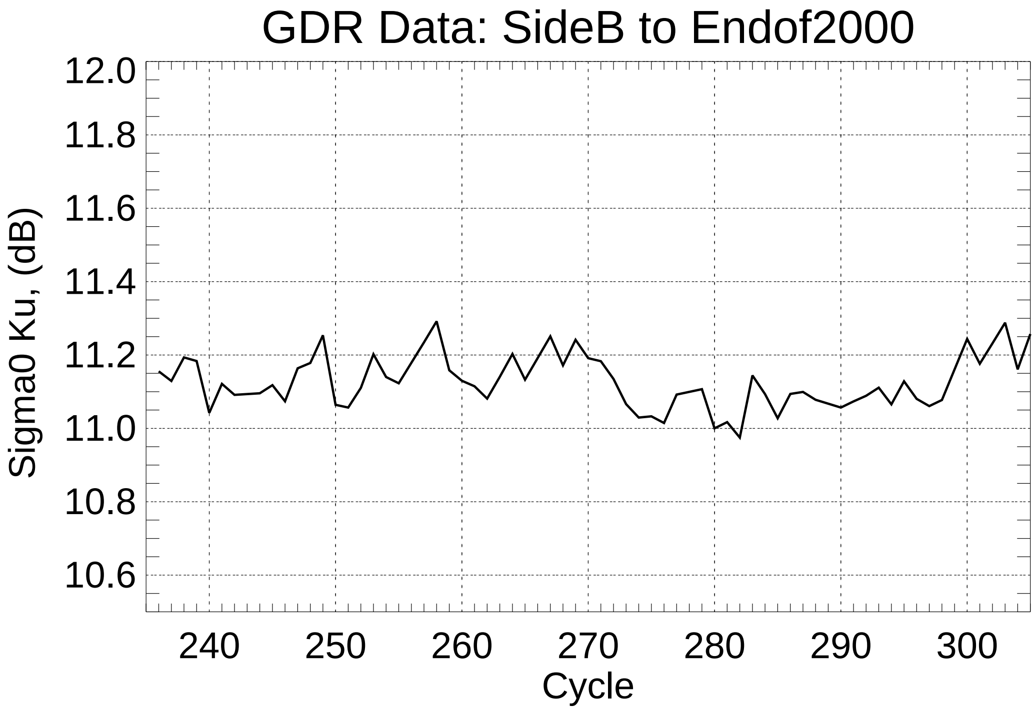

Figure 2-6 Cycle-Average Ku-Band Sigma0 in dB

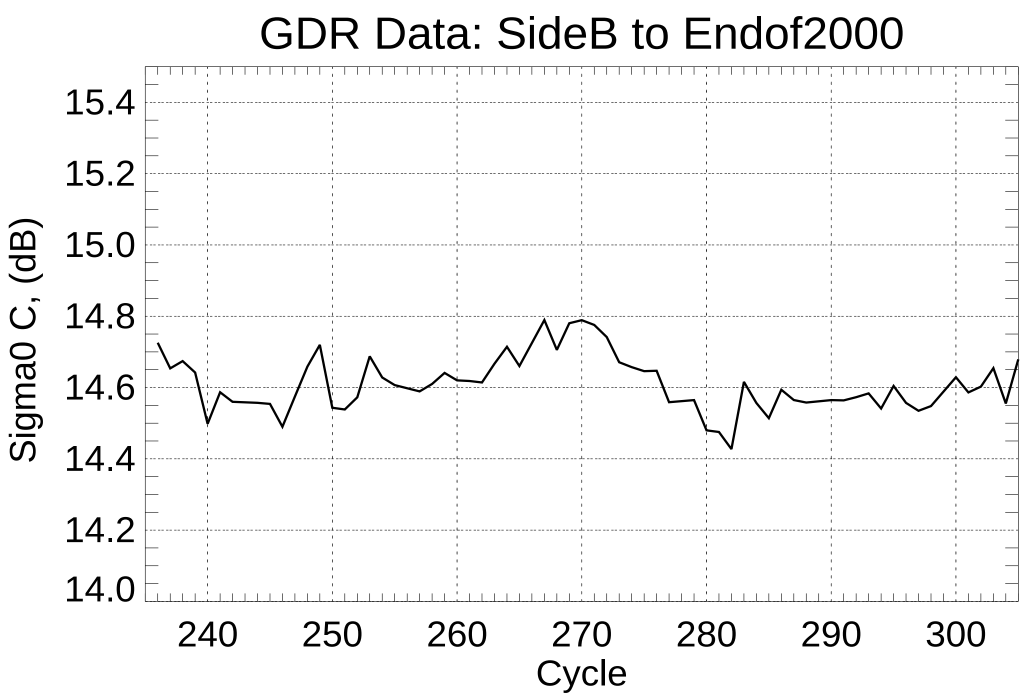

Figure 2-7 Cycle-Average C-Band Sigma0 in dB

2.2.3 Significant Wave Height

Ku-Band cycle-averages for significant wave height (SWH) are shown in Figure 2-8 "Cycle-Average Ku-Band Significant Wave Height in Meters". Seasonal trends in SWH are observable.

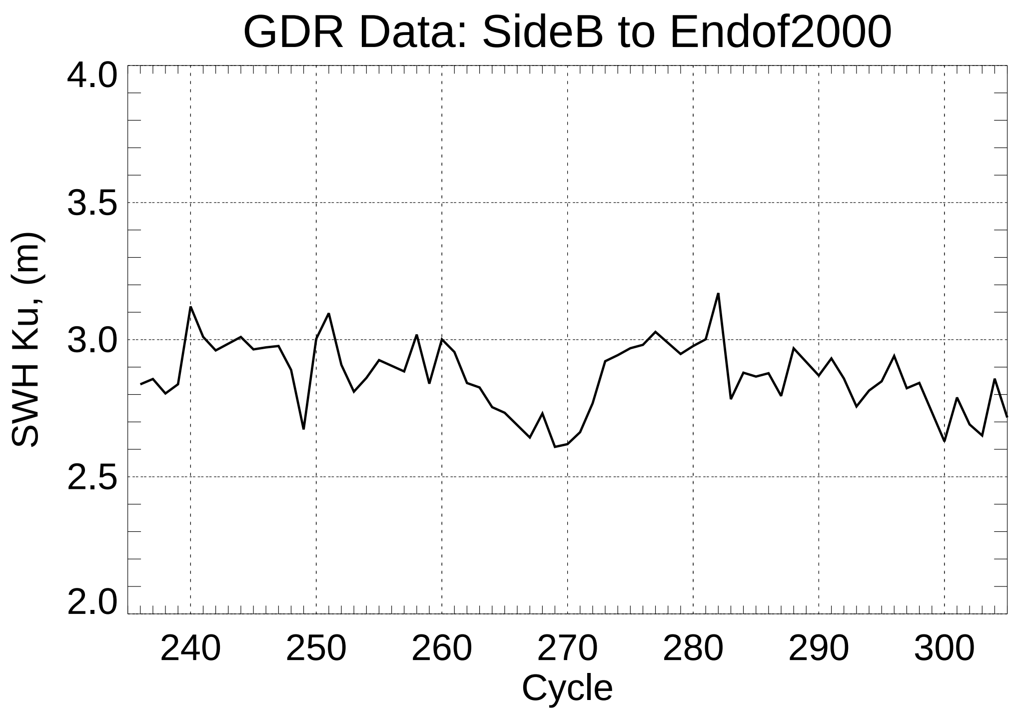

Figure 2-8 Cycle-Average Ku-Band Significant Wave Height in Meters

2.2.4 Range RMS

The calculated Ku-Band range rms values depicted in Figure 2-9 "Cycle-Average Ku-Band Range RMS in Millimeters" on page 2-10 are based on the rms derivation described in Section 5.1.1 of the February 1994 Engineering Assessment Report. An expected correlation with SWH is apparent.

2.2.5 Waveform Monitoring

Selected telemetered waveform gates during CAL-2 and STANDBY modes are monitored daily, to discern waveform changes throughout the mission. CAL-2 waveform sets are generally available twice per day, during calibrations. STANDBY waveforms are generally available four times per day, since the altimeter passes through STANDBY mode just prior to and immediately after each CALIBRATE mode. The relationship of telemetered waveform sample numbers to the onboard waveform-sample numbers is listed in Table 6.2.1 of the February 1994 Engineering Assessment Report.

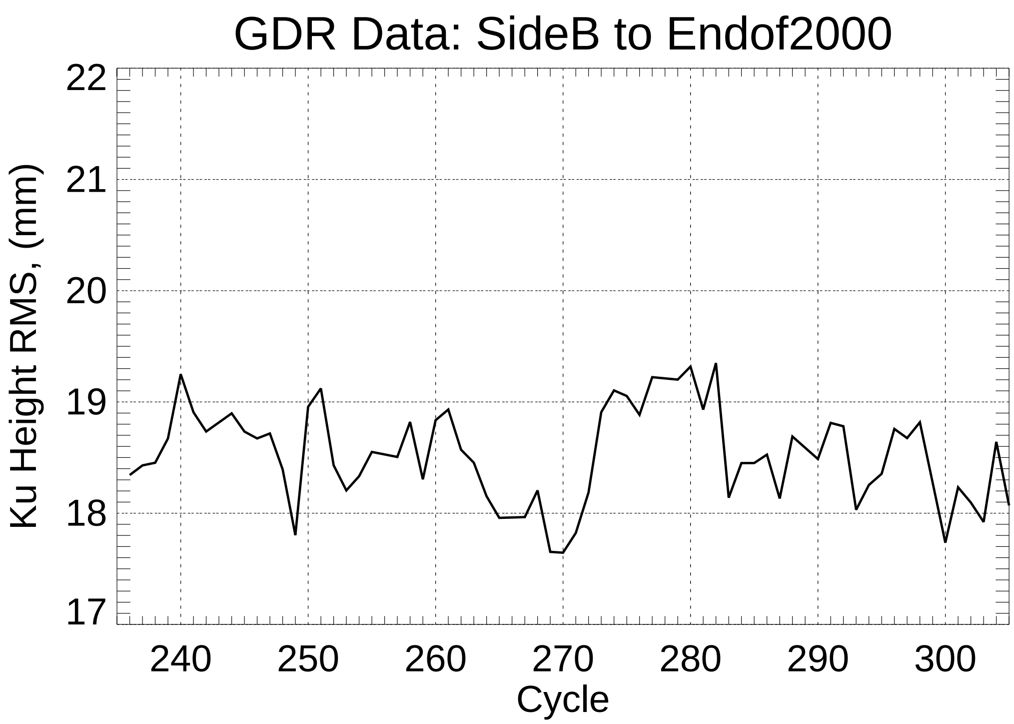

Figure 2-9 Cycle-Average Ku-Band Range RMS in Millimeters

For both Ku-Band and C-Band, the monitored waveform samples are as follows: CAL-2 gates 23, 29, 48, and 93; and STANDBY gates 38, 39, 68, and 69. The Ku-Band waveform sample history is shown in Figure 2-10 "Ku-Band CAL-2 Waveform Sample History" on page 2-11 and in Figure 2-11 "Ku-Band STANDBY Waveform Sample History" on page 2-12for CAL-2 and STANDBY, respectively. The C-Band waveform history is depicted in Figure 2-12 "C-Band CAL-2 Waveform Sample History" on page 2-13 and in Figure 2-13 "C-Band STANDBY Waveform Sample History" on page 2-14, respectively, for CAL-2 and STANDBY.

The monitored Ku-Band CAL-2 waveform samples for Sides B in Figure 2-10 have each varied less than 1% throughout the mission, and exhibit little or no temperature dependence.

The Ku-Band STANDBY waveform samples in Figure 2-11, in contrast, have a slight inverse dependence on temperature (launch-to-date temperatures are shown in Figure 2-14 on the same horizontal time scale as the waveform samples). From the time of Side B turn-on, each of the four sampled gates quickly increased between 5% and 20%, and has then remained fairly steady. Gate 69 is decreasing slightly.

The Side B C-Band CAL-2 waveforms samples, shown in Figure 2-12, are similar to the Ku-Band CAL-2 waveforms in that they have varied less than about 1%, and exhibit no apparent temperature dependence.

The C-Band STANDBY waveform samples, shown in Figure 2-13, are also similar to their counterpart Ku-Band STANDBY waveforms. Gates 38, 39, 68, and 69 have an

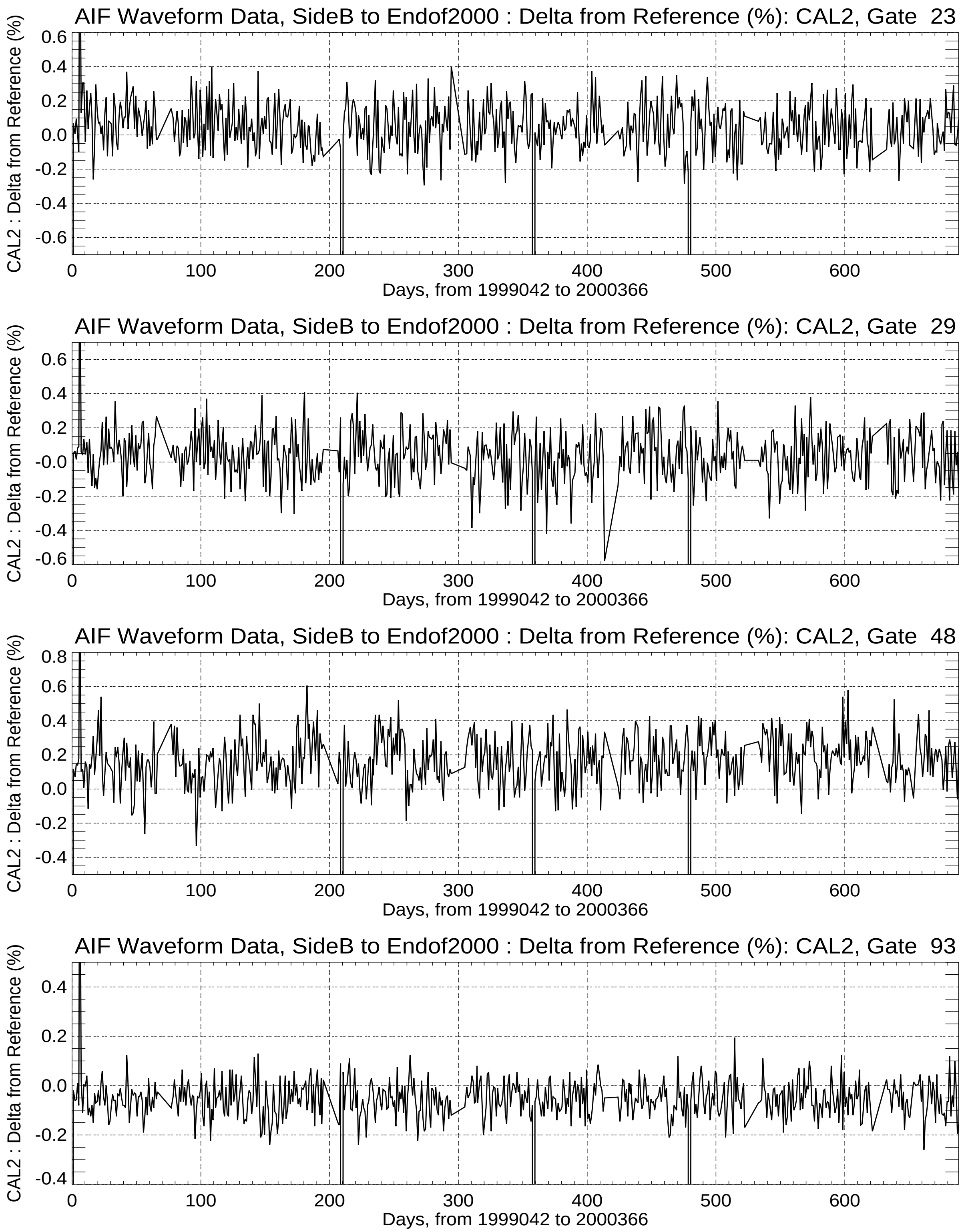

Figure 2-10 Ku-Band CAL-2 Waveform Sample History

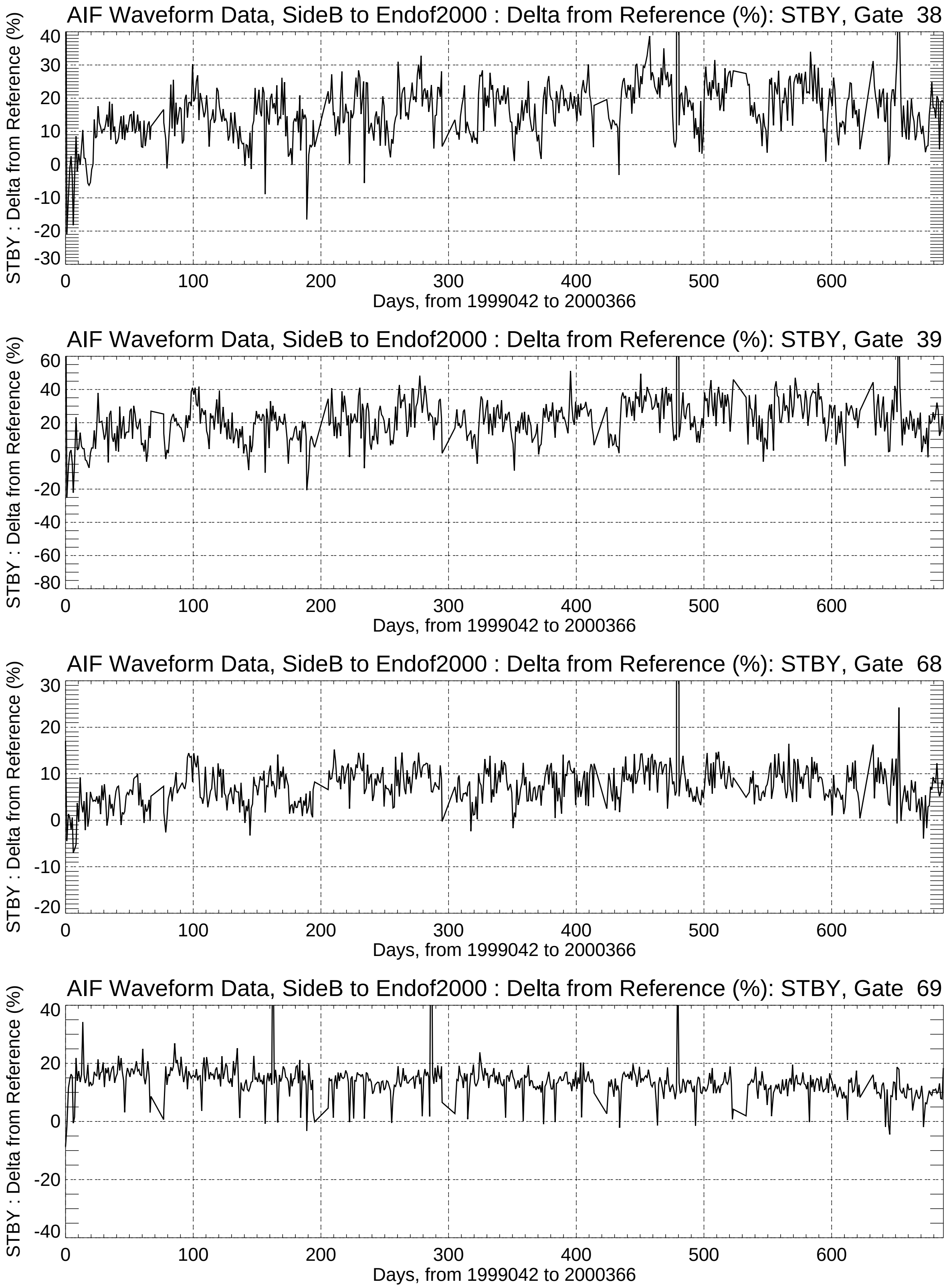

Figure 2-11 Ku-Band STANDBY Waveform Sample History

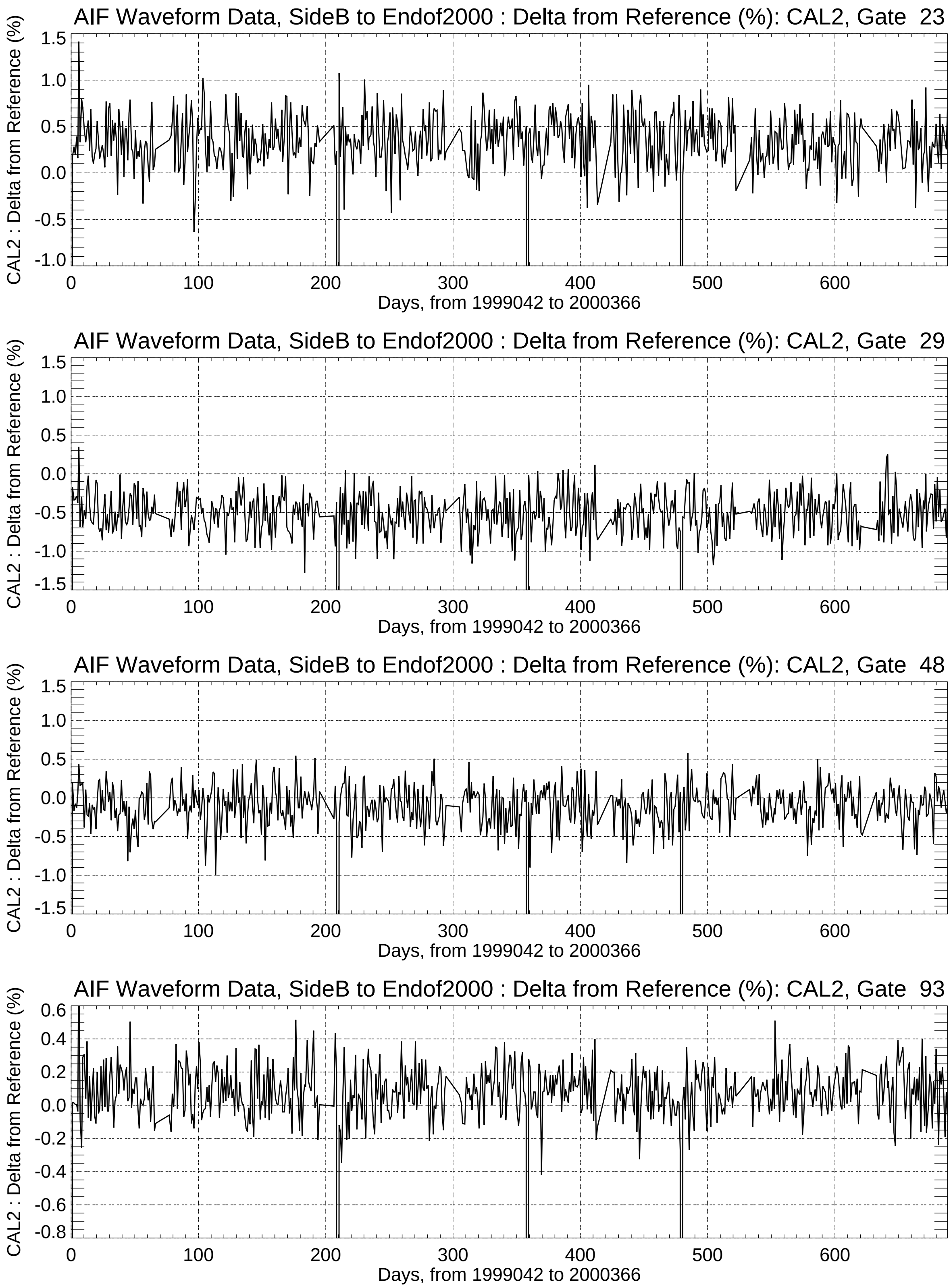

Figure 2-12 C-Band CAL-2 Waveform Sample History

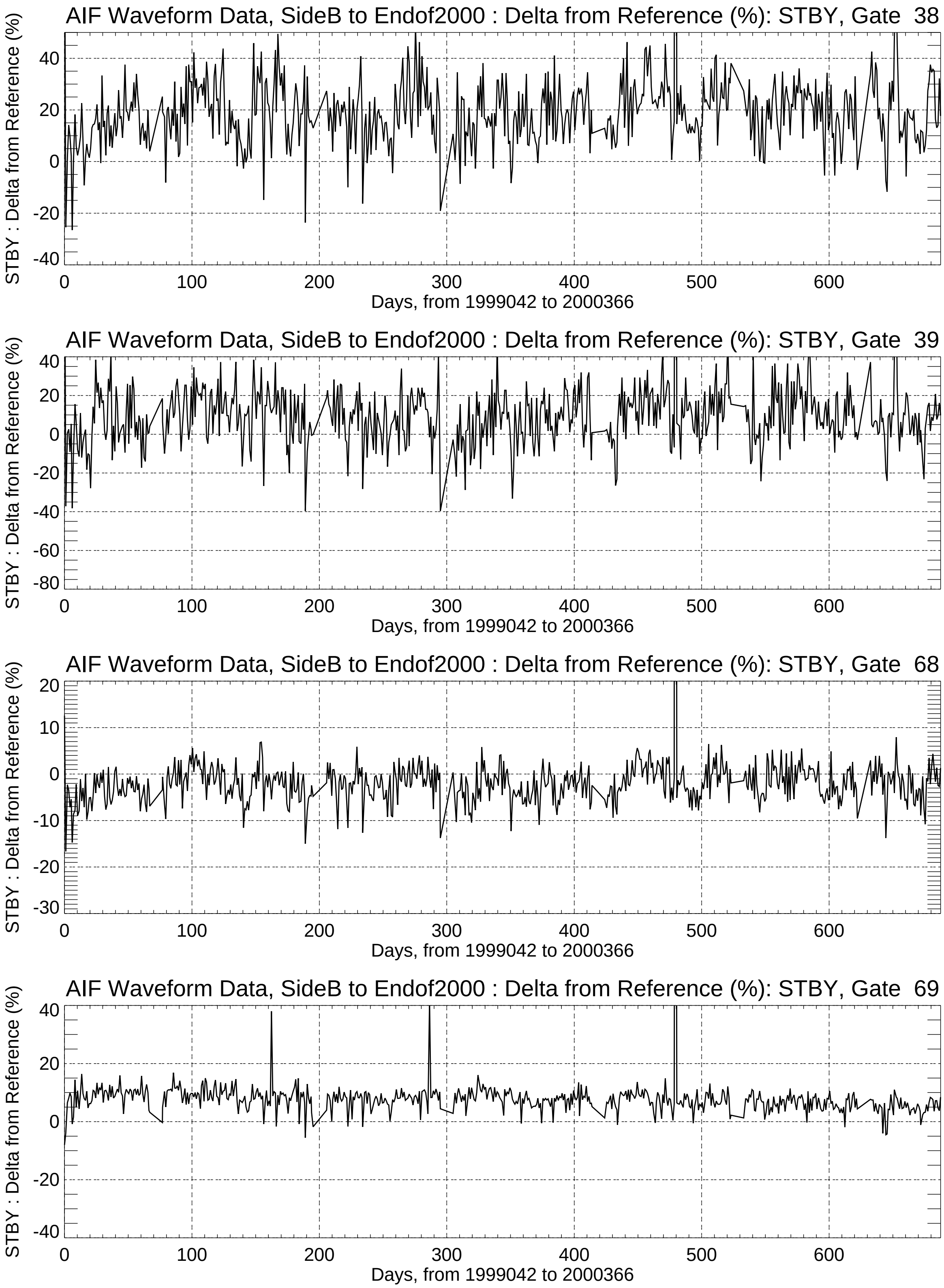

Figure 2-13 C-Band STANDBY Waveform Sample History

inverse dependence on temperature, and have each experienced increases shortly after turn-on. Gate 69 appears to have a downward trend similar to Ku-Band.

In Figure 2-12, "C-Band CAL-2 Waveform Samples", and Figure 2-13, "C-Band STANDBY Waveform Samples", there are waveform spikes at the labeled days of 210, 359 and 480. The reasons for these spikes are posted in the "Side B Key Events", section 2.3, Table 2-2. They are: Day 210 - 1999 / 252, Digital Filter Bank Calibration; Day 359 - 2000 / 036, Digital Filter Bank Calibration; Day 480 - 2000 / 157, Improper SEU recovery from a Digital Filter Bank Interface Lockup.

2.2.6 Engineering Monitors

Altimeter temperatures, voltages, powers and currents continue to be monitored. The system remains very stable, with no significant changes since Side B turn-on. The engineering monitor plots presented in this section contain data based on 24-hour time periods, showing the average, the minimum, and the maximum values during each 24-hour period.

2.2.6.1 Temperatures

The temperatures of all 26 internal thermistors continued to be within the design temperature range and, except for the DCG Gate Array, are within the ranges experienced during the pre-launch Hot and Cold Balance Tests. The minimum / maximum values for each of the thermistors during TRACK mode remained within the bounds listed in Table 7.1 of the *TOPEX Mission Engineering Assessment Report*, February 1994, and they compose plots 2 through 27 in Figure 2-14 "Engineering Monitor Histories" on page 2-16.

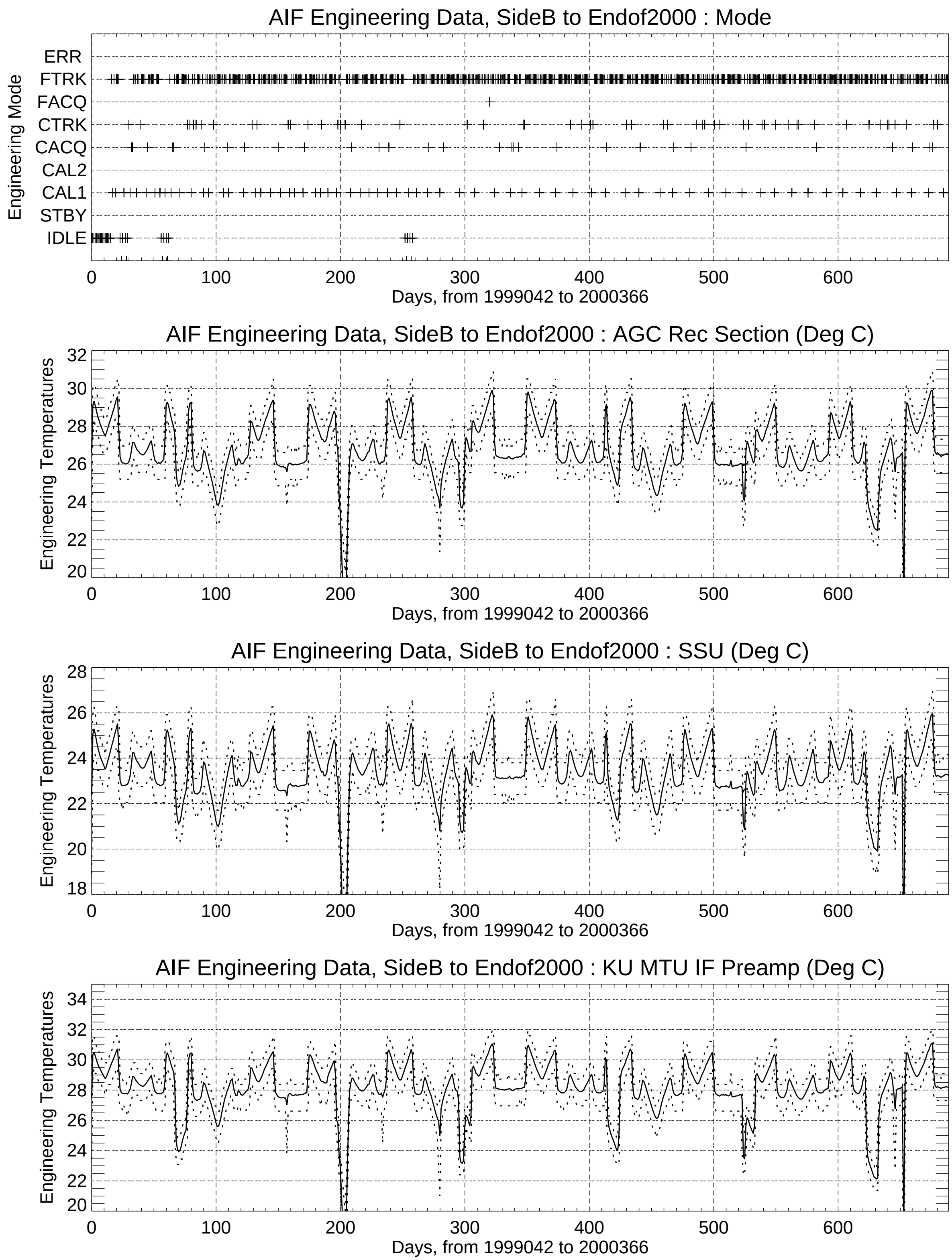

Figure 2-14 Engineering Monitor Histories

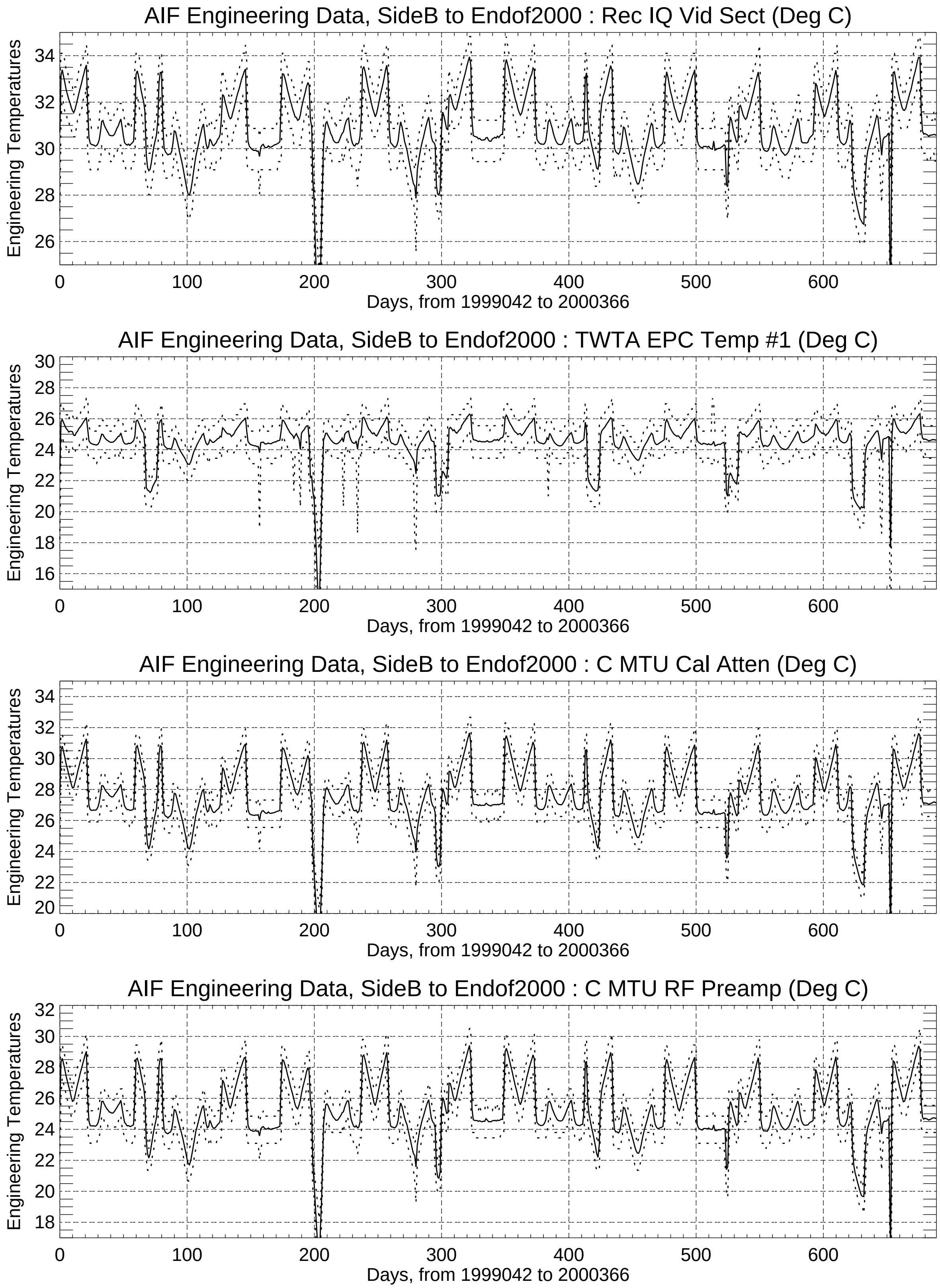

Figure 2-14 Engineering Monitor Histories (Continued)

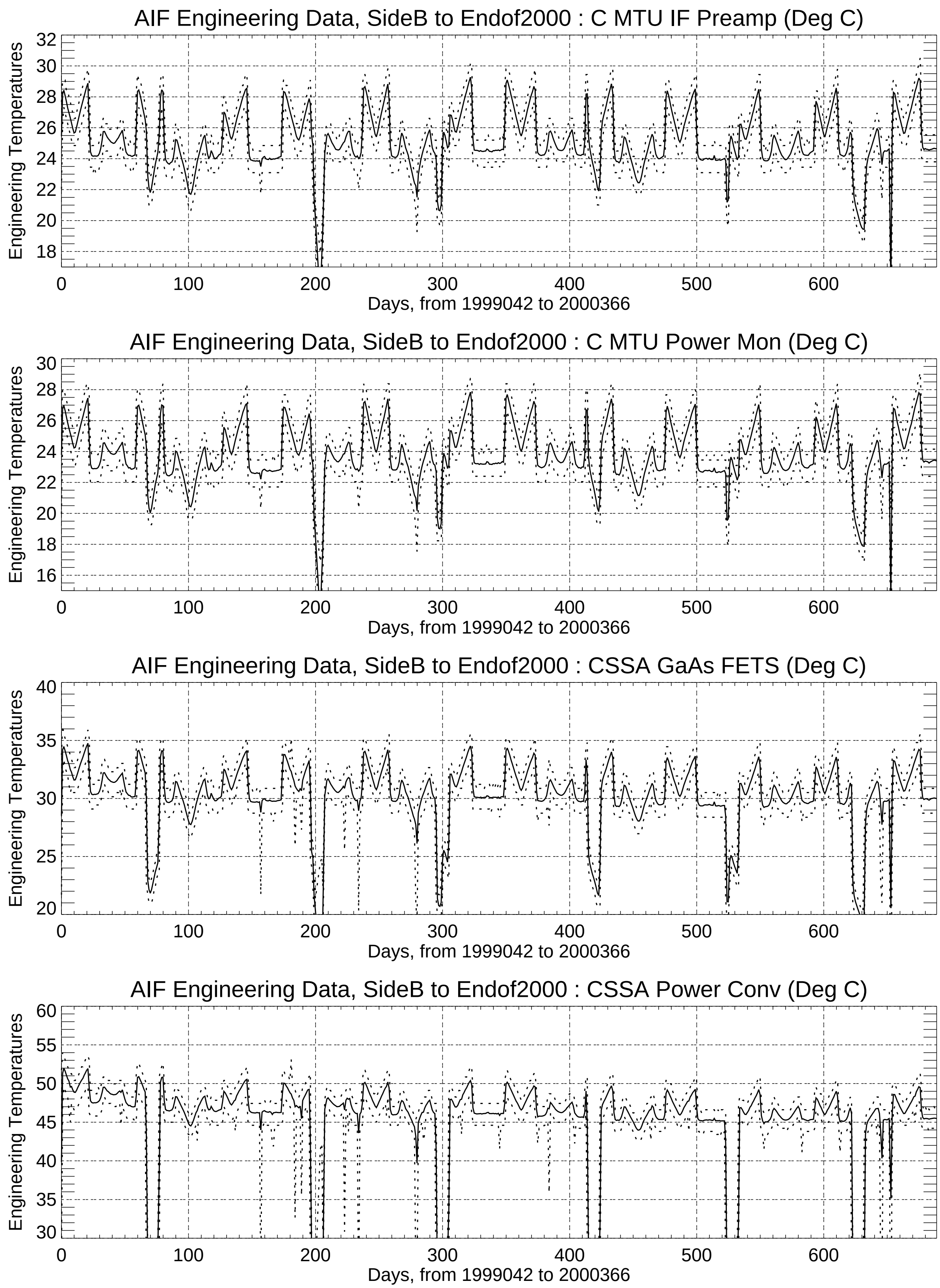

Figure 2-14 Engineering Monitor Histories (Continued)

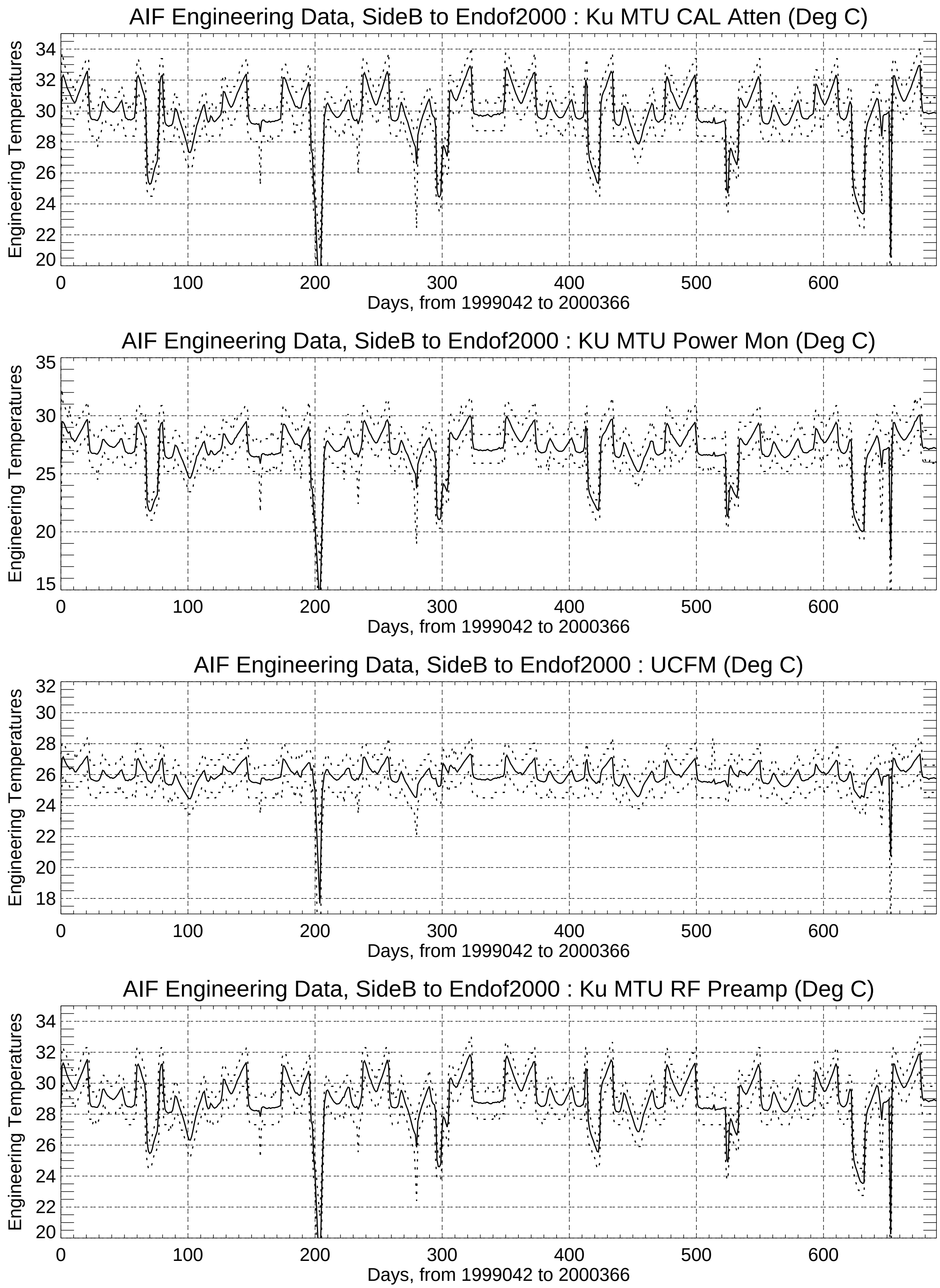

Figure 2-14 Engineering Monitor Histories (Continued)

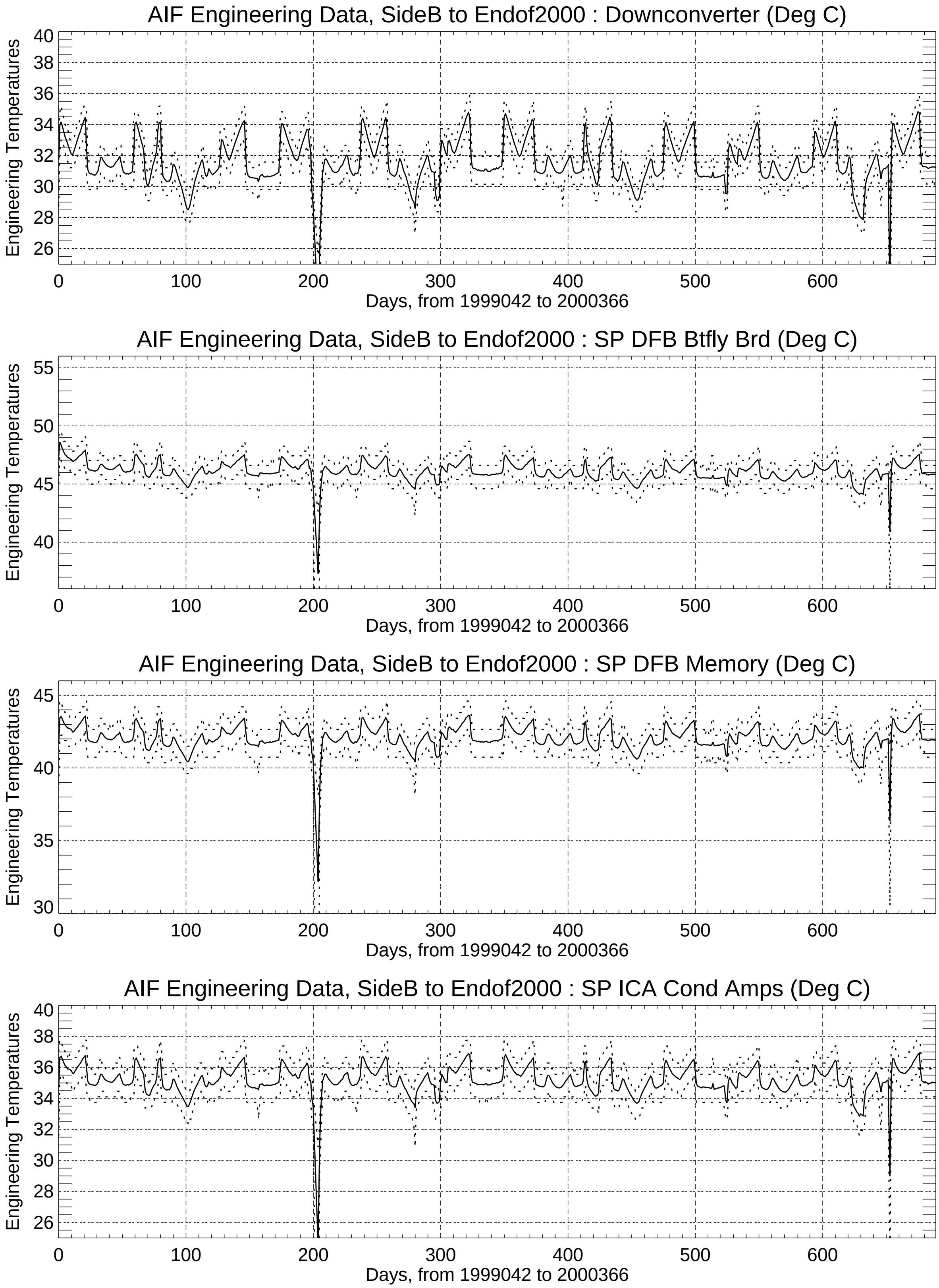

Figure 2-14 Engineering Monitor Histories (Continued)

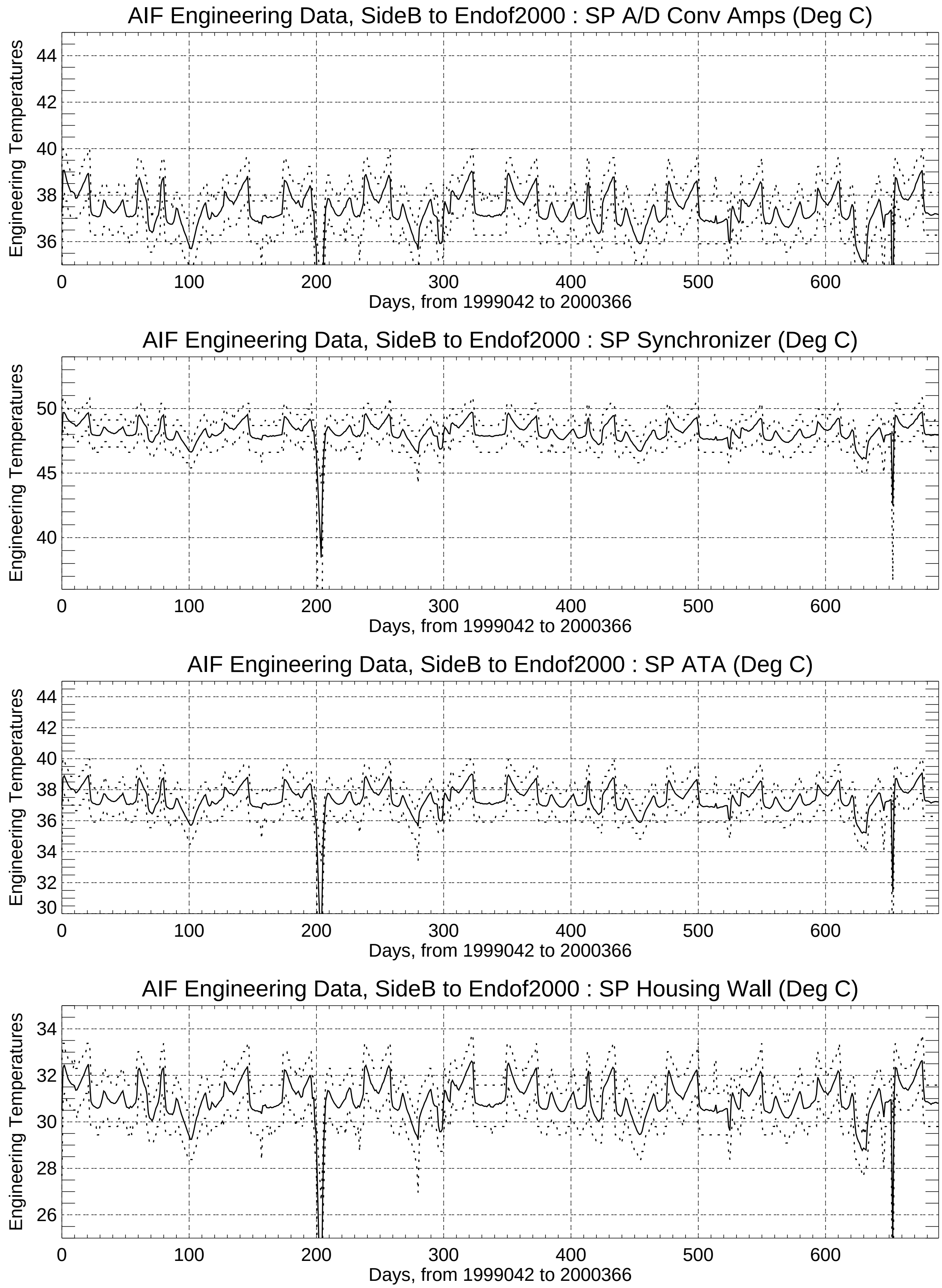

Figure 2-14 Engineering Monitor Histories (Continued)

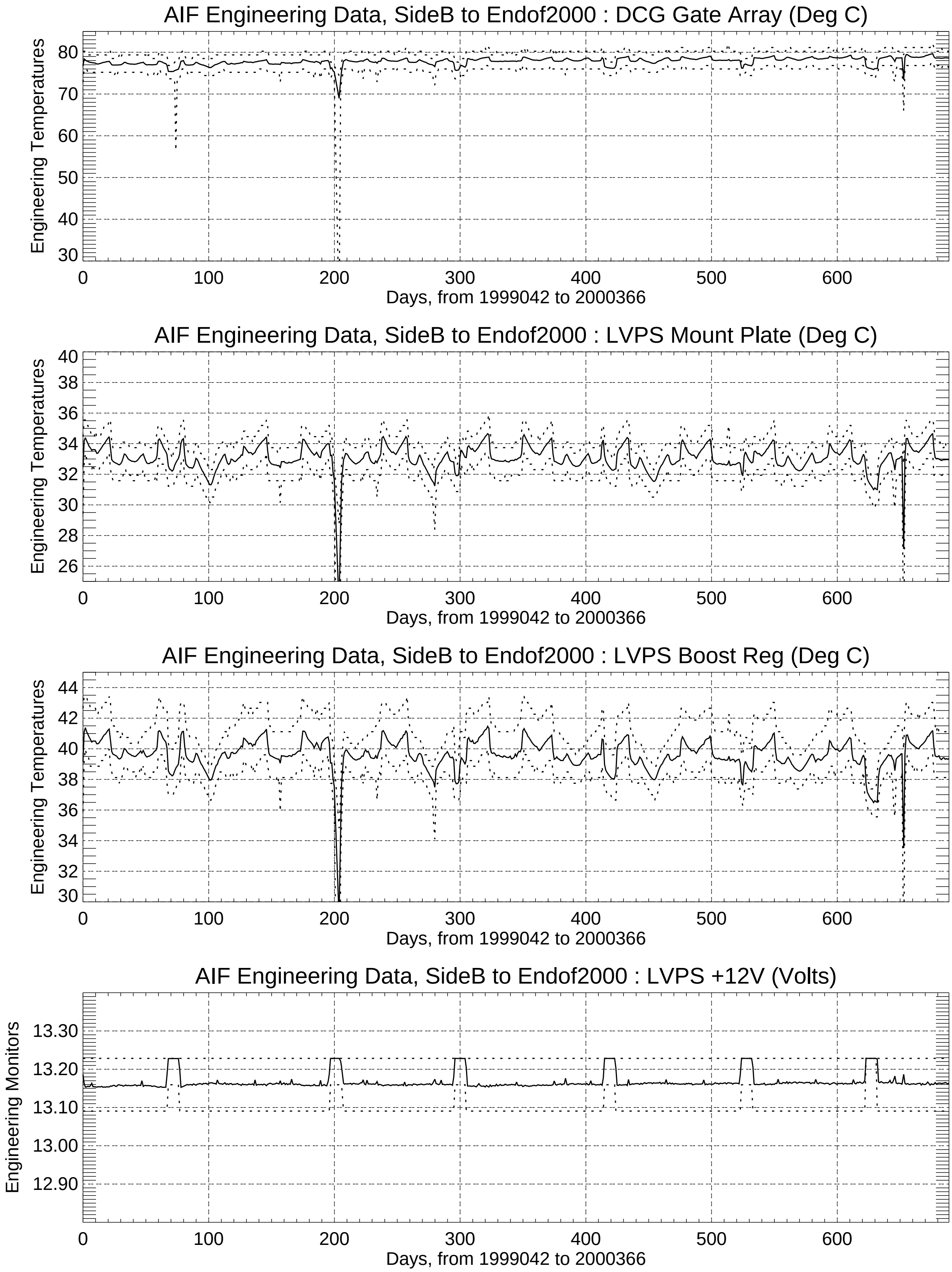

Figure 2-14 Engineering Monitor Histories (Continued)

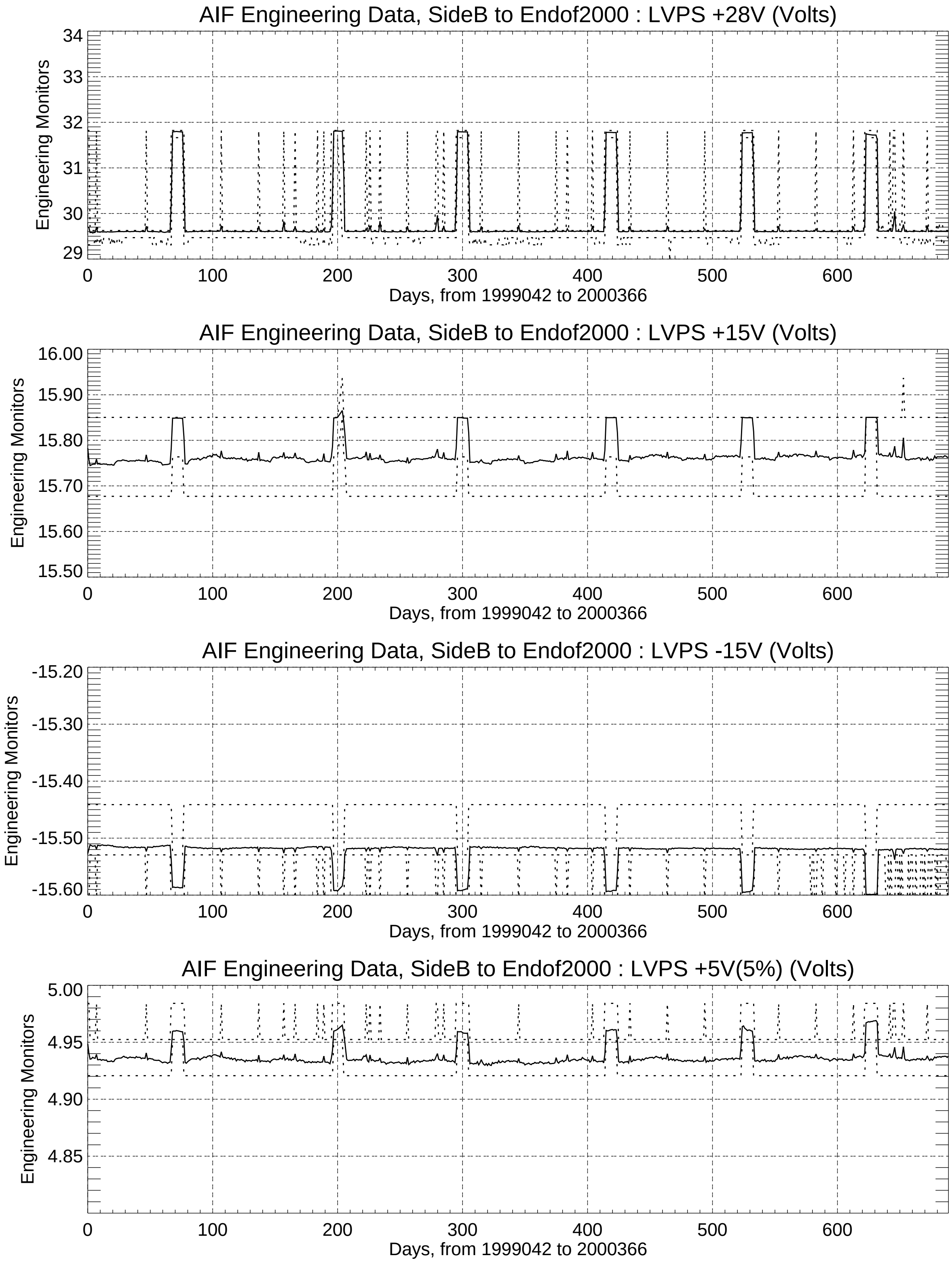

Figure 2-14 Engineering Monitor Histories (Continued)

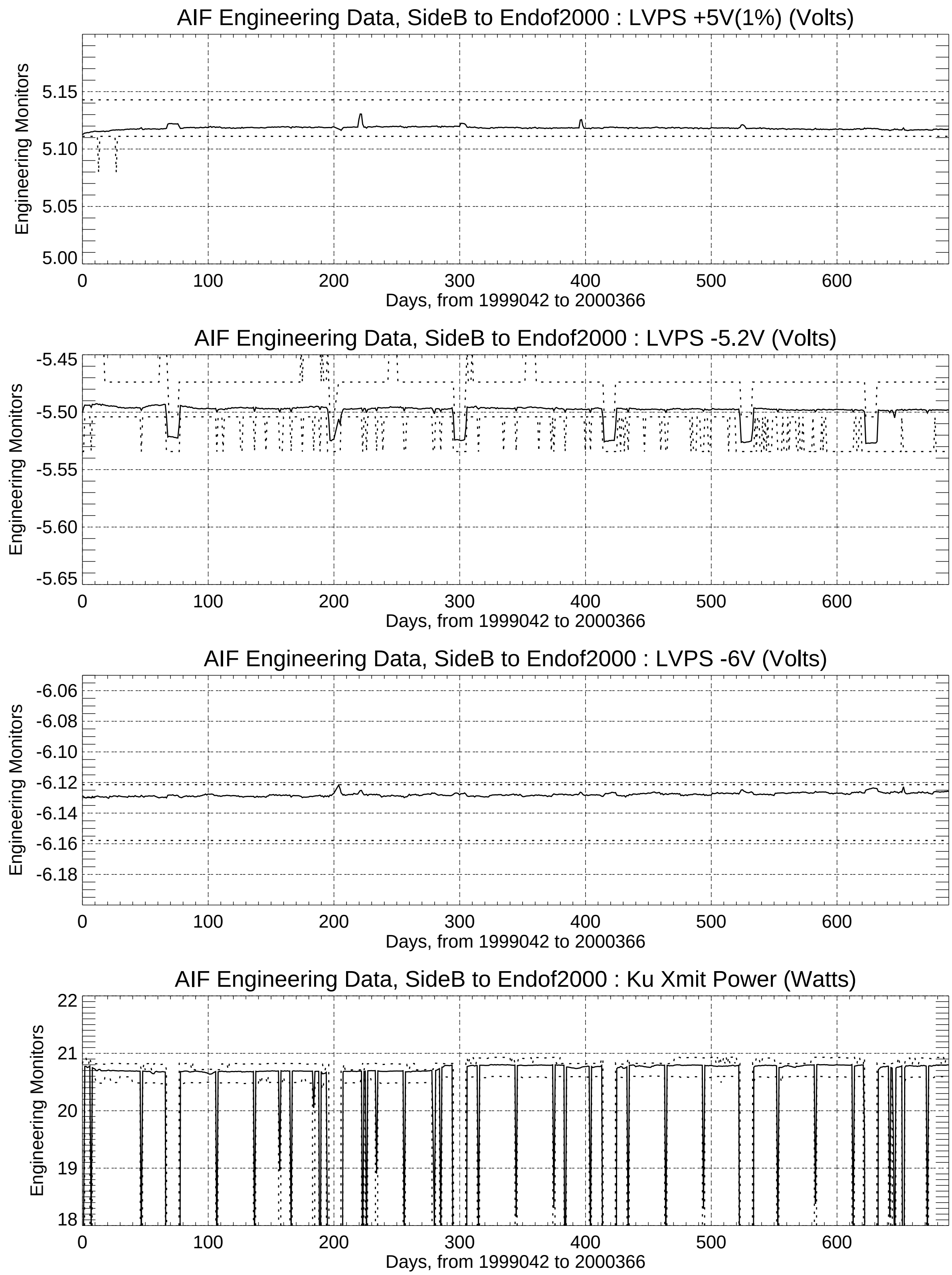

Figure 2-14 Engineering Monitor Histories (Continued)

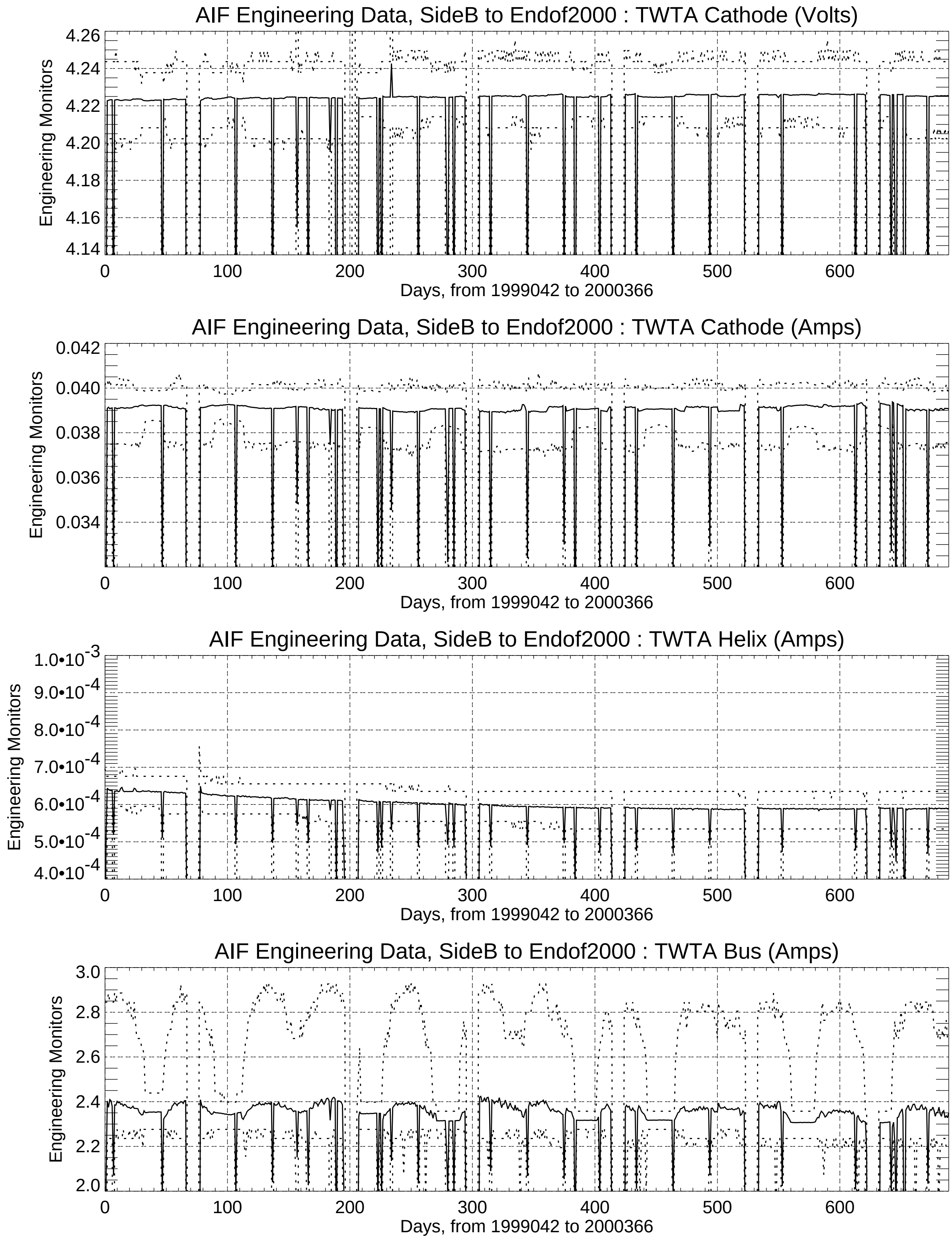

Figure 2-14 Engineering Monitor Histories (Continued)

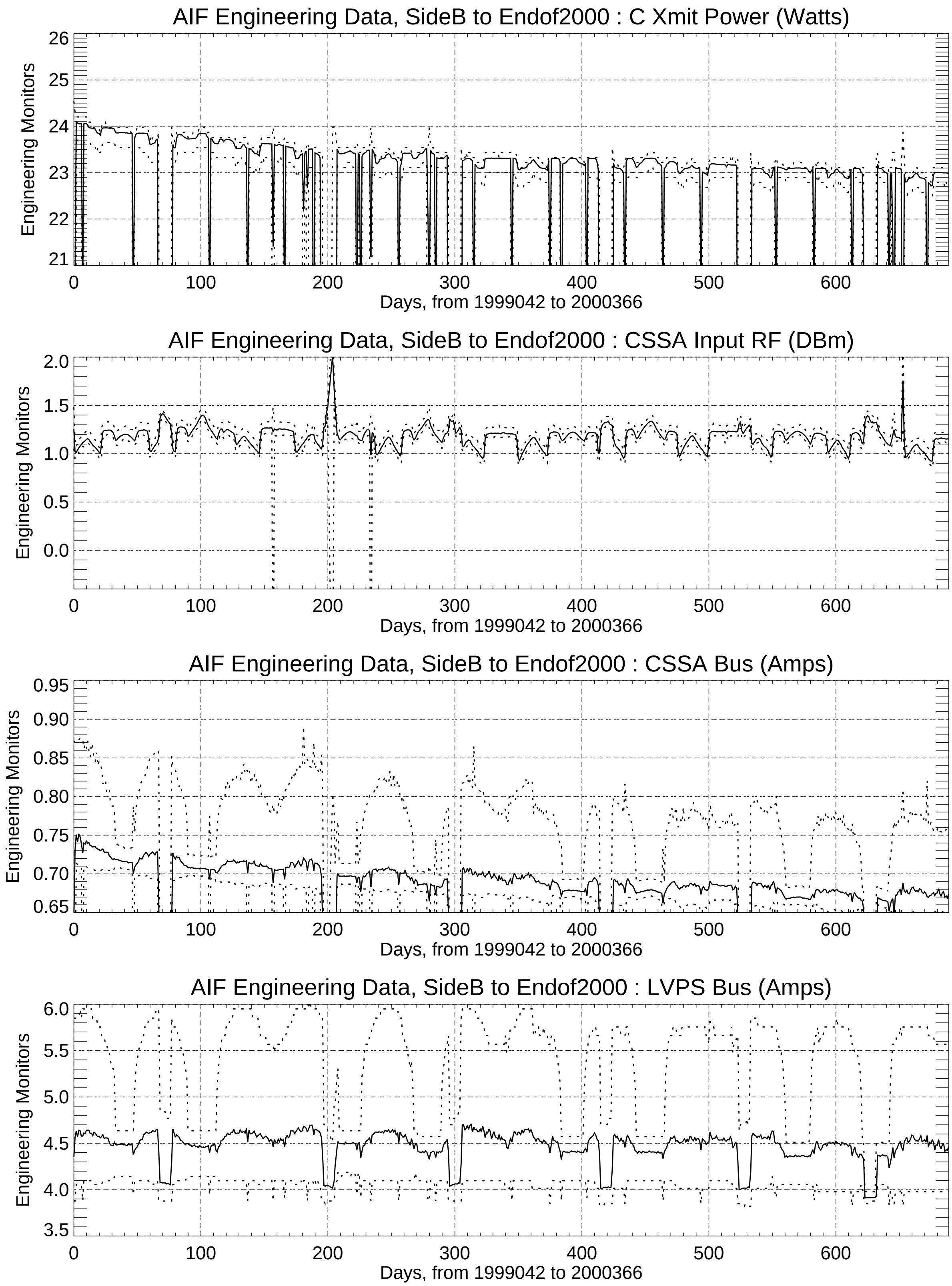

Figure 2-14 Engineering Monitor Histories (Continued)

As noted in last year's assessment report, the DCG Gate Array temperature is about 30 degrees higher than that experienced during pre-launch testing. However, the temperature has remained stable since Side B turn-on, and a lifetime thermal analysis of a similar DCG Gate Array unit indicates no concern.

Although not used during our routine monitoring, several of the altimeter-related baseplate temperature monitors serviced by Remote Interface Unit (RIU) 6B became uncalibrated on day 17 of 1995. The affected temperature monitors are listed in Section 2.2.6.1 of the 1996 Engineering Assessment Report. An abrupt change in the values occurred on that date, apparently due to a change in the current which is applied to the thermistor circuits.

2.2.6.2 Voltages, Powers and Currents

The altimeter's 17 monitors for voltages, powers and currents remained at consistent levels, with little deviations. Their Side B to end of 2000 histories are also shown in Figure 2-14 "Engineering Monitor Histories" on page 2-16.

The eight voltages [LVPS +12V, LVPS +28V, LVPS +15V, LVPS -15V, LVPS +5V(5%), LVPS +5V(1%), LVPS -5.2V and LVPS -6V], have changed very little since Side B turn-on.

The following changes since turn-on of Side B are noted:

- The TWA Helix current has decreased about 0.05 milliamperes.
- The C-Band Transmit Power has decreased approximately 1.0 watt since turn-on.
- There has been a gradual decrease in the CSSA Bus current level; the level has decreased 0.08 amp since turn-on.

2.2.7 Single Event Upsets

There have been a total of 104 Single Event Upsets (SEUs) from the initial turn-on of Side B to the end of 2000, an average of one SEU per 6.6 days. The vast majority of the SEUs occurred in the South Atlantic Anomaly, as shown in Figure 2-15 "Locations of SEU Occurrences" on page 2-28. The dots in Figure 2-15 denote the locations of normal SEU occurrences, while the diamonds indicate that the SEU was abnormal.

The altimeter processor automatically recovered from 95 of the SEUs; the other nine required manual (ground-based command) resets. The automatic resets, generally, resulted in the loss of only a few seconds of data.

As of January 1, 2001, there have been a total of eleven anomalous Side B resets (the nine manual resets plus two additional abnormal automatic resets). Table 2-1 "Anomalous Single Event Upsets" on page 2-28 lists the dates of these eleven SEUs, along with the type of on-board reset and the duration of the effect on the data.

Regarding the two abnormal automatic resets:

- Day 1999-280 - The waveforms were not updating and a range sweep was processed. The altimeter reset itself.

- Day 2000-056 - The SEU reset resulted in corrupted engineering spare word. A memory reload corrected the problem. The altimeter science data, in the interim between the SEU and the memory reload, was apparently not affected.

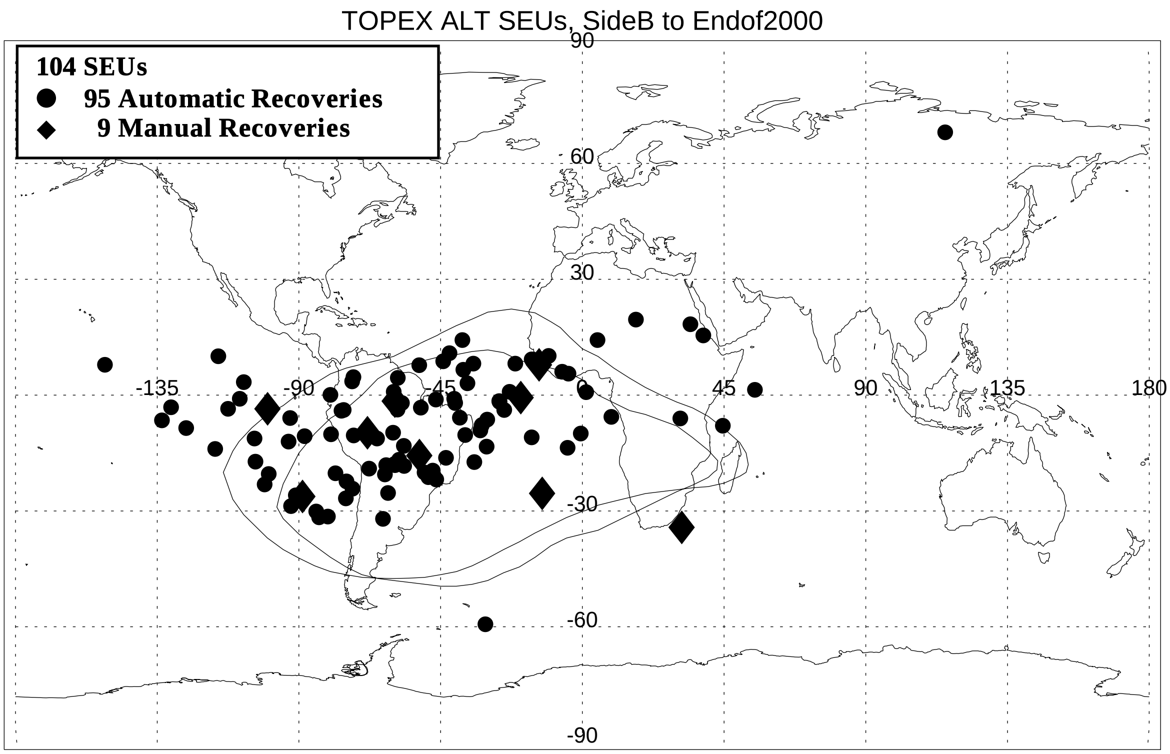

Figure 2-15 Locations of SEU Occurrences

Table 2-1 Anomalous Single Event Upsets

Year	Day	Duration (Hr)	Reset Type	Type SEU
		Side B		
1999	071	0.7	Manual	DFB Interface Lockup
1999	198	5.6	Manual	C MTU Xmit
1999	223	1.6	Manual	Memory Corrupted
1999	246	13.0	Manual	Eng. Interface Lockup
1999	276	3.1	Manual	Ku MTU Xmit
1999	280	0.1	Automatic	No waveform update/Range Sweep
2000	056	0.1	Automatic	Eng. Spare Word Corrupted
2000	067	5.8	Manual	Sci. Telemetry Lockup

Table 2-1 Anomalous Single Event Upsets (Continued)

Year	Day	Duration (Hr)	Reset Type	Type SEU
2000	157	1.9	Manual	DFB Interface Lockup
2000	227	1.4	Manual	Sci. Telemetry Lockup
2000	275	1.1	Manual	DFB Interface Lockup
		Total = 34.4 Hrs		

2.3 Side B Key Events

The key events for TOPEX Altimeter Side B since its on-orbit turn-on are summarized in Table 2-2 "NASA Altimeter Side B - Key Events".

Table 2-2 NASA Altimeter Side B - Key Events

Day	Event
1999/041	Commanded Side B to IDLE Mode and Uploaded Memory Patches
1999/042	Commanded Side B to STANDBY and then to TRACK Mode
1999/042	Side B Testing, including: Mode Checks, Cal-Sweep, and Waveform Leakage Tests
1999/043	Additional Testing, including: Cal-Sweep, Waveform Leakage Tests, and Gate-Shift Tests
1999/048	Gate Shift Tests (lost 3.1 hours of data)
1999/049	Cal-Sweep Test (lost 0.4 hours of overland data)
1999/049-050	Off-Nadir Tests
1999/050	Began First Side B Operational Cycle [Cycle 237]
1999/071	Improper SEU Recovery (lost 0.7 hours of data)
1999/089	Cal-Sweep Test (lost 0.4 hours of overland data)
1999/109	Cal-Sweep Test (lost 0.4 hours of overland data)
1999/109	Changed to IDLE Mode for SSALT
1999/119	Returned to TRACK Mode
1999/119	Cal-Sweep Test (lost 0.4 hours of overland data)
1999/149	Cal-Sweep Test (lost 0.4 hours of overland data)
1999/179	Cal-Sweep Test (lost 0.4 hours of overland data)

Table 2-2 NASA Altimeter Side B - Key Events (Continued)

Day	Event
1999/198-199	C-Band Autonomously Switched to Side A Transmit (lost 5.6 hours of data)
1999/209	Cal-Sweep Test (lost 0.4 hours of overland data)
1999/223	C-Band CAMPIN Autonomously Disabled (lost 1.6 hours of data). Some corruption of Non-Protected Memory
1999/226	Unsuccessful Restoration of Non-Protected Memory, due to Command Table Error (lost 0.6 hours of overland data)
1999/231	Successful Restoration of Non-Protected Memory (lost 1.1 hours of mostly overland data)
1999/236	Commanding for New Parameter File, to Increase AGC Minimum from 13 to 15 dB (lost 0.1 hours of overland data).
1999/237	Cal-Sweep Test (lost 0.4 hours of overland data)
1999/238	Changed to IDLE Mode for SSALT
1999/243	Spacecraft Safehold, after a reset of central data processing unit. ALT was automatically turned OFF.
1999/243	Commanded ALT back to IDLE Mode. Total OFF time was 15.7 hours.
1999/244	Uploaded full memory dump command. ALT remains in IDLE.
1999/245	ALT turned OFF during Attitude Control Electronics switchover
1999/246	Commanded ALT back to IDLE Mode and Uploaded full memory dump command. ALT remains in IDLE. OFF time was 7.9 hours.
1999/248	Returned to TRACK Mode
1999/252	Digital Filter Bank Calibration (lost 0.3 hours of overland data)
1999/265	Sent Commands in Attempt to Improve Acquisition. Lost 1.1 hours of land and ocean data. Commanding was Unsuccessful.
1999/268	Cal-Sweep Test (lost 0.4 hours of overland data)
1999/276	Ku-Band Autonomously Switched to Side A Transmit (lost 3.1 hours of data)
1999/298	Cal-Sweep Test (lost 0.4 hours of overland data)
1999/327	Cal-Sweep Test (lost 0.4 hours of overland data)
1999/337	Changed to IDLE Mode for SSALT
1999/347	Returned to TRACK Mode

Table 2-2 NASA Altimeter Side B - Key Events (Continued)

Day	Event
1999/357	Cal-Sweep Test (lost 0.4 hours of overland data)
1999/360	SEU resulted in corruption of the engineering Pass Count value. No apparent effect on ALT science data.
2000/012	Orbital Maneuver #13 (affected 1.2 hours of data)
2000/022	Cal-Sweep Test (lost 0.4 hours of overland data)
2000/036	Digital Filter Bank Calibration (lost 0.3 hours of overland data)
2000/052	Cal-Sweep Test (lost 0.4 hours of overland data)
2000/056-061	SEU at 056/141130 UTC resulted in corrupted engineering spare word. Memory reload on 061/070828 UTC corrected problem. ALT science data quality during the interim was apparently not affected.
2000/061	Reloaded memory to rectify engineering memory corruption which began on day 056. Lost 0.9 hours of mostly overland data. This memory reload also restored the engineering Pass Count value which had been corrupted by an earlier SEU on 1999/360.
2000/067	Improper SEU recovery (lost 5.8 hours of data)
2000/081	Cal-Sweep Test (lost 0.4 hours of overland data)
2000/091	Changed to IDLE Mode for SSALT
2000/101	Returned to TRACK Mode
2000/111	Cal-Sweep Test (lost 0.4 hours of overland data)
2000/141	Cal-Sweep Test (lost 0.4 hours of overland data)
2000/157	Improper SEU recovery (lost 1.9 hours of data)
2000/171	Cal-Sweep Test (lost 0.4 hours of overland data)
2000/200	Cal-Sweep Test (lost 0.4 hours of overland data)
2000/200	Changed to IDLE Mode for SSALT
2000/210	Returned to TRACK Mode
2000/227	Improper SEU recovery (lost 1.4 hours of data)
2000/230	Cal-Sweep Test (lost 0.4 hours of overland data)
2000/260	Cal-Sweep Test (lost 0.4 hours of overland data)
2000/275	Improper SEU recovery (lost 1.1 hours of data)

Table 2-2 NASA Altimeter Side B - Key Events (Continued)

Day	Event
2000/290	Cal-Sweep Test (lost 0.4 hours of overland data)
2000/299	Changed to IDLE Mode for SSALT
2000/309	Returned to TRACK Mode
2000/319	Cal-Sweep Test (lost 0.4 hours of overland data)
2000/322	Changed to IDLE Mode for Leonid Meteor Shower (lost 2.0 hours of data)
2000/329	Spacecraft Safehold, ALT was automatically turned OFF due to bad ephemeris load.
2000/330	Commanded Alt back to Track. Total off time was 27.1 hours.
2000/349	Cal-Sweep Test (lost 0.4 hours of overland data)

The listing of key events includes Cal Sweeps. In response to the altimeter's PTR change during Side A, a Cal Sweep software patch was developed, and was uploaded on day 250 of 1998. The purpose of this patch is to monitor the shape of the altimeter's CAL-1 waveform, looking for changes over time. Cal Sweeps are now regularly performed every 30 days, beginning with Side A on day 251 of 1998 and continuing through Side B operations. The results of the Side B Cal Sweeps are discussed in Section 3.3.

2.4 Side B Abnormalities

2.4.1 Land-to-Water Acquisition Times

In the summer of 1999, it was brought to our attention by colleague Joel Dorandeu of Collecte Localisation Satellites (CLS) that a few of the Side B land-to-water acquisition times were anomalously slow. Our subsequent analysis at that time indicated that these occasional slow land-to-water acquisitions had occurred since the time of Side B turn-on.

Although these abnormal acquisitions resulted in a loss of only about 0.02% of ocean-tracking data, we wished to understand and rectify the anomalies. The parameter file C3502840 (which had been in use since February 1995) was modified in 1999 to increase the AGC Minimum (bytes 67-70) from a value of 13 dB to a value of 15 dB, and the new parameter file was named AGCMIN15. Uploading of this file had no observed positive, or negative, effect on the occasional acquisition delays.

Subsequent to a spacecraft-level Safehold on day 243 of 1999, the acquisition anomaly was no longer in evidence. Plots depicting pre- and post-Safehold acquisitions are shown in Section 2 of the *TOPEX Radar Altimeter Engineering Assessment Report, Update: Side B Turn-On to January 1, 2000*, September 2000.

Throughout the year 2000, we monitored the land-to-water acquisitions, and the anomaly has not recurred. We continue to monitor the acquisition times, and we continue to use the AGCMIN15 parameter file as our standard.

2.4.2 Attitude Anomaly

There was a brief anomalous attitude variation in TOPEX 2000 day 352 data, during cycle 304, pass 082. The attitude exhibited an excursion to about 0.21 degrees, approximately twice the normal off-nadir angle for over-ocean attitude estimates. The attitude behavior was similar to significantly-shorter-duration “Gyro spikes” observed a couple of other times over the past two years. This attitude excursion had a duration about 2000 seconds, and the attitude change vs. time was roughly linear. After the system recovered, we saw the resumption of the normal attitude variation, between approximately 0.0 and 0.1 degrees.

The attitude anomaly began at a J2000 time of approximately 30349500 seconds; the waveform-estimated attitude at that time was very low, about 0.02 degrees. Then the attitude increased in a relatively straight-line manner, to a value of about 0.21 degrees at time 30351600. At that time, the attitude values became unavailable due to TOPEX being over land or ice near its extreme southern latitude. Valid attitude estimates became available again at approximately 30352050 seconds, and the attitude then decreased rapidly as the spacecraft pointing system recovered from the apparent gyro spike. The recovery was complete within another 500 seconds, and the attitude behavior thereafter appeared normal.

The range noise, the AGC, and the SWH values appeared reasonable throughout this attitude anomaly. There should be no consequence to the TOPEX data users, because the TOPEX data corrections are valid for attitudes out to 0.4 degrees.

Section 3

Assessment of Instrument Performance (Cycles 236 through 305)

3.1 Range

The following range discussion is restricted to TOPEX Side B, from its start on 1999 day 040 through the end of year 2000. Earlier years' assessment updates have supplied cumulative results for Side A from launch to the end of the assessment update period, and the assessment update published in August 1999 provides the entire set of TOPEX Side A results from launch through Side A turnoff on 10 February 1999.

This report section discusses the Side B CAL-1 Step-5 Ku- and C-band delta ranges. The Calibration Mode was briefly reviewed in Section 2.1. The Ku- and C-band delta ranges have been processed to form a set of delta combined range values, where "combined" refers to the weighted sum of Ku- and C-band delta ranges which compensates for the ionospheric electron path delay. There are about twenty combined delta ranges for each TOPEX cycle, corresponding to two calibrations per day during the 10-day cycle. Early in Side A operation we developed a CAL-1 processing scheme to remove the effects of a 7.3 mm range quantization in the TOPEX internal calibration mode. The Side B is almost identical to Side A, the same calibration mode quantization is present in the CAL-1 delta range data, and we have used the same processing method to remove these quantization effects.

In previous years we had found that the Side A delta ranges had a temperature dependence. There are about two dozen different temperatures monitored within the TOPEX altimeter, and it is not possible to determine which of these is the most important to range bias. For our Side A analysis we had used the temperature of the upconverter / frequency multiplier unit (the UCFM), designating this temperature as Tu. The Ku-band delta range and the combined delta range varied somewhat with Tu, and we had found a simple quadratic correction of the combined delta range for Tu variation. Our previous years' assessment updates had tables of the range bias results with and without the correction for Tu, and we recommended that the TOPEX GDR data end user (who does not have easy access to the temperature data) should use the Side A combined delta range results that were NOT corrected for temperature Tu.

For Side B the behavior of delta range with temperature is somewhat different. We found that the Ku-band range shows practically no temperature effect but that the C-band result does exhibit a temperature dependence. We found that the C-band variation was more highly correlated with the receiver AGC temperature (designated Tagc here) than with Tu. Figure 3-1 on page 3-2 shows the full set of Side B Tagc values during the calibrations through the end of year 2000. Figure 3-2 on page 3-3 and Figure 3-3 on page 3-3 compare the Side B Ku-band CAL-1 Step 5 delta range values for the same time span, before and after fitting a thermal correction which is quadratic in Tagc, and it can be seen that the Tagc correction term has very little effect on the results. Figure 3-4 on page 3-4 and Figure 3-5 on page 3-4 compare the corresponding

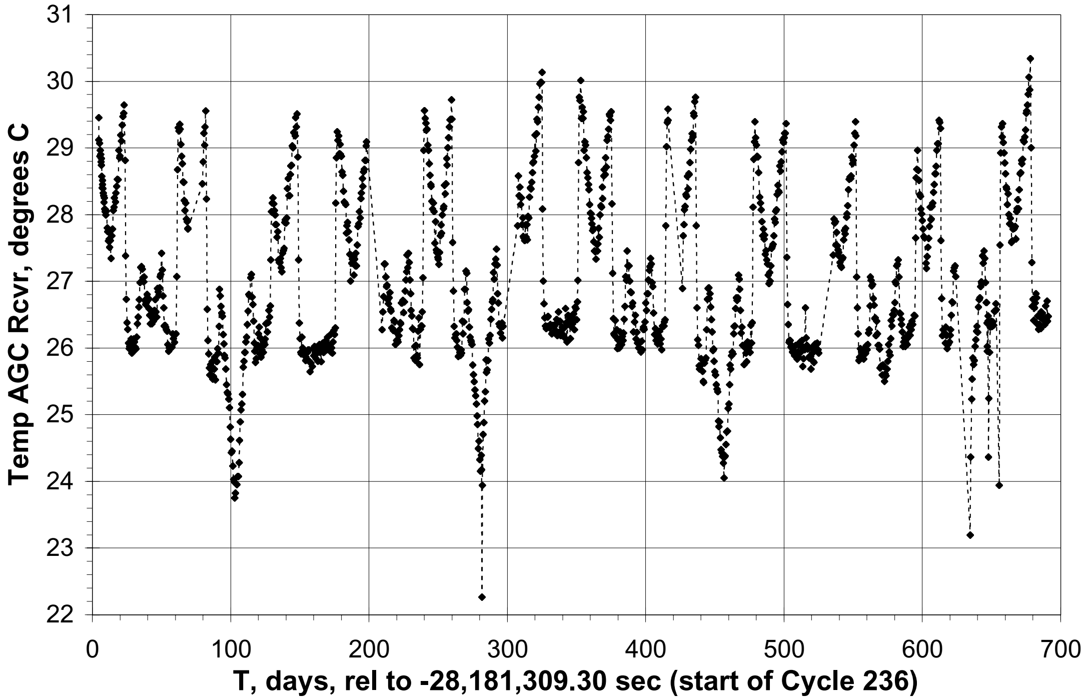

Figure 3-1 AGC Receiver Temperature vs. Time
Data for Side B Cycles 236-305

Side B C-band delta range values through the end of year 2000, before and after Tagc correction, and it can be seen that the Tagc correction term does eliminate some of the variations of the individual data relative to the general trend. Finally, Figure 3-6 on page 3-5 and Figure 3-7 on page 3-5 compare the Side B combined delta range results with and without Tagc corrections and, similar to the Ku-band figures, the Tagc corrections have little discernible effect.

As for Side A, the general trend of delta ranges is slow enough that corrections can and should be made based on cycle averages of the CAL-based delta ranges. Figure 3-8 on page 3-6 and Figure 3-9 on page 3-6 show the Side B Ku- and C-band cycle averages of the delta height. Figure 3-10 on page 3-7 shows the set of cycle averages of the combined height delta ranges with NO temperature correction applied, and these Figure 3-10 values are printed in Table 3-1 on page 3-7. These values are also available at our TOPEX web site

http://topex.wff.nasa.gov/docs/RangeStabUpdate.html,

and that web site is updated every month or so. The web site table also has the delta ranges which are temperature corrected for Tu using the correction developed for Side A. It was a mistake to calculate the Side A correction for the Side B data on the web site, and the Tu correction should be ignored. The simple rule for Side B is to use the delta range that has NO temperature correction.

To correct the GDR range data for the range calibration drift, one would use

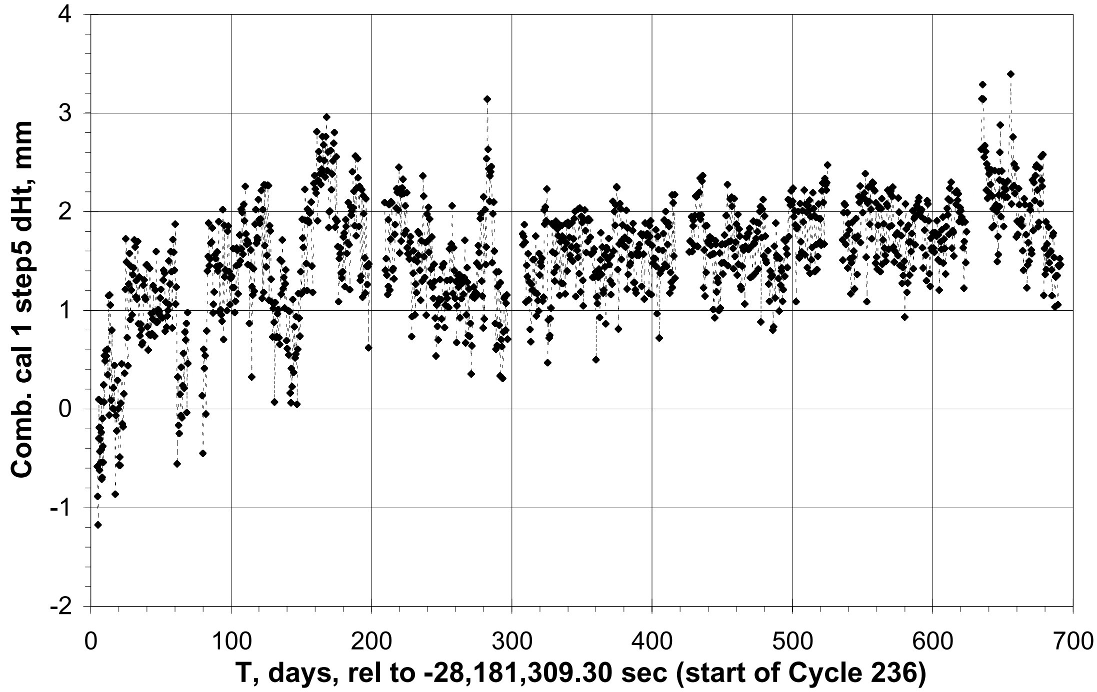

Figure 3-2 Ku-Band CAL-1 Step 5 Delta Height vs. Time for Side B Data, Cycles 236-305, not Temperature-Corrected

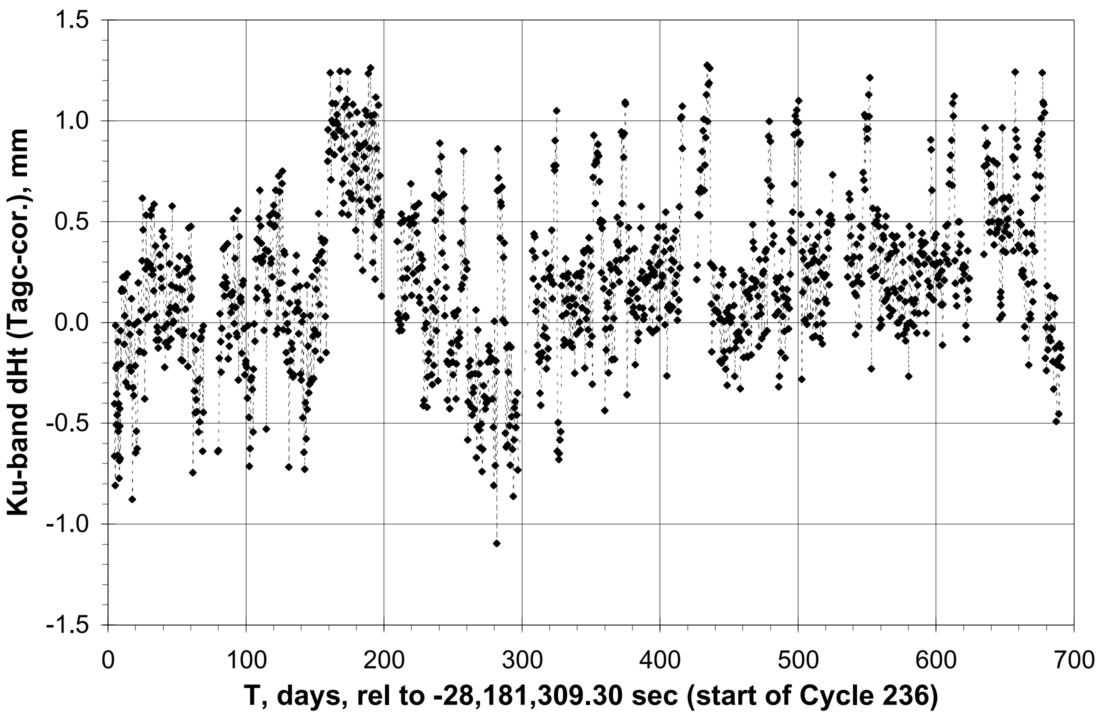

Figure 3-3 Ku-Band CAL-1 Step 5 Delta Height vs. Time for Side B Data, Cycles 236-305, Corrected for AGC Temperature

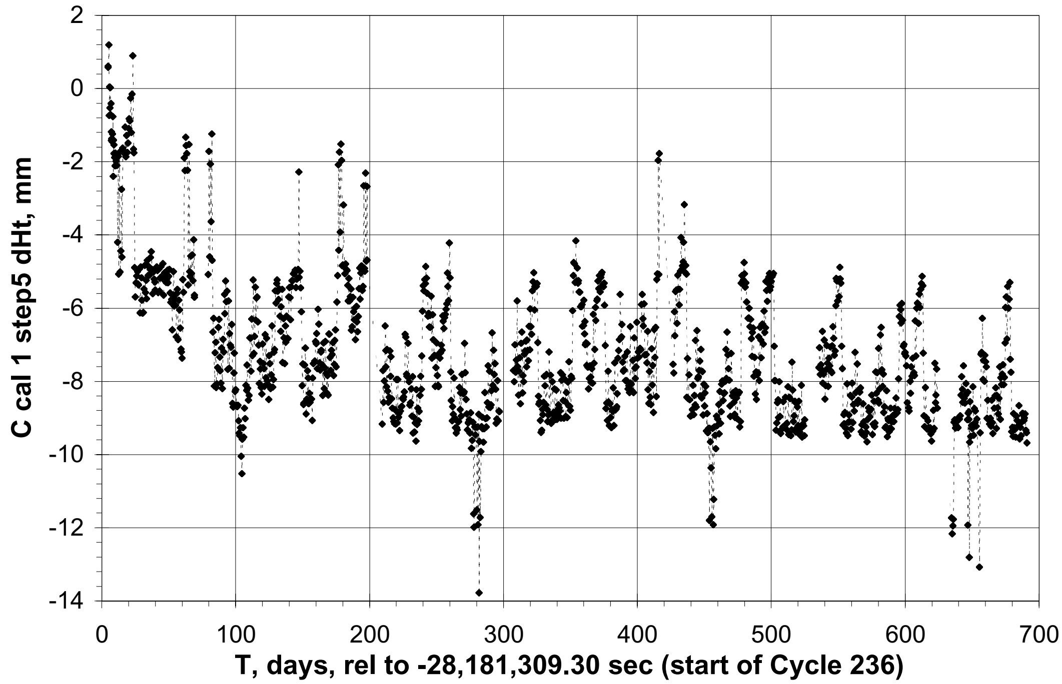

Figure 3-4 C-Band CAL-1 Step 5 Delta Height vs. Time for Side B Data, Cycles 236-305, Not Temperature-Corrected

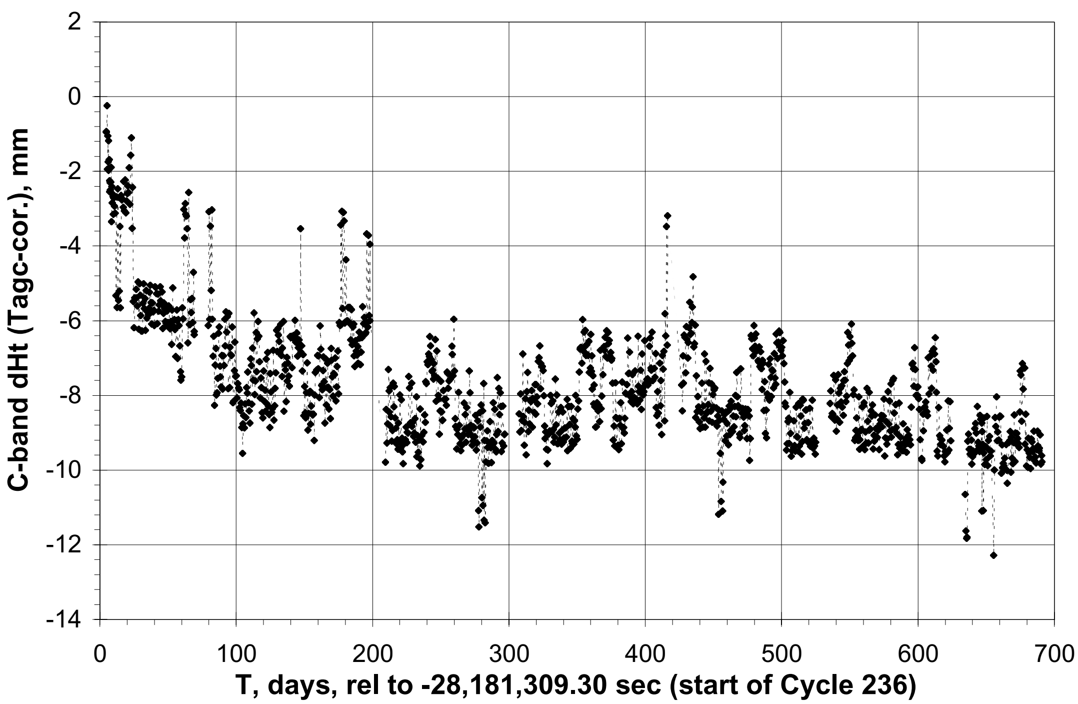

Figure 3-5 C-Band CAL-1 Step 5 Delta Height vs. Time for Side B Data, Cycles 236-305, Corrected for AGC Temperature

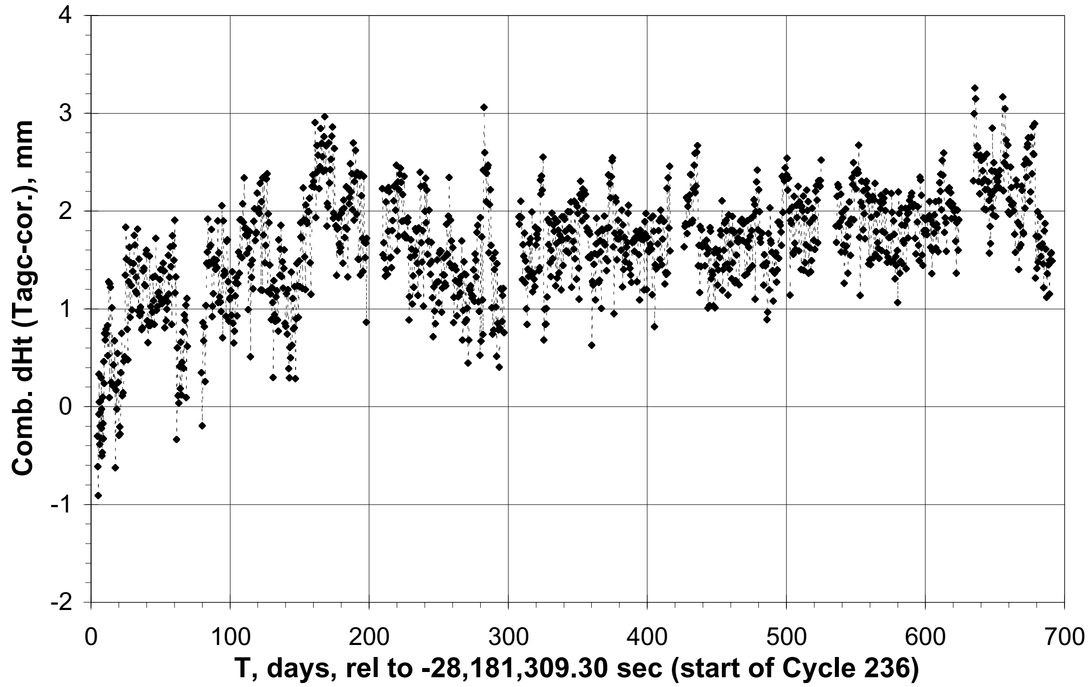

Figure 3-6 Ku & C Combined CAL-1 Step 5 Delta Height vs. Time Side B Data, Cycles 236-305, Not Corrected for AGC Temperature

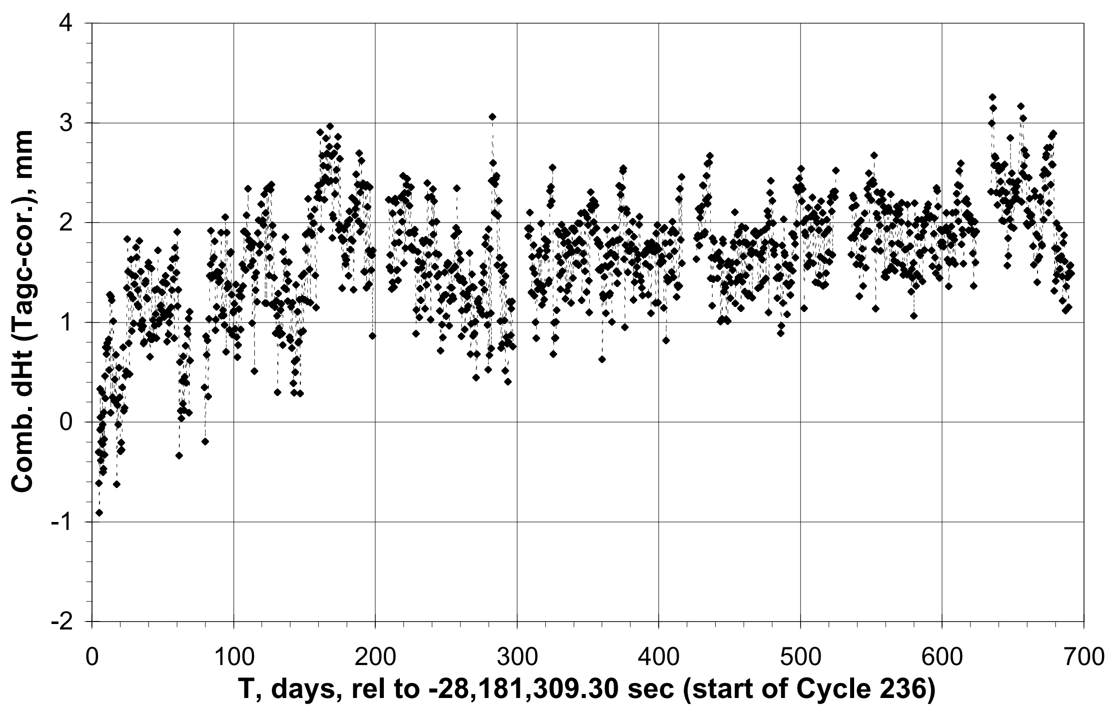

Figure 3-7 Ku & C Combined CAL-1 Step 5 Delta Height vs. Time Side B Data, Cycles 236-305, Corrected for AGC Temperature

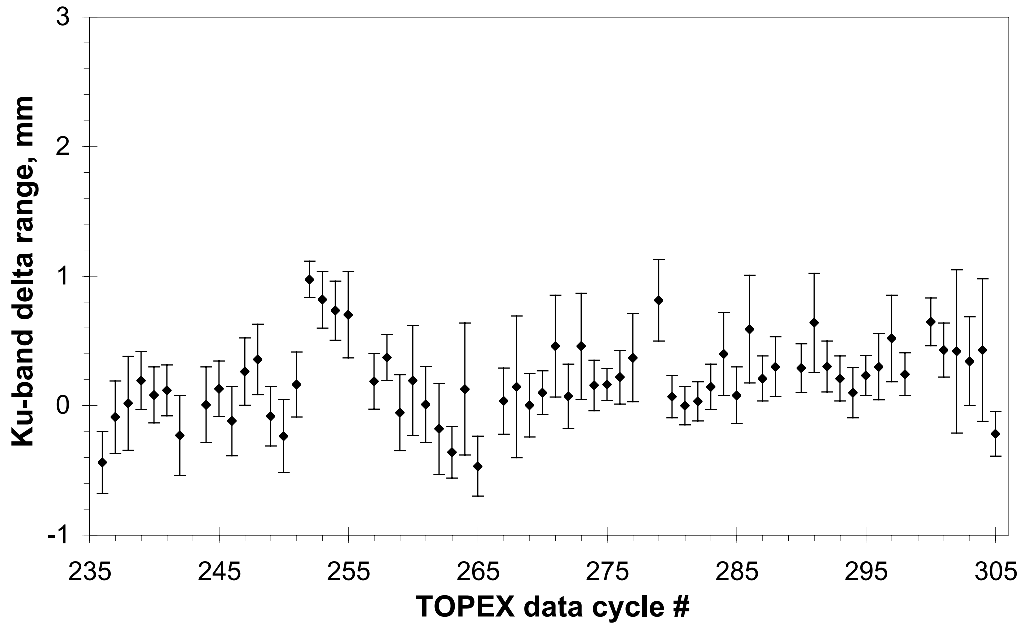

Figure 3-8 Side B Ku-Band Delta Range Cycle Averages, Not Corrected for Temperature

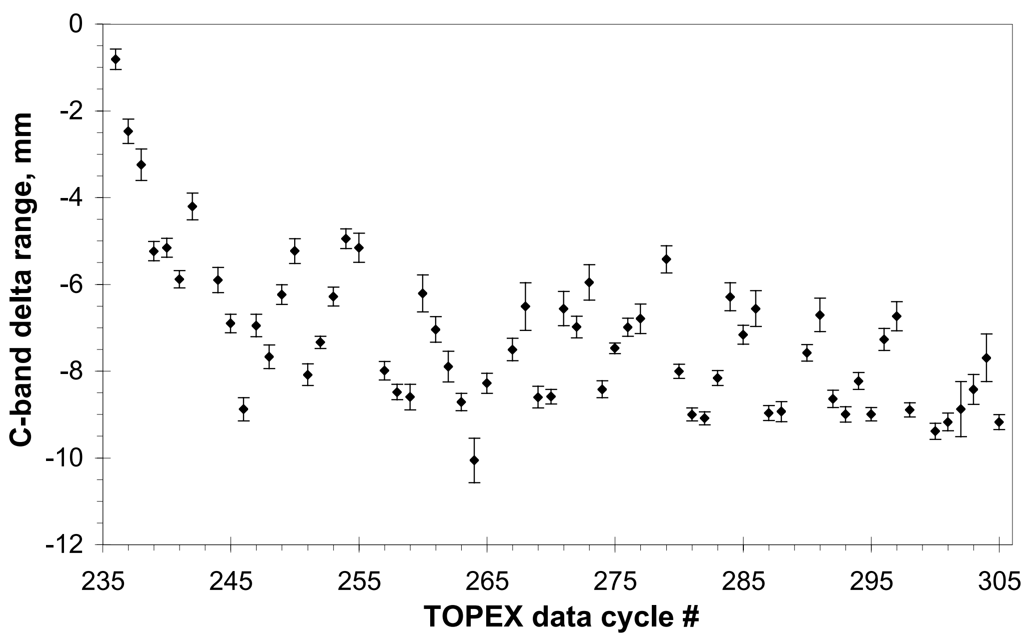

Figure 3-9 Side B C-Band Delta Range Cycle Averages, not Corrected for Temperature

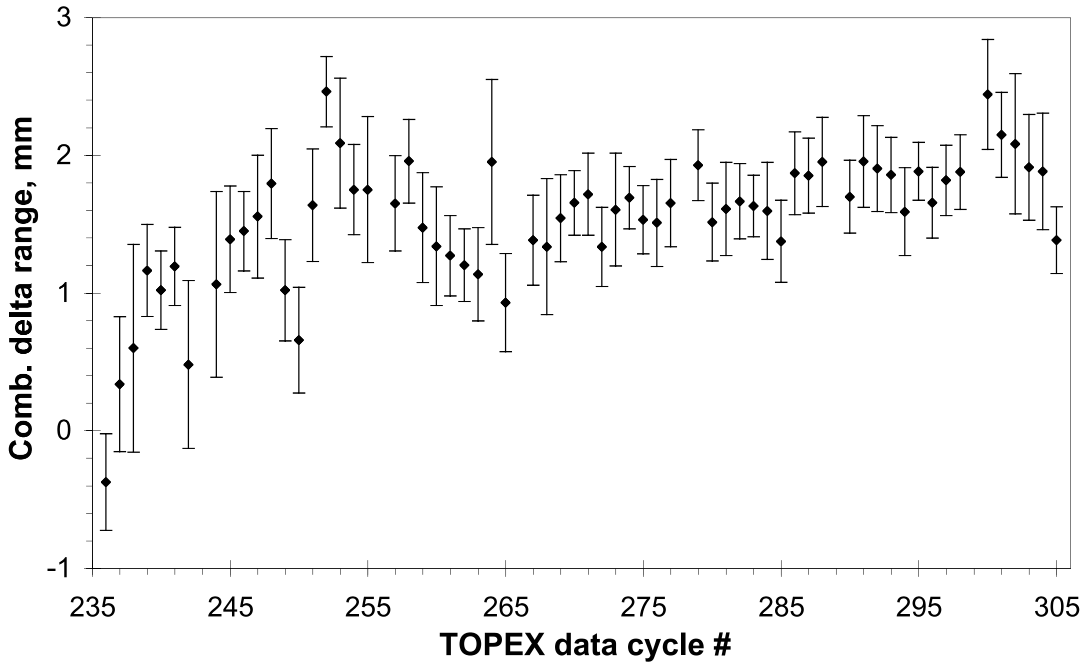

Figure 3-10 Side B Combined (Ku & C) Delta Range Cycle Averages, not Corrected for Temperature

Corrected Range = GDR range - dR_av_N, where dR_av_N is the cycle-average delta combined range value of Table 3-1 (as plotted in Figure 3-10). Note that the delta ranges are all given relative to a constant but arbitrary range offset, so this correction will provide only a relative range drift correction. The corresponding expression for correcting the GDR sea surface height (SSH) is

Corrected SSH= GDR SSH + dR_av_N.

Table 3-1 TOPEX Range Bias Change, From CAL-1 Step 5, No Temperature Correction

Cycle	Count	Cycle Average dRange (comb), mm	Cycle Standard Deviation dRange (comb), mm
236	21	-0.37	+0.35
237	21	+0.34	+0.49
238	20	+0.60	+0.75
239	19	+1.16	+0.33
240	20	+1.02	+0.28
241	20	+1.19	+0.28

Table 3-1 TOPEX Range Bias Change, From CAL-1 Step 5, No Temperature Correction (Continued)

Cycle	Count	Cycle Average dRange (comb), mm	Cycle Standard Deviation dRange (comb), mm
242	21	+0.48	+0.61
244	20	+1.06	+0.67
245	19	+1.39	+0.39
246	20	+1.45	+0.29
247	20	+1.55	+0.45
248	20	+1.79	+0.40
249	20	+1.02	+0.37
250	20	+0.66	+0.38
251	19	+1.64	+0.41
252	19	+2.46	+0.26
253	20	+2.09	+0.47
254	22	+1.75	+0.33
255	21	+1.75	+0.53
257	18	+1.65	+0.35
258	20	+1.96	+0.30
259	20	+1.47	+0.40
260	20	+1.34	+0.43
261	20	+1.27	+0.29
262	20	+1.20	+0.26
263	19	+1.13	+0.34
264	21	+1.95	+0.60
265	20	+0.93	+0.36
267	20	+1.38	+0.33
268	20	+1.33	+0.49
269	19	+1.54	+0.32
270	20	+1.65	+0.23
271	20	+1.72	+0.30
272	21	+1.33	+0.29
273	20	+1.60	+0.41

Table 3-1   TOPEX Range Bias Change, From CAL-1 Step 5, No Temperature Correction (Continued)

Cycle	Count	Cycle Average dRange (comb), mm	Cycle Standard Deviation dRange (comb), mm
274	20	+1.69	+0.23
275	18	+1.53	+0.25
276	19	+1.51	+0.32
277	21	+1.65	+0.32
279	20	+1.93	+0.26
280	19	+1.51	+0.28
281	19	+1.61	+0.34
282	20	+1.66	+0.27
283	19	+1.63	+0.22
284	19	+1.60	+0.35
285	20	+1.37	+0.30
286	20	+1.87	+0.30
287	18	+1.85	+0.27
288	20	+1.95	+0.32
290	20	+1.70	+0.26
291	20	+1.95	+0.33
292	20	+1.90	+0.31
293	18	+1.86	+0.27
294	20	+1.59	+0.32
295	19	+1.88	+0.21
296	19	+1.65	+0.26
297	20	+1.82	+0.25
298	18	+1.88	+0.27
300	20	+2.44	+0.40
301	23	+2.15	+0.31
302	19	+2.08	+0.51
303	19	+1.91	+0.38
304	19	+1.88	+0.42
305	19	+1.38	+0.24

3.2 AGC/Sigma0

The ocean surface's radar backscattering cross section, one of the quantities estimated by the TOPEX radar altimeter, is designated by σ^0 which for typographical convenience is often referred to as sigma0 or sigma-naught; in this report section we use sigma0. Most altimeters will eventually drift in their power estimation, hence in their sigma0 estimation. To correct for such drift, the TOPEX ground data processing includes a lookup table of sigma0 corrections. We will refer to that table as the "Cal Table" (the relevant TOPEX ground data processing system filename is SPA_ALT_CALPAR.TXT). In this section we describe the sigma0 trends from start of Side B (cycle 236) through cycle 305, the last cycle in year 2000.Our sigma0 trend analyses use the sigma0 **before** the Cal Table corrections have been applied, and we refer to this as sigma0_uncorr.

3.2.1 Processing of Calibration Mode Results and Global Sigma0 Averages

As part of our continuing TOPEX support, we do daily quick-look processing of all TOPEX altimeter data for performance monitoring, providing performance summaries for the engineering and science data. The daily processing results are used to update a launch-to-date engineering database. Also, data are processed from the twice-daily execution of the altimeter's internal calibration mode (with submodes CAL-1 and CAL-2) and these results are used to update a WFF launch-to-date calibration database. We also process the intermediate geophysical data record (IGDR) data as they become available for network access, normally several days after the altimeter acquires the data. The IGDR data are processed for altimeter performance, and 1-minute summary records are produced and are added to a WFF launch-to-date GDR database. When the final GDR data become available, they replace the IGDR data already in our database. There is no difference however between sigma0 data on the IGDR and the GDR, because no further sigma0 corrections are made in going from the IGDR to the GDR.

We have been very concerned about possible contamination of the data by what we have called "sigma0 blooms", regions of over-ocean altimeter data characterized by unusually high apparent sigma0 values accompanied by unusual altimeter waveform shapes. Generally the Ku-and the C-band sigma0 show the same behavior in a bloom region. Such blooms in the TOPEX data can persist for several tens of seconds, and the waveforms in a bloom region generally have too rapid a plateau decay. Many of these waveforms are too sharply peaked ("specular"), indicating a breakdown in the general incoherent scattering theory used to characterize the rough surface scattering. The sigma0 blooms exist in perhaps 5% of all TOPEX over-ocean data (there is additional sigma0 bloom information at http://topex.wff.nasa.gov/blooms/blooms.html). For input to our GDR database 1-minute averages, we require all the available altimeter flags to show normal tracking and the land/water flag to show deep water. When the data are extracted from this database for the sigma0 calibration, all records are rejected having Ku-band sigma0 estimates of 16 dB or greater or having waveform-estimated attitude angles of 0.12 degrees or greater. These editing criteria delete most of the sigma0 blooms.

Because our analysis is based on sigma0_uncorr, we need to know what Cal Table values have been already applied to the GDR (or IGDR) data in order to "undo" these corrections.

3.2.2 History of Cal Table Values Used in GDR Production

There were eighteen Cal Table adjustments during the TOPEX Side A operation. For Side B operation there have been five Cal Table adjustments after the initial Side B Cal Table was set. There exists no single summary of exactly when each of the Cal Table changes was implemented in the TOPEX Side B ground processing so we will provide that summary here. The Side A Cal Table history has been described year by year in earlier Engineering Assessment Updates, and the entire Side A history is summarized at http://topex.wff.nasa.gov/docs/Sigma0Cal_A_All.pdf.

Each time that the Cal Table contents are changed in the TOPEX ground data processing at JPL, there are at least these three items created within the Mission Operations System (MOS):

1) the MOS Change Request Form (the MCR) bears an origination date, describes the change to be made and the desired operational date for the change, and also has the date when the MCR was approved (by a change control board at JPL);
2) the Parameter File is the text file to be actually used in the data processing and contains the Cal Table values for each cycle; and
3) the File Release Form contains the Parameter File creation date, the release approval date, and the date at which file execution is to begin.

The MCR Form is typically accompanied by other supporting information from WFF describing why the change is being requested. In Table 3-2 "TOPEX Side B Sigma0 Calibration MCR Information Summary" on page 3-12, we have summarized information from copies of the sigma0-related MCRs and File Release Forms relevant to the re-released GDRs and the MGDR-Bs. Columns 1 to 3 of Table 3-2 are transcribed from the MCR Forms, columns 4 and 5 from the File Release Forms, column 6 contains a brief indication of what change the MCR made and why, and column 7 of Table 3-2 indicates which of the TOPEX Side B GDRs were governed by each MCR.

3.2.3 Brief Review of Side A Behavior and Initial Approach to Corrections in Side B

In TOPEX Side A there were indications that the time trend of the CAL-1 AGC differed from the time trend of the over-ocean cycle-averaged sigma0 in both the Ku- and the C-band systems. We were forced to use the time trend of the over-ocean sigma0 cycle-averages to produce the sigma0 Cal Table entries. We tried to make these corrections only for relatively long times, avoiding responding to cycle-to-cycle noise. Correcting a noisy process by making trend estimates projections is a frustrating activity at best, and the Side A Cal Table has several places where we failed to detect trend changes or to correct our trend projections soon enough. After TOPEX was switched to its Side B in early February 1999 we described the entire Side A Cal Table history in “TOPEX Sigma0 Calibration Table History for All Side A Data”, G. S.

Table 3-2 TOPEX Side B Sigma0 Calibration MCR Information Summary

From MCR Form			From File Release Form		Additional Information	
(1) MCR #	**(2) MCR Origination Date**	**(3) Comments on MCR Form**	**(4) File Creation Date**	**(5) Release Approval Date**	**(6) Comments on MCR Actions and Reasons**	**(7) Cycles Distributed Under This MCR**
690	1999/05/26, 1999-146	After indicated parameter & constant changes, produce IGDrs and GDRs from all Alt-B data to date	1999/05/25, 1999-145	1999/05/28	After initial Cal/Val activity, set constant Ku and C biases with values chosen to make smooth connection to Side A results	236 - 247
692	1999/06/16, 1999-167	see attached request memo from Callahan asking that cycle 248 be reprocessed	1999/06/17, 1999-168	6/17/99	C-band has a trend estimated from first 12 cycles (1st C-band change is at cycle 242), Ku-band has zero trend.	248-258
701	2000/01/10, 2000-010	Begin use for cycle 259.	2000/01/13, 2000-013	1/13/00	Put in linear trend for Ku, and changed linear trend for C. Still assuming single linear trends from cycle 236 for Ku and for C.	259-276
703	2000/04/03, 2000-094	Begin use for cycle 279	2000/04/04, 2000-095	4/4/00	Hold fixed correction at cycle 276 for Ku-band and 279 for C-band; the assumed single linear trends from cycle 236 are getting away from actual data.	278 - 284; but these were reprocessed & re released under MCR 708

Table 3-2 TOPEX Side B Sigma0 Calibration MCR Information Summary (Continued)

From MCR Form			From File Release Form		Additional Information	
(1) MCR #	(2) MCR Origination Date	(3) Comments on MCR Form	(4) File Creation Date	(5) Release Approval Date	(6) Comments on MCR Actions and Reasons	(7) Cycles Distributed Under This MCR
708	2000/07/18, 2000-200	Begin use for cycle 288 (SSALT); repro-cess 277-287	2000/07/ 19, 2000-201	7/19/00	Replace single linear trends by pair of trends with discontinuity at the cycle 256 safe hold.	277 - 299
720	2000/12/06, 2000-341	Begin use for cycle 303; repro-cess cycles 300-302	2000/12/ 07, 2000-342	12/7/00	Make a trend tweak by adjust-ing the second part of the trends (i.e., after cycle 256)	300-

Hayne and D. W. Hancock III, 27 July 1999, available at http://topex.wff.nasa.gov/docs/Sigma0Cal_A_All.pdf. In that paper we produced our best guess at what values the Cal Table should have included, based on a quadratic trend fit to the entire Side A set of over-ocean cycle-averages of sigma0.

When Side B was turned on, we continued to do as we had done for Side A. The initial Side B Cal Table entries were chosen in a committee process, involving Phil Callahan and others, so that there was no obvious discontinuity in over-ocean sigma0 from Side A to Side B. These initial Cal Table values were held constant about a dozen cycles until trends became apparent.

The Side B C-band Cal Table values were changed beginning with cycle 248 to correct for an apparent downward trend in the C-band over-ocean sigma0. No corrections were made to the Side B Ku-band Cal Table until cycle 259 when it became clear that there was an upward trend in the Ku-band over-ocean sigma0. Both the Ku- and the C-band Cal Table values were produced by assuming a linear trend in the over-ocean sigma0. The Ku-band system was particularly surprising in showing an increase in over-ocean sigma0 estimates before correction. Eventually it became clear that the linear trends in the Cal Table were overcorrecting the data, and the Cal Table values were held constant until the data trends caught up with the correction; this Cal Table freeze was made at cycle 274 for Ku-band and at cycle 278 for C-band. At the end of cycle 287 we had reassessed the trends, and a new set of Cal Table values was produced and the GDRs for cycles 277 - 284 were reprocessed and re-released. GDRs for cycles 285 onward were released only with the new Cal Table values. One additional trend adjustment was made at cycle 300.

Table 3-3 "TOPEX Side B Cal Table Entries for Distributed GDRs" on page 3-17 summarizes the Side B Cal Table values used for the distributed GDRs. Table 3-3 applies to the re-released cycles 277 - 284, not the originally released data for those cycles. Column 1 of Table 3-3 is the data cycle number, column 2 indicates the applicable MCR, and columns 3 and 4 give the Ku- and C-band Cal Table values which were used in producing the TOPEX GDR data product.

3.2.4 Current Approach to Side B Corrections, Based on CAL-1

Figure 3-11 "Ku-Band Side B Cycle Average CAL-1 and CAL-2 Delta AGC and Sigma0 (Cal Table Corrections Removed)" summarizes the Side B Ku-band altimeter's CAL-1, CAL-2, transmit power monitor, and over-ocean sigma0 cycle averages for cycles 236 - 284, and Figure 3-12 "C-Band Side B Cycle Average CAL-1 and CAL-2 Delta AGC and Sigma0 (Cal Table Corrections Removed" on page 3-15 presents the corresponding information for the C-band altimeter. A small seasonal correction, derived from the entire set of Side A sigma0 data, has been applied to the over-ocean sigma0 averages. Notice that the Cal Table corrections have been removed from the over-ocean sigma0 in these figures, because our purpose is to see the trends in absence of Cal Table corrections. In Figure 3-11 and Figure 3-12 the CAL-11 delta AGC trend is in quite good agreement with the over-ocean sigma0 trend, suggesting that the CAL-1 AGC change would provide an adequate basis for the Side B Cal Table (unlike the Side A altimeter for which the CAL-1 trend differed from the over-ocean sigma0 trend).

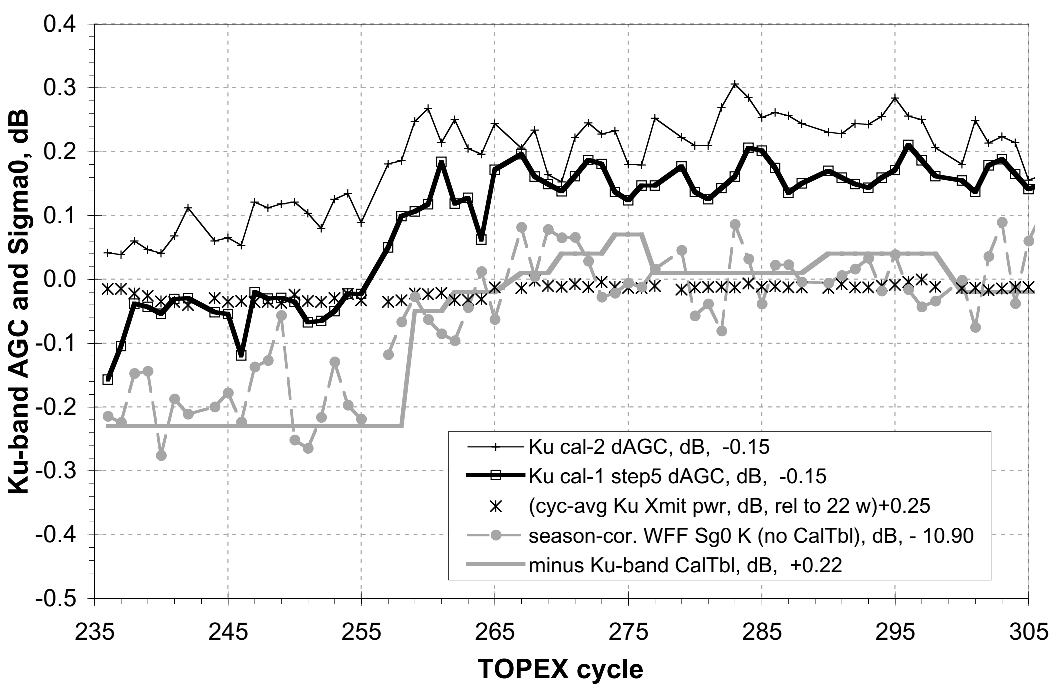

Figure 3-11 Ku-Band Side B Cycle Average CAL-1 and CAL-2 Delta AGC and Sigma0 (Cal Table Corrections Removed)

Another effect visible in Figure 3-11 is an apparent step-change in both the Ku-band CAL-1 AGC and the Ku-band over-ocean sigma0. This step occurred at cycle 256, a SSALT cycle, during which a satellite safe hold occurred resulting in the TOPEX

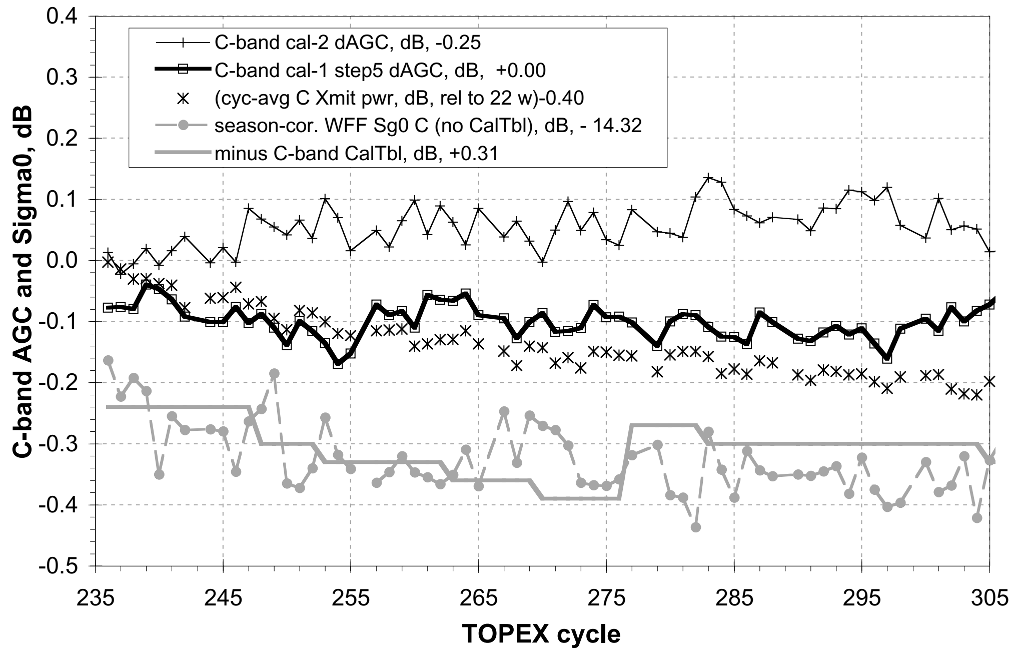

Figure 3-12 C-Band Side B Cycle Average CAL-1 and CAL-2 Delta AGC and Sigma0 (Cal Table Corrections Removed

altimeter’s being powered off during most of cycle 256 (cycle 256 started on 1999 day 238, 26 August). During a normal SSALT cycle the TOPEX altimeter is still powered but is in its standby mode. We don’t know why but the TOPEX altimeter apparently behaved differently before and after this cycle 256 event. There is a visible step-change seen in Figure 3-11, and there was also a change in the Ku-band altimeter’s track acquisition behavior in land-to-water transitions. Before cycle 256 there were occasional cases of the Ku-band altimeter’s requiring several tens of seconds for acquisition, but after the cycle 256 safe hold the Ku-band land-to-water track transitions no longer showed the occasional anomalous long acquisition times. For whatever unknown reason, the Side B altimeter behaves differently after the cycle 256 safe hold. The C-band altimeter Figure 3-12 shows less magnitude of effect than the Ku-band Figure 3-11, but there does appear to be a small C-band step change at cycle 256 in Figure 3-12.

Another TOPEX satellite safe hold occurred on day 329, 23 November, of year 2000. The TOPEX altimeter was off from about 04:45 to 23:19 of 2000d329 and, following commanding and software reloading, was put back into track mode at 07:50 on 2000d330. The altimeter temperatures dropped during the safe hold, but normal operating conditions had been reached by the end of 2000d331. Unlike the cycle 256 safe hold, there were no apparent changes in the TOPEX AGC and sigma0 associated with the 2000d329 safe hold.

One additional feature shown in Figure 3-11 and Figure 3-12 is that both the Ku- and C-band sigma0 and CAL-1 AGC have been quite stable for the last year, with effectively zero slope to their time trends.

3.2.5 CAL-1 Fitted Trends for Estimation of Cal Table Values

Based on Figure 3-11 and Figure 3-12, we decided to use the CAL-1 data as the basis for the Side B sigma0 Cal Table. A year or so ago we decided to fit straight line segments to the Side B CAL-1 data, with different slope and intercept values before and after cycle 256 to allow for a possible step change in altimeter characteristics. More recently we decided to fit the CAL-1 data after cycle 256 by **two** straight line segments, requiring the fit to have continuous values but allowing a discontinuity in the slope. The cycle at which the slope changed was one of the variable fit parameters. So our fits consist of three straight-line segments with the latter two connected to each other. Figure 3-13 on page 3-16 shows the Ku-band Side B CAL-1 AGC and the fitted line segments, and Figure 3-14 on page 3-17 shows the same thing for C-band. The error bars shown in Figure 3-13 and Figure 3-14 are the estimated individual standard deviations of the 20 calibration mode results from which the cycle averages are formed, but in the least squares fit for the straight line segments the cycle means were equally weighted.

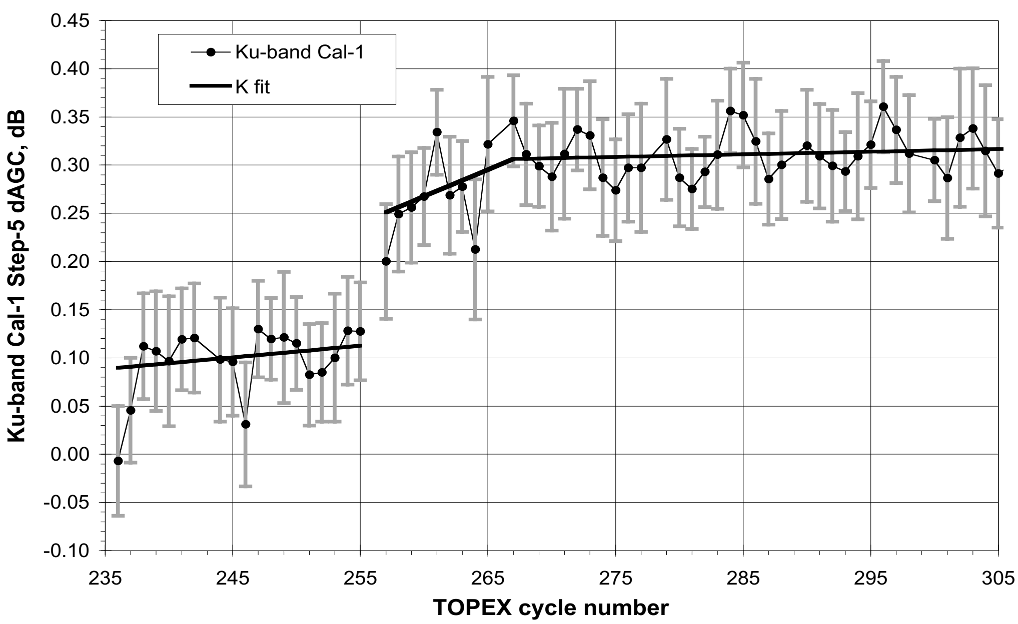

Figure 3-13 TOPEX Side B Ku-Band Cal-1 Step-5 Delta AGC vs. Cycle, Fitted by 3 Straight-Line Segments

The (negatives of) Figure 3-13 and Figure 3-14 data provide a relative correction, and it was arbitrarily decided to set the CAL-1-based corrections to zero at cycle 240; that is, we assumed that +0.45 dB was the correct Ku-band Cal Table value and that +0.55 dB was the correct C-band Cal Table value at cycle 240. This allows us to calculate the values given in columns 5 and 6 of Table 3-3. These are our best current guess at the values which should have been in the Cal Table, and if one were to recalculate GDRs one should use the column 4 and 5 numbers as replacements for the values in columns 3 and 4 which were used in the original GDR production.

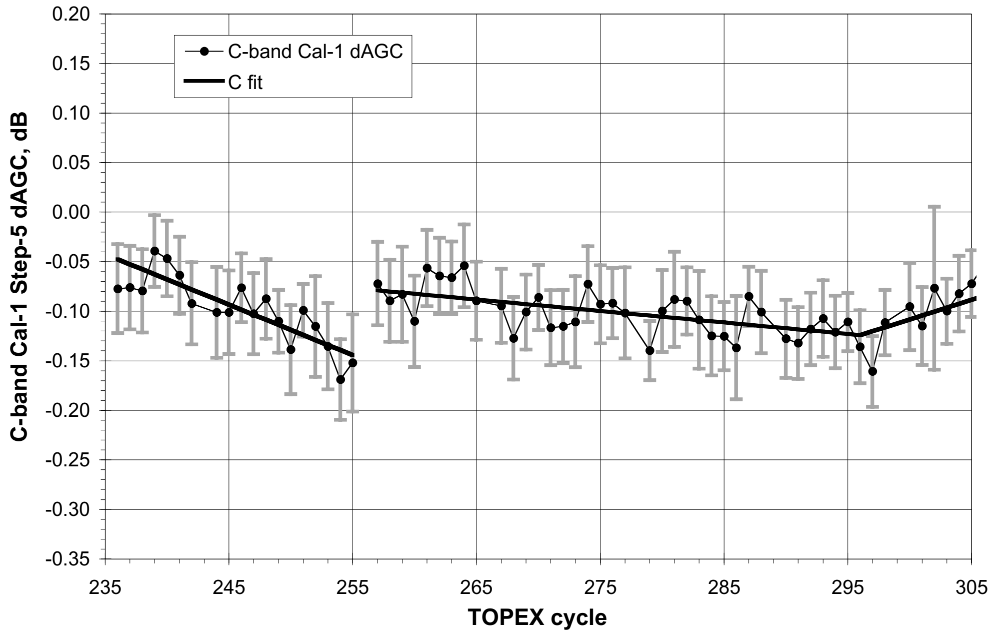

Figure 3-14 TOPEX Side B C-Band Cal-1 Step-5 Delta AGC vs. Cycle, Fitted by 3 Straight-Line Segments

Table 3-3 TOPEX Side B Cal Table Entries for Distributed GDRs

		Cal Table Values Used in Already-Distributed Data		Best Fit Cal Table Values from 3-Segment Fit to CAL-1		Adjustment for Already-Distributed Data	
(1) TOPEX Cycle	(2) Applicable MCR #	(3) Ku-Band Cal Table, dB	(4) C-Band Cal Table, dB	(5) Best Fit Ku-Band Cal Table, dB	(6) Best Fit C-Band Cal Table, dB	(7) Ku-Band Adjust, dB	(8) C-Band Adjust, dB
236	690	+0.45	+0.55	+0.455	+0.530	+0.005	-0.020
237	690	+0.45	+0.55	+0.454	+0.535	+0.004	-0.015
238	690	+0.45	+0.55	+0.452	+0.540	+0.002	-0.010
239	690	+0.45	+0.55	+0.451	+0.545	+0.001	-0.005
240	690	+0.45	+0.55	+0.450	+0.550	+0.000	+0.000
241	690	+0.45	+0.55	+0.449	+0.555	-0.001	+0.005
242	690	+0.45	+0.55	+0.448	+0.560	-0.002	+0.010
244	690	+0.45	+0.55	+0.445	+0.570	-0.005	+0.020
245	690	+0.45	+0.55	+0.444	+0.575	-0.006	+0.025
246	690	+0.45	+0.55	+0.443	+0.581	-0.007	+0.031
247	690	+0.45	+0.55	+0.442	+0.586	-0.008	+0.036
248	692	+0.45	+0.61	+0.440	+0.591	-0.010	-0.019

Table 3-3 TOPEX Side B Cal Table Entries for Distributed GDRs (Continued)

		Cal Table Values Used in Already-Distributed Data		Best Fit Cal Table Values from 3-Segment Fit to CAL-1		Adjustment for Already-Distributed Data	
(1) TOPEX Cycle	(2) Applicable MCR #	(3) Ku-Band Cal Table, dB	(4) C-Band Cal Table, dB	(5) Best Fit Ku-Band Cal Table, dB	(6) Best Fit C-Band Cal Table, dB	(7) Ku-Band Adjust, dB	(8) C-Band Adjust, dB
249	692	+0.45	+0.61	+0.439	+0.596	-0.011	-0.014
250	692	+0.45	+0.61	+0.438	+0.601	-0.012	-0.009
251	692	+0.45	+0.61	+0.437	+0.606	-0.013	-0.004
252	692	+0.45	+0.61	+0.436	+0.611	-0.014	+0.001
253	692	+0.45	+0.64	+0.434	+0.616	-0.016	-0.024
254	692	+0.45	+0.64	+0.433	+0.621	-0.017	-0.019
255	692	+0.45	+0.64	+0.432	+0.626	-0.018	-0.014
257	692	+0.45	+0.64	+0.294	+0.561	-0.156	-0.079
258	692	+0.45	+0.64	+0.288	+0.562	-0.162	-0.078
259	701	+0.27	+0.64	+0.282	+0.563	+0.012	-0.077
260	701	+0.27	+0.64	+0.277	+0.565	+0.007	-0.075
261	701	+0.27	+0.64	+0.271	+0.566	+0.001	-0.074
262	701	+0.24	+0.64	+0.266	+0.567	+0.026	-0.073
263	701	+0.24	+0.67	+0.260	+0.568	+0.020	-0.102
264	701	+0.24	+0.67	+0.255	+0.569	+0.015	-0.101
265	701	+0.24	+0.67	+0.249	+0.570	+0.009	-0.100
267	701	+0.21	+0.67	+0.238	+0.573	+0.028	-0.097
268	701	+0.21	+0.67	+0.238	+0.574	+0.028	-0.096
269	701	+0.21	+0.67	+0.238	+0.575	+0.028	-0.095
270	701	+0.18	+0.70	+0.237	+0.576	+0.057	-0.124
271	701	+0.18	+0.70	+0.237	+0.577	+0.057	-0.123
272	701	+0.18	+0.70	+0.237	+0.578	+0.057	-0.122
273	701	+0.18	+0.70	+0.237	+0.580	+0.057	-0.120
274	701	+0.15	+0.70	+0.236	+0.581	+0.086	-0.119
275	701	+0.15	+0.70	+0.236	+0.582	+0.086	-0.118
276	701	+0.15	+0.70	+0.236	+0.583	+0.086	-0.117
277	708	+0.21	+0.58	+0.235	+0.584	+0.025	+0.004

Table 3-3 TOPEX Side B Cal Table Entries for Distributed GDRs (Continued)

		Cal Table Values Used in Already-Distributed Data		Best Fit Cal Table Values from 3-Segment Fit to CAL-1		Adjustment for Already-Distributed Data	
(1) TOPEX Cycle	(2) Applicable MCR #	(3) Ku-Band Cal Table, dB	(4) C-Band Cal Table, dB	(5) Best Fit Ku-Band Cal Table, dB	(6) Best Fit C-Band Cal Table, dB	(7) Ku-Band Adjust, dB	(8) C-Band Adjust, dB
279	708	+0.21	+0.58	+0.235	+0.587	+0.025	+0.007
280	708	+0.21	+0.58	+0.235	+0.588	+0.025	+0.008
281	708	+0.21	+0.58	+0.234	+0.589	+0.024	+0.009
282	708	+0.21	+0.58	+0.234	+0.590	+0.024	+0.010
283	708	+0.21	+0.61	+0.234	+0.591	+0.024	-0.019
284	708	+0.21	+0.61	+0.234	+0.592	+0.024	-0.018
285	708	+0.21	+0.61	+0.233	+0.594	+0.023	-0.016
286	708	+0.21	+0.61	+0.233	+0.595	+0.023	-0.015
287	708	+0.21	+0.61	+0.233	+0.596	+0.023	-0.014
288	708	+0.21	+0.61	+0.233	+0.597	+0.023	-0.013
290	708	+0.18	+0.61	+0.232	+0.599	+0.052	-0.011
291	708	+0.18	+0.61	+0.232	+0.600	+0.052	-0.010
292	708	+0.18	+0.61	+0.231	+0.602	+0.051	-0.008
293	708	+0.18	+0.61	+0.231	+0.603	+0.051	-0.007
294	708	+0.18	+0.61	+0.231	+0.604	+0.051	-0.006
295	708	+0.18	+0.61	+0.231	+0.605	+0.051	-0.005
296	708	+0.18	+0.61	+0.230	+0.606	+0.050	-0.004
297	708	+0.18	+0.61	+0.230	+0.602	+0.050	-0.008
298	708	+0.18	+0.61	+0.230	+0.598	+0.050	-0.012
300	720	+0.24	+0.61	+0.229	+0.590	-0.011	-0.020
301	720	+0.24	+0.61	+0.229	+0.586	-0.011	-0.024
302	720	+0.24	+0.61	+0.229	+0.583	-0.011	-0.027
303	720	+0.24	+0.61	+0.228	+0.579	-0.012	-0.031
304	720	+0.24	+0.61	+0.228	+0.575	-0.012	-0.035
305	720	+0.24	+0.64	+0.228	+0.571	-0.012	-0.069
306	720	+0.24	+0.64	+0.228	+0.567	-0.012	-0.073
308	720	+0.24	+0.64	+0.227	+0.559	-0.013	-0.081

Table 3-3 TOPEX Side B Cal Table Entries for Distributed GDRs (Continued)

		Cal Table Values Used in Already-Distributed Data		Best Fit Cal Table Values from 3-Segment Fit to CAL-1		Adjustment for Already-Distributed Data	
(1) TOPEX Cycle	(2) Applicable MCR #	(3) Ku-Band Cal Table, dB	(4) C-Band Cal Table, dB	(5) Best Fit Ku-Band Cal Table, dB	(6) Best Fit C-Band Cal Table, dB	(7) Ku-Band Adjust, dB	(8) C-Band Adjust, dB
309	720	+0.24	+0.64	+0.227	+0.555	-0.013	-0.085
310	720	+0.24	+0.64	+0.227	+0.551	-0.013	-0.089
311	720	+0.24	+0.64	+0.226	+0.547	-0.014	-0.093
312	720	+0.24	+0.64	+0.226	+0.543	-0.014	-0.097
313	720	+0.24	+0.64	+0.226	+0.539	-0.014	-0.101

Figure 3-15 on page 3-20 compares the sigma0 Cal Table values actually used in the distributed GDRs and the best guess revised Cal Table values, for both TOPEX Ku- and C-band. In practical terms we can find the “delta correction” values to be added to the current GDR sigma0 values to produce those sigma0 values which would have been obtained if the ground processing had used the values given by columns 5 and 6 of Table 3-3 instead of the values in columns 3 and 4 of that table. These delta correction values are given in columns 7 and 8 of Table 3-3, and are plotted in Figure 3-16 on page 3-21. This figure shows that the Ku-band sigma0 values for cycles 257 and 258 are the most in need of additional adjustment. This is not surprising, given that no change in the Ku Cal Table was made from start of Side B until cycle 259.

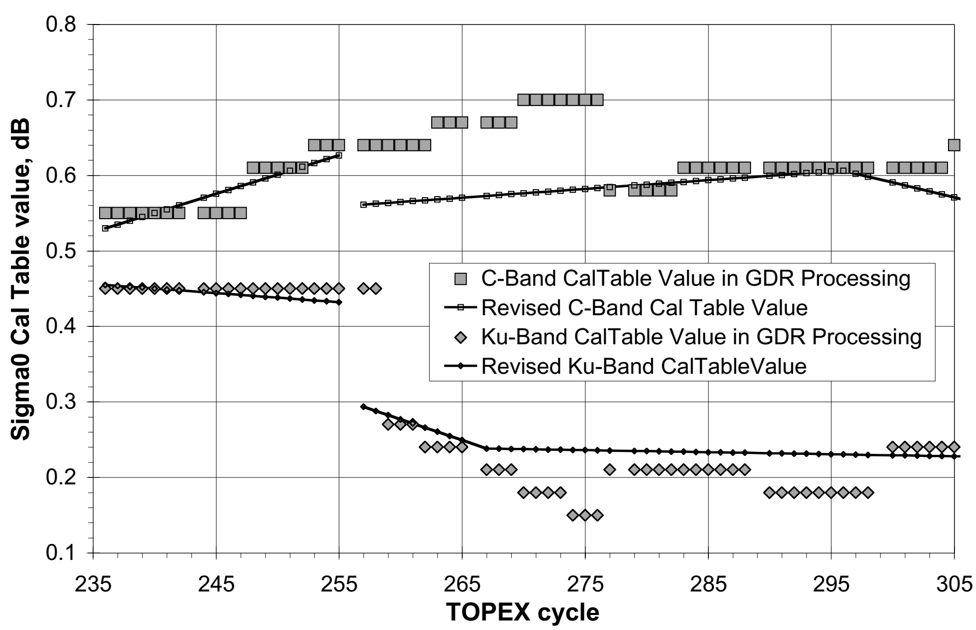

Figure 3-15 TOPEX Side B Ku- and C-band Sigma0 Calibration Table Values

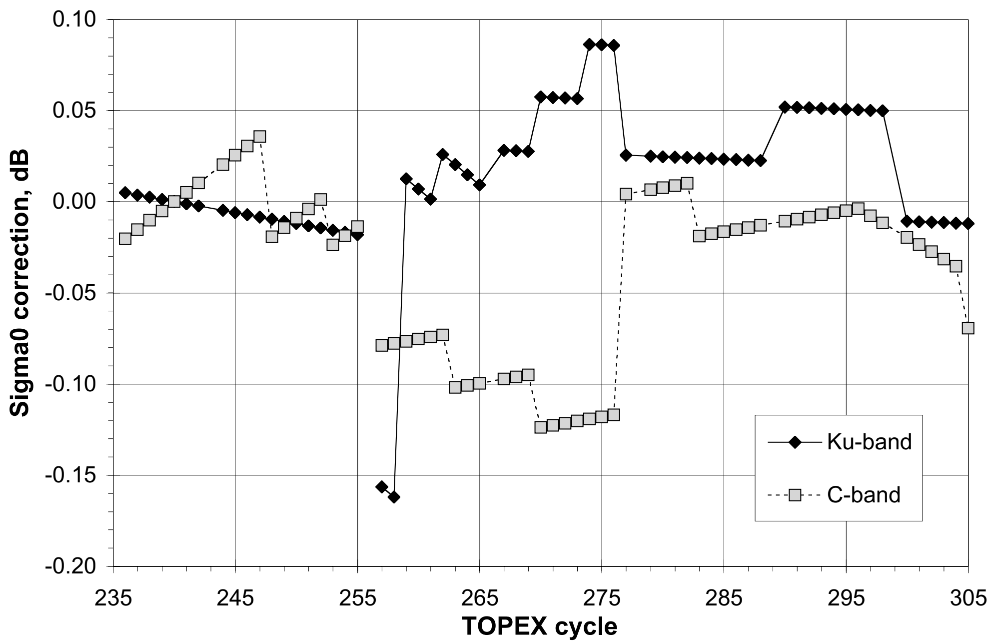

Figure 3-16 Correction for Already-Distributed TOPEX Side B Data, to Adjust All Cycles by 3-Segment CAL-1 Fit

3.3 Side B Point Target Response

Changes in the TOPEX Side A altimeter became apparent around the middle of 1998. The first symptoms of the changes were an increase in the altimeter's SWH estimates and an increase in the range rms. Subsequent investigation revealed apparent changes in the altimeter's point target response (PTR); these changes were shown by the waveform data in the altimeter's Calibration Mode 1 (CAL-1). The Side A PTR changes were the reason that the altimeter was switched to its Side B in February 1999 near the start of cycle 236.

The normal TOPEX CAL-1 has been executed at least twice daily throughout the entire TOPEX operation. In CAL-1 a portion of the transmitted signal is fed back into the altimeter receiver through a special calibration attenuator and the altimeter tracks this transmitted signal using a special tracking algorithm. During the preflight testing a special calibration mode sweep test (the CalSweep) had been developed in which the altimeter did not automatically track the PTR; instead the AGC level was frozen at a preset level and the altimeter's fine-height word was incremented through its entire range (equivalent to 8 waveform sample positions). The CalSweep waveforms can be processed to give a "fine-grained" look at the PTR. After the Side A overestimates of SWH became apparent, a software patch was uploaded to TOPEX to allow the CalSweep to be executed on-orbit. The CalSweep was executed approximately monthly from mid-1998 through the end of the Side A operation. The year 1998 Engineering Assessment Update (published in August 1999) contains a more detailed discussion of the Side A PTR observation by CAL-1 and CalSweep, and the consequences of the Side A PTR change.

The CalSweep has continued to be executed about once a month for the entire time of Side B operation. Figure 3-17 on page 3-23 shows the comparison of an early Side B CalSweep (1999 day 042) and the last Ku-band CalSweep of year 2000 (2000 day 349). Figure 3-18 on page 3-23 shows the same comparison for the Side B C-band altimeter. As a reference, the theoretical model for the PTR is shown by the pure sinc^2 plotted in Figure 3-17 and Figure 3-18. Only the central lobe and the first five sidelobes are shown in these figures. To within the accuracy and repeatability of the CalSweep, there has been practically no perceptible change in the Side B Ku- and C-band CalSweeps from start of Side B through the end of year 2000. If there have been any changes at all in the Side B CalSweeps, these changes have been less than the size of the plot symbols in Figure 3-17 and Figure 3-18.

In addition to the CalSweep, further information on the PTR is available from the waveform data in the normal CAL-1 which is executed about twenty times in each TOPEX repeat cycle. While the CalSweep "paints" the PTR in fine-grained detail, the CAL-1 waveform only provides a single sample at about the peak of each of the PTR sidelobes. We keep a database of waveforms from the first two CAL-1 modes in each repeat cycle, and this provides another way of assessing possible PTR changes as a function of cycle. We will use the CAL-1 step 5 waveforms for the following discussion because the AGC level of step 5 is about the same level as in the TOPEX normal over-ocean fine track.

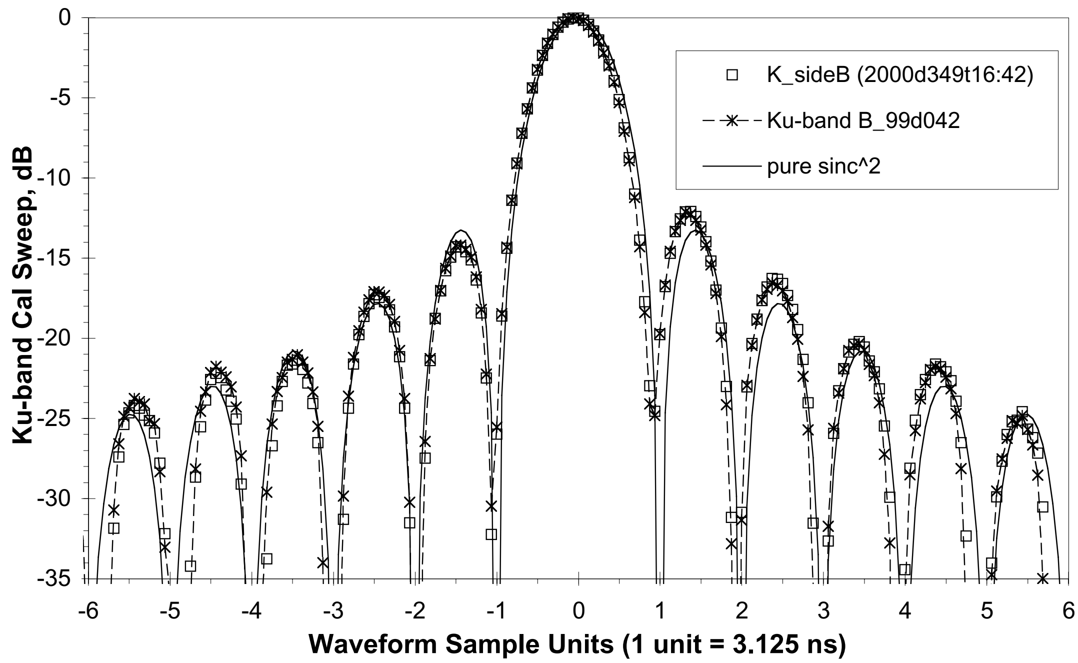

Figure 3-17 TOPEX Side B Ku-Band Cal Sweep 2000 Day 349 Compared to 1999 Day 042

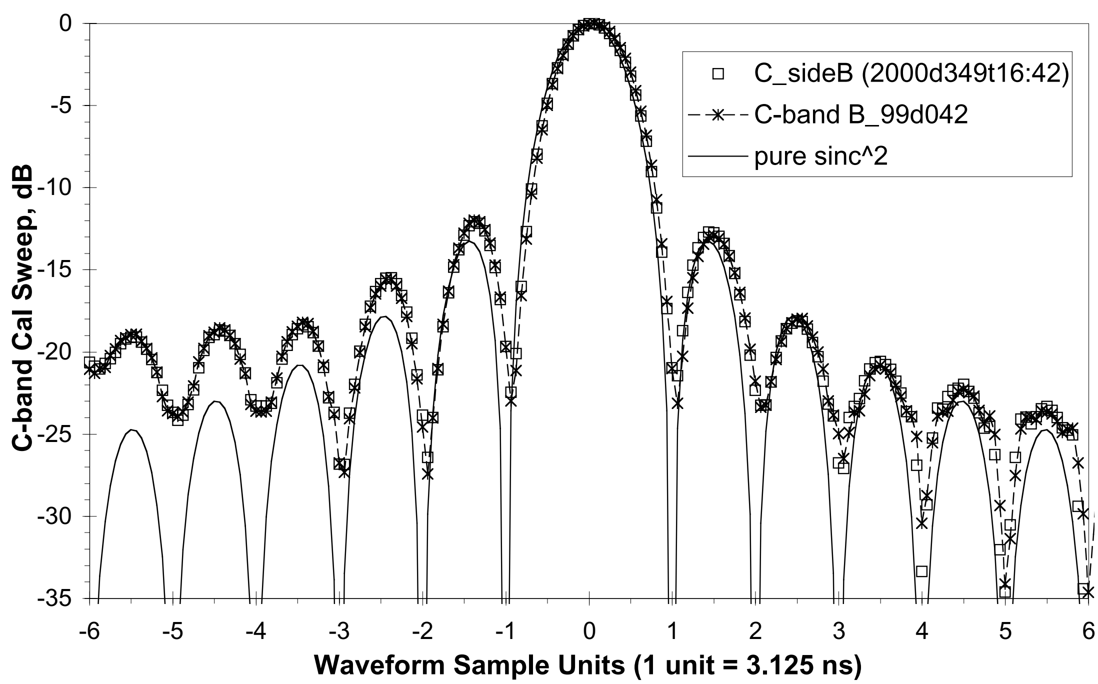

Figure 3-18 TOPEX Side B C-Band Cal Sweep 2000 Day 349 Compared to 1999 Day 042

For the TOPEX Side B Ku-band system, Figure 3-19 on page 3-24 shows the time his-

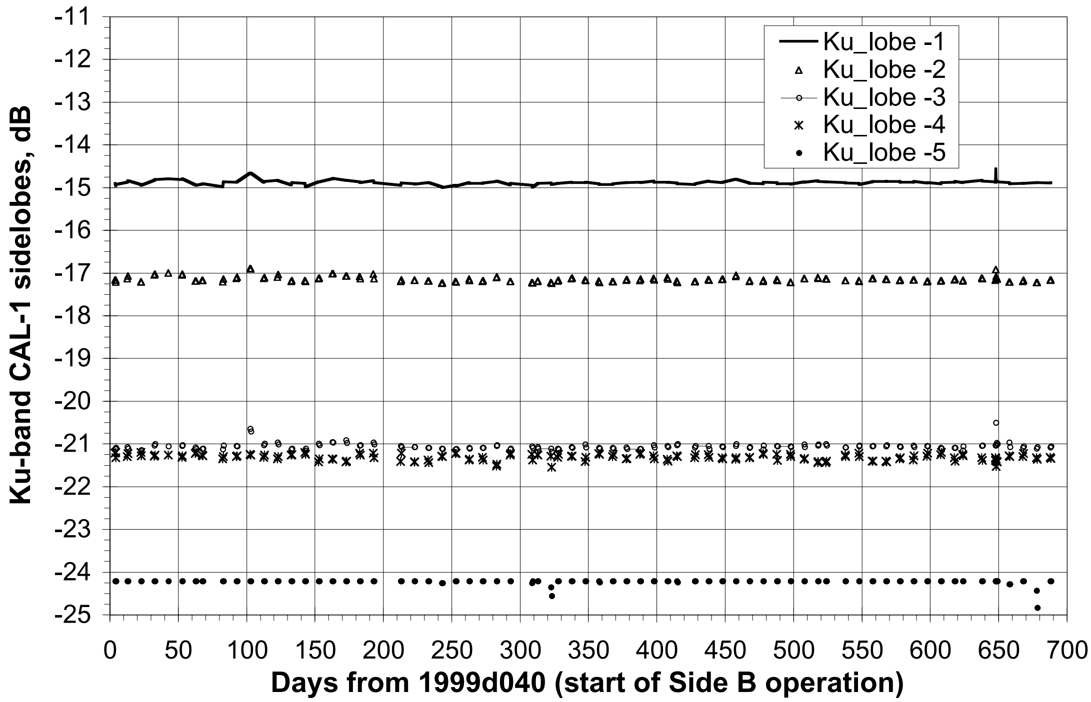

Figure 3-19 Side B Ku-Band CAL-1 Step 5 Lower Sidelobes Relative to Peak Value

tory of the first five PTR lobes below the main peak and Figure 3-20 on page 3-25 shows the first five lobes above the main peak. These two figures show the Ku-band data from start of Side B operation through the end of year 2000, and none of the sidelobe peak values exhibit any significant time trend. For the Side B C-band system, Figure 3-21 on page 3-25 shows the first five PTR lobes below the main peak and Figure 3-22 on page 3-26 shows the first five sidelobes above the main peak. While the lower five C-band Side B PTR sidelobes in Figure 3-21 show no significant time trends, there are possible small trends in a couple of the upper five C-band sidelobes in Figure 3-22. The +2 sidelobe shows an increase of about a quarter dB from start of Side B through the end of year 2000, and the +3 sidelobe shows about an increase for about half dB over this time. Figure 3-22 may possibly show a step change in these sidelobes at the cycle 256 safehold about 208 days after the start of Side B operation. We think that these changes are too small to have any practical consequences in the TOPEX range or SWH estimation, but future CalSweep and CAL-1 waveform trend results will be closely watched for possible further changes.

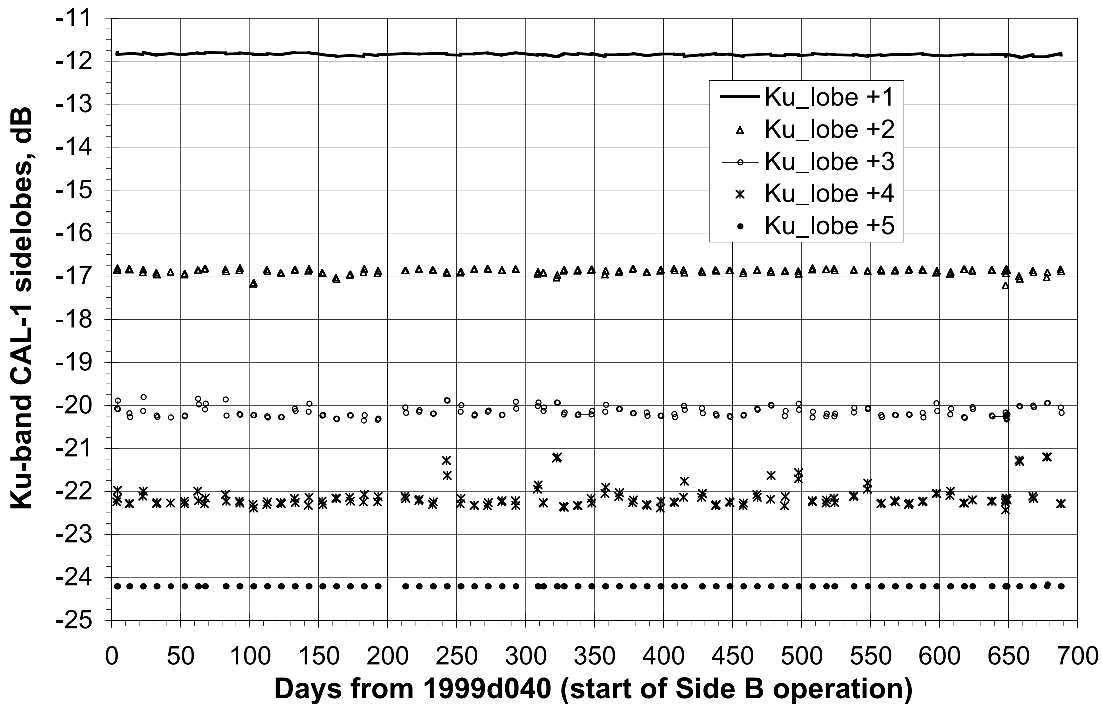

Figure 3-20 Side B Ku-Band CAL-1 Step 5 Higher Sidelobes Relative to Peak Value

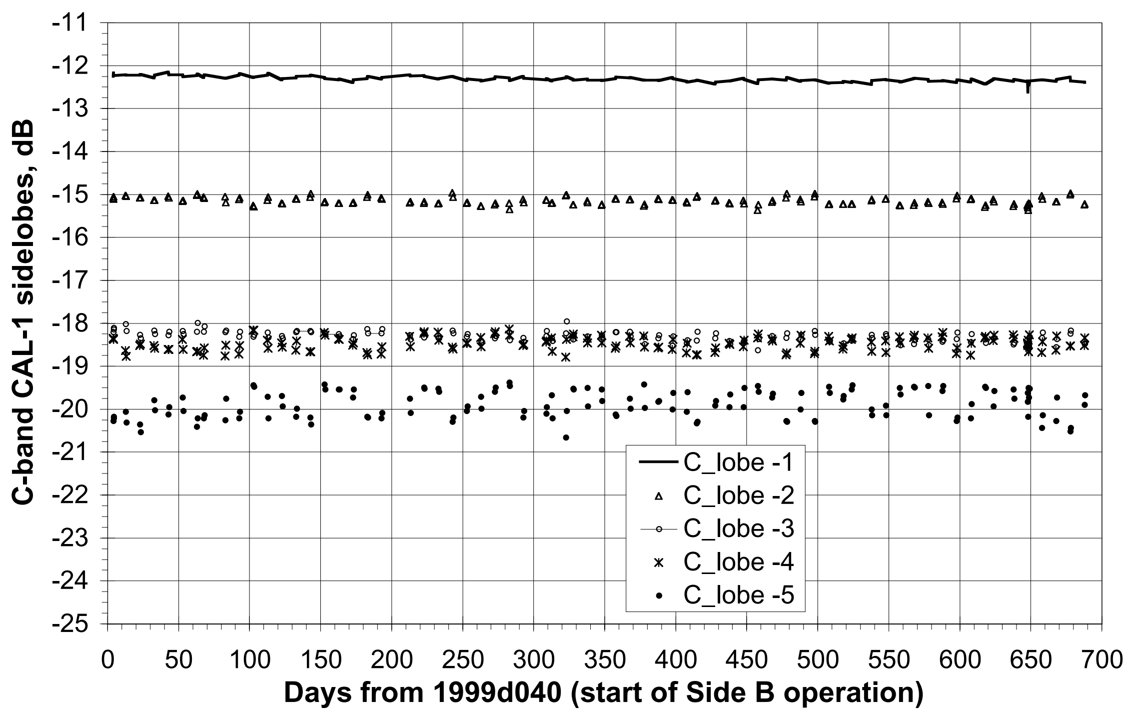

Figure 3-21 Side B C-Band CAL-1 Step 5 Lower Sidelobes Relative to Peak Value

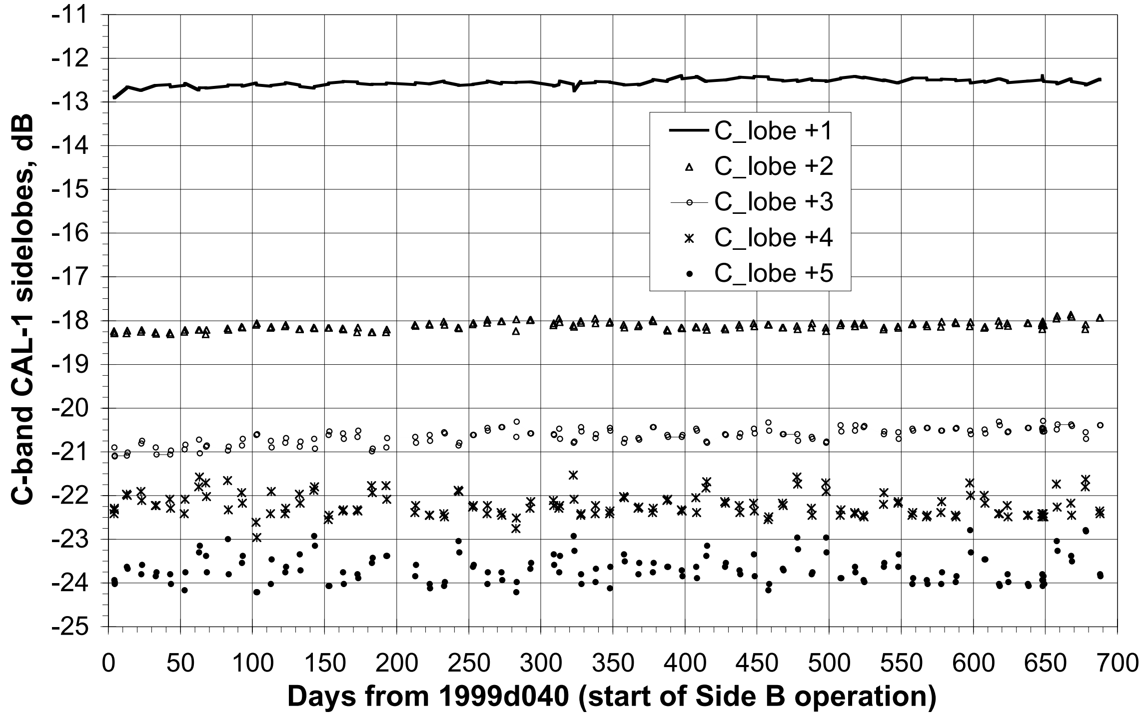

Figure 3-22 Side B C-Band CAL-1 Step 5 Higher Sidelobes Relative to Peak Value

Section 4

Other Studies

4.1 Possible Drift in the Radar-derived Ionospheric Corrections for TOPEX, from work contributed by Doug Vandemark et al

Analysis indicates that the average difference between DORIS and TOPEX radar-derived (ALT) ionospheric corrections is varying, and is generally on the increase since TOPEX/Poseidon (T/P) cycle 190. This mm-scale trend was first pointed out by J. Dorandeau, and Figure 4-1 on page 4-3 comes from MGDRB data supplied by J. Dorandeau. The filtering versus time of day and latitude is unknown and may well be the global average.

The question that arises - is the increase observed in Figure 4-1 subsequent to cycle 190 due to some radar-specific problem in the ionospheric correction? The answer is not obvious because the trend not only correlates with the T/P cycle, but also correlates with increased solar activity that started to ramp upward in 1998 towards a maximum that occurred around the end of 2000 (about cycle 300). This is T/P's first exposure to this substantial ionospheric delay signal and thus is the first large signal test for the DORIS-ALT comparison.

Attempts were made to determine, using the MGDR data, if the ALT correction was somehow drifting with time due to some long-term sensor error. The approach was to filter through the T/P over-ocean data and average over various night-time subsets and for various latitude bands to see if the DORIS-ALT 'drift' was evident for those cases of very low ionospheric content after cycle 190. All indications are that the drift does reside in any filtering combination one might try. But the data also indicate the mean ionospheric delay (be it from DORIS or TOPEX) is also increasing since cycle 190. That is, the night-time delay also changes with the solar cycle. Thus, the observed difference may also represent an actual DORIS vs. TOPEX difference due to the alternate techniques (e.g., sampling or model characteristics that had not been observed prior to the solar max.)

The following figures provide some limited documentation of the DORIS-ALT difference. The data are not entirely conclusive for either possibility. That will likely have to wait until ionospheric delay levels lessen towards the solar minimum.

Figure 4-2 on page 4-4 through Figure 4-5 on page 4-5 are from data near the equator where the delay levels are generally elevated, but where the seasonal solar cycle signal is fairly dramatic. The intent was to record the DORIS-ALT difference over a varying mean. The top part of Figure 4-2 illustrates the average ionospheric differences and standard deviations versus cycle number for local daytime (1000-1800 hours), while the bottom part of the figure is for local nighttime (0000-0800 hours). Both data sets are based on MGDR-B values, and are from the latitude boundaries of $\pm$15 degrees. Every third T/P pass was used in forming the average.

Figure 4-3 on page 4-4 depicts scatterplots of the ionospheric difference and of the standard deviations of the differences (from the Figure 4-2 data) versus the TOPEX-based ionospheric corrections. As in the prior figure, the top plots are for local daytime and the bottom plots are for local nighttime. A five-cycle smoothed product is additionally shown by the asterisks in the two left panels.

The correlation coefficient between the drift and the mean ionospheric level is computed to be (R) = 0.96 for cycles 190-303, while R=0.86 versus the T/P cycle number. This is the strongest indication that the drift is associated with actual DORIS –ALT techniques as they change versus mean electron content, and is not a radar problem. Other evidence, given as background, includes the fact that the difference standard deviation from Figure 4-3 also scatters tightly against the mean ionospheric level. Truncated ionospheric difference plots, for cycles 150-303 only, are shown by the solid lines in Figure 4-4 on page 4-5 where, again, the top part is for daytime and the bottom represents the nighttime. The dashed line is the TOPEX-based ionospheric correction divided by -10.

One views the PDF of the ionospheric corrections for any given cycle in Figure 4-5 on page 4-5. It is clear that they can differ (DORIS vs. ALT) markedly. Some of the differences observed may simply reside in close examination of statistics derived from these PDFs. In Figure 4-5, the TOPEX-based trace (the darker of the two) has been shifted to the left by 0.008 m to account for the baseline offset evident from the start of the mission. Note that sample population is always greater for the night subset.

Figure 4-6 on page 4-6 and Figure 4-7 on page 4-6 are for mid-latitudes, and are included to show that the absolute difference level and the absolute level of change with time can be difficult to quantify at better than the 2 mm level. These last plots are for 30-50 deg. in latitude for both hemispheres where the delay level is generally smaller; and every third T/P pass has been used to form the average.

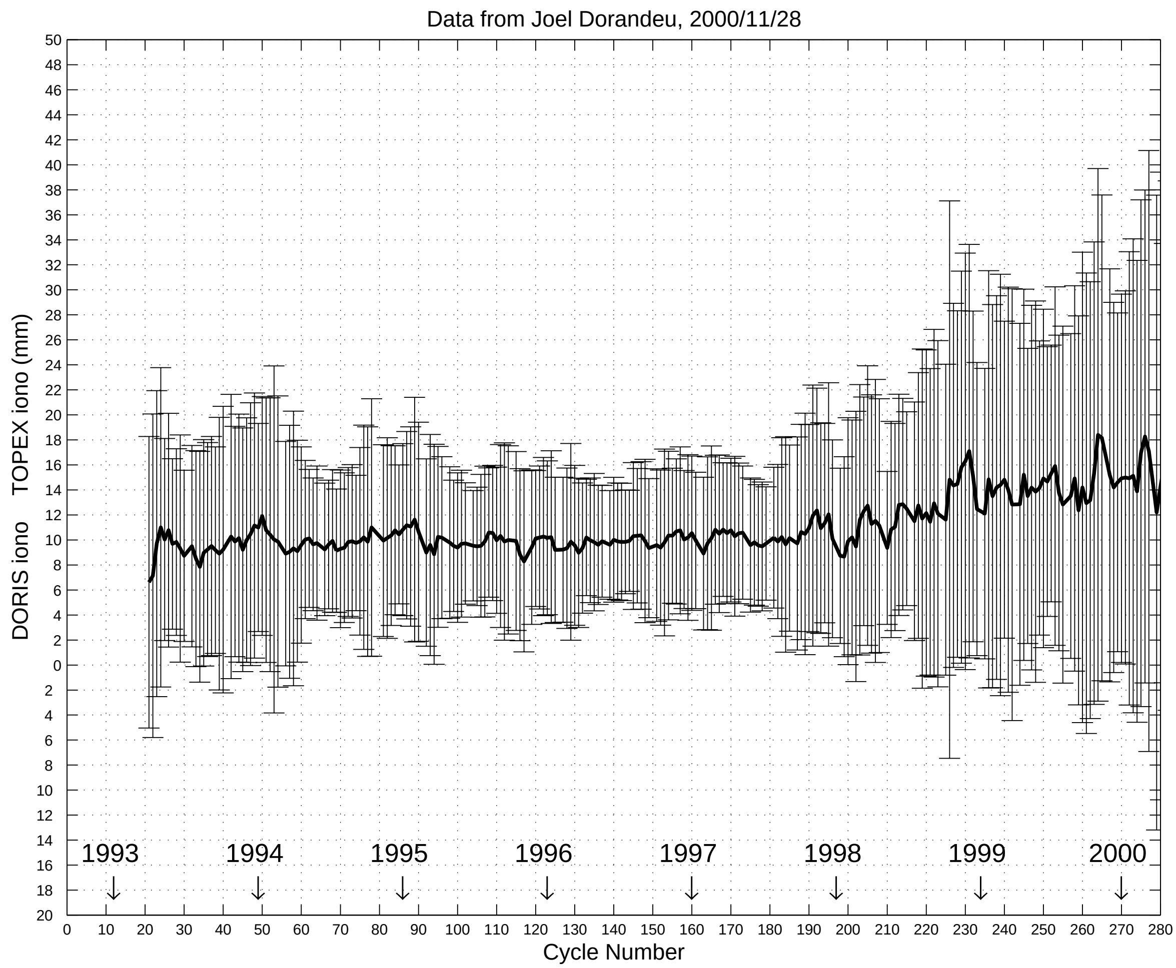

Figure 4-1 Average Ionospheric Difference (in mm) vs. T/P Cycle from Data Supplied by J. Dorandeau. (Error bars indicate the estimated standard deviation.)

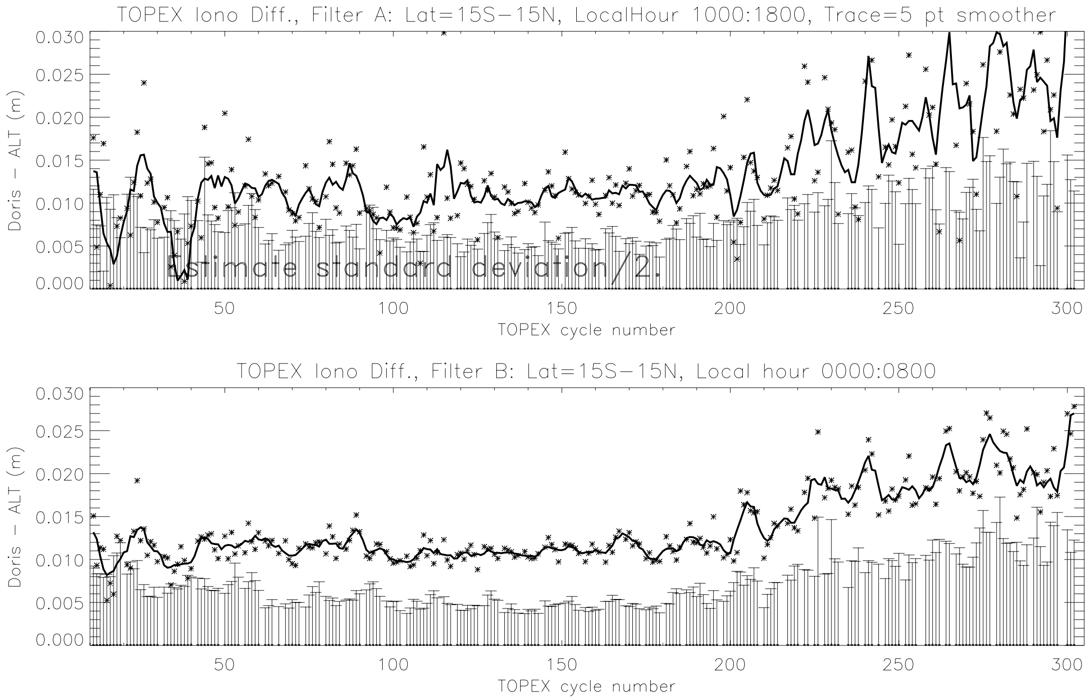

Figure 4-2 Average Ionospheric Difference (in m) vs. T/P Cycle for Local Day (upper) and Night (bottom) and only for the Zonal Band from –15 to +15 in Latitude.

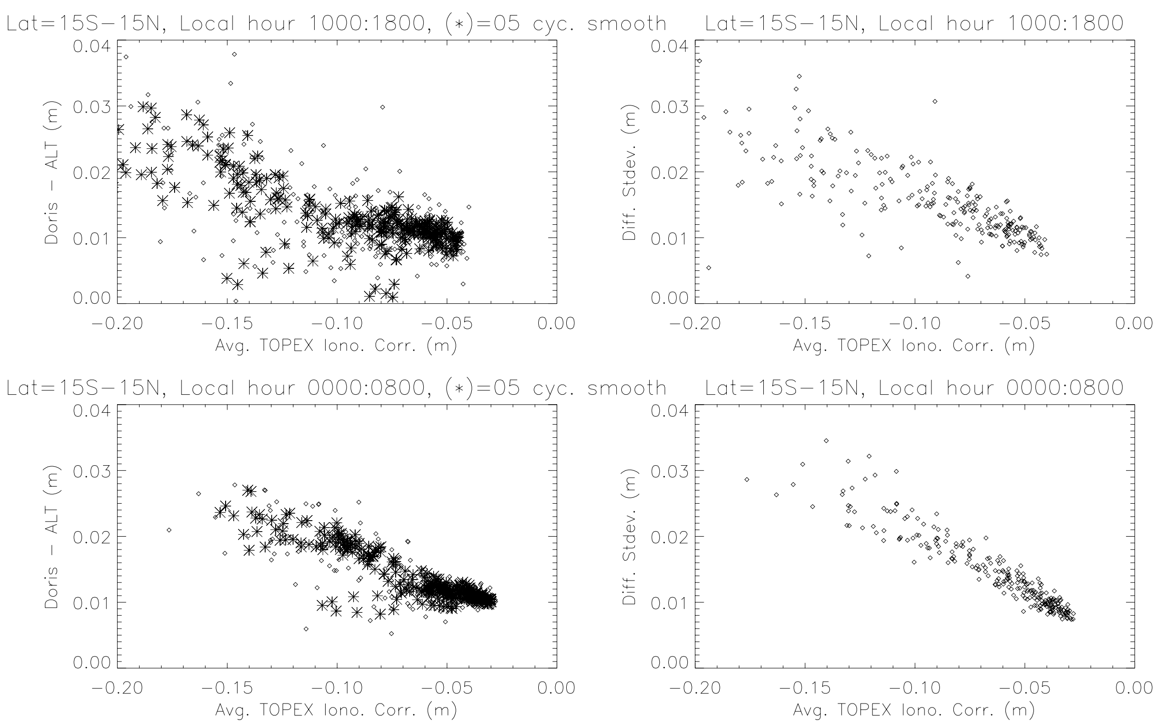

Figure 4-3 Scatterplots of the Average Ionospheric Difference and Difference Standard Deviation vs. the Mean ALT Ionospheric Correction for the Complete T/P Mission up to Cycle 303.

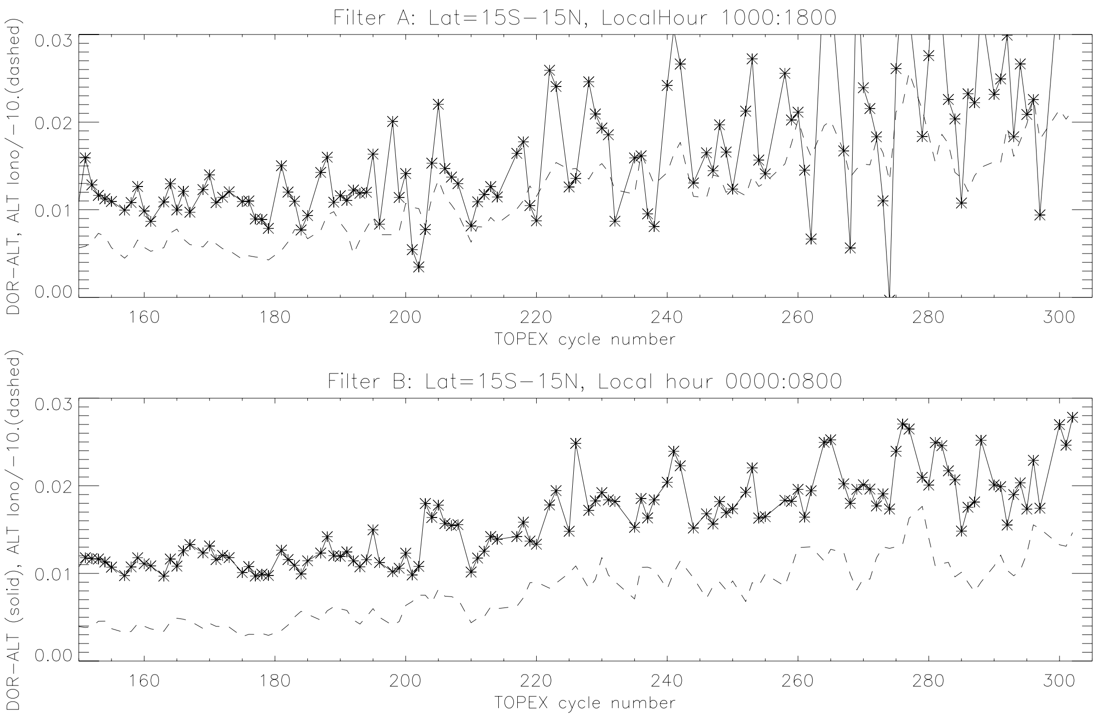

Figure 4-4 Difference and the Mean Ionospheric Correction (scaled to fit on the plot as indicated) vs. T/P Cycle for both the Day and Night Data Sets.

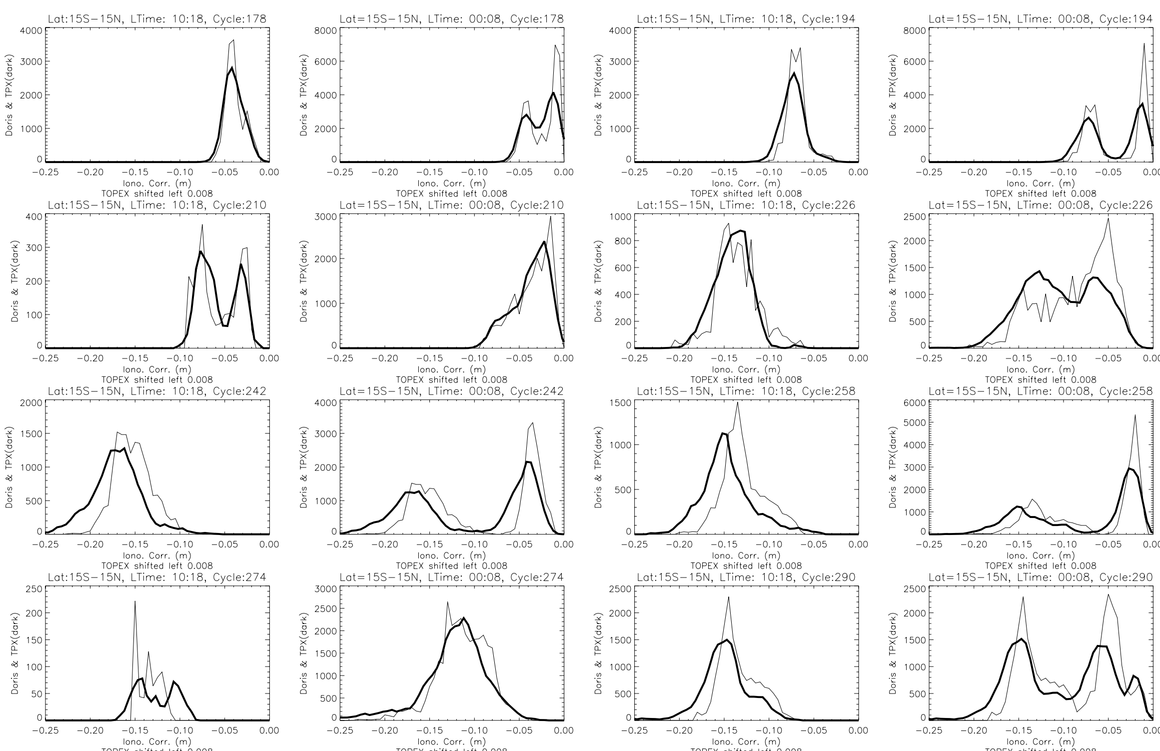

Figure 4-5 Representative Probability Density Functions of the ALT and DORIS Ionospheric Corrections for the Indicated Cycles (Local day and night are also indicated.)

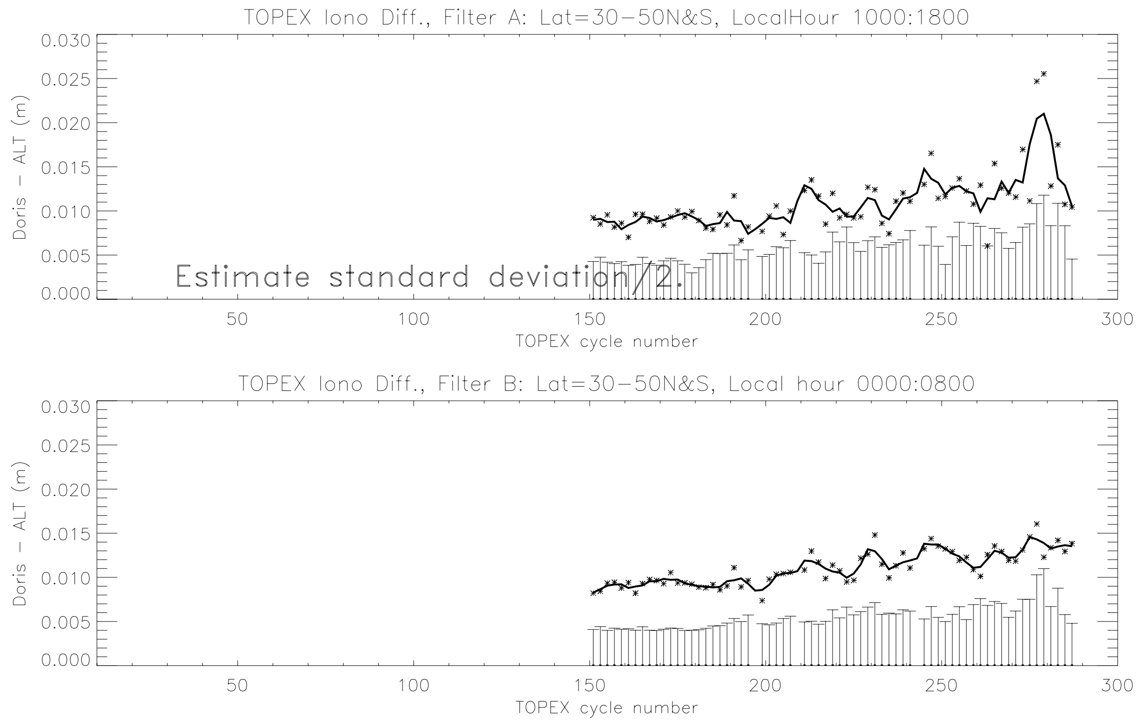

Figure 4-6 Average Ionospheric Difference (in m) versus T/P Cycle for Local Day (upper) and Night (bottom) and only for the Zonal Band from 30 to 50 Latitude in both Hemispheres

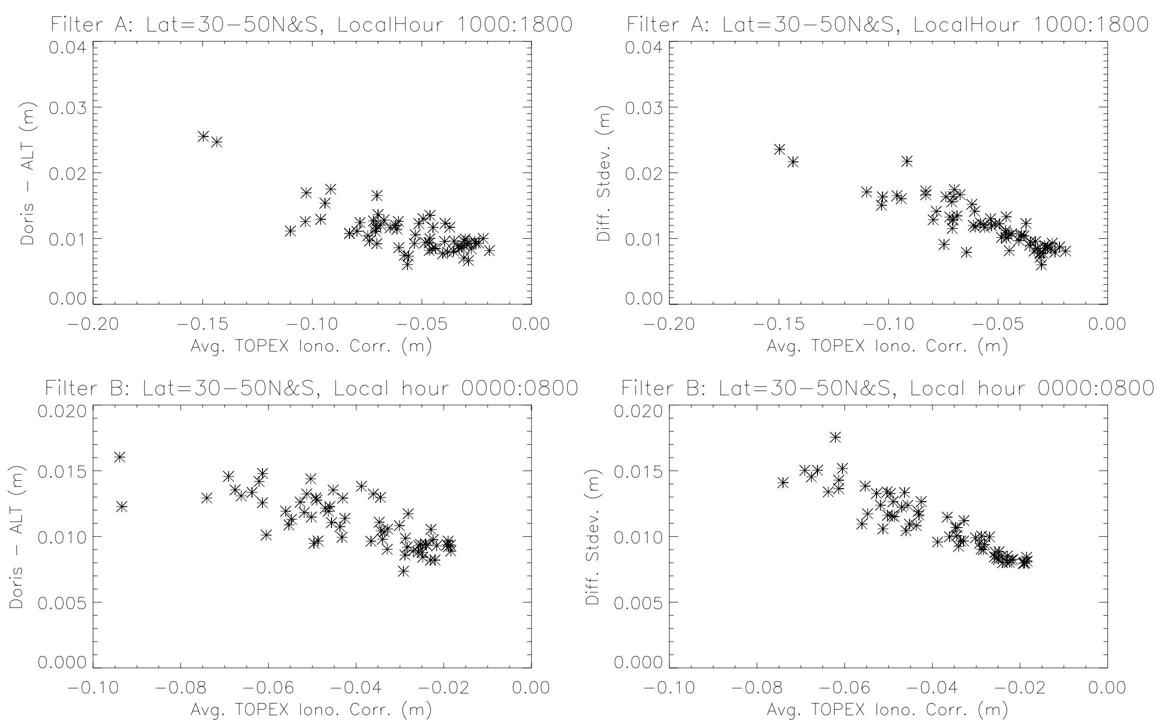

Figure 4-7 Scatterplots of the Average Ionospheric Difference and Difference Standard Deviation vs. the Mean ALT Ionospheric Correction for the T/P Mission, Cycles 150-288.

4.2 Assessment of the Cycle-by-Cycle TOPEX Altimeter Noise Level by High-Pass Filtering 1-Hz Data, from work contributed by Ngan Tran et al

4.2.1 Introduction

Based on recent results from Driscoll and Sailor [2001], we compute and test a second TOPEX altimeter noise estimation technique. The technique we have been using to this point is based on computing the 1-minute Ku-band range RMS. The range noise of the TOPEX Ku-band altimeter is assessed by calculating the RMS of one-per-frame Ku-minus-C height differences, after a linear fit over a 1-minute interval. The height RMS for the Ku-band is then determined by scaling the rms-of-fit by the ratio of the Ku / C noise. For more details, the rms derivation is described in Section 5.1.1 of the February 1994 Engineering Assessment Report. As pointed out in this cited document, this method takes the effects of geoid noise out of the calculation that would be present on a straight fit to either frequency, since both frequencies follow the same geoid tracking. This method has been developed specifically for a dual-frequency altimeter as TOPEX and cannot be used for a single-frequency altimeter.

Driscoll and Sailor [2001] have developed a new approach that works by high-pass filtering 1-Hz data. Indeed, the altimeter instrument noise can be characterized as a white noise process with a specified average power that differs for each altimeter analyzed [Sailor and Driscoll, 1992]. In fact, the empirical “white noise floor” observed in altimeter data is not solely due to the instrument's contribution to noise (it is affected in part by environmental factors such as sea state), but for the purposes of defining a measure of the quality of on-orbit performance of an altimeter, a measure such as the white noise level is one way of comparing the quality of different altimeters.

Previous estimations of altimeter white noise are based on the analysis of segments of nearly collinear repeat tracks [Sailor and Driscoll, 1992; Sailor and LeSchack, 1987]. The raw altimeter output is the sum of the geoid signal, the oceanography, and instrument noise. The instrument noise is at the few centimeter level while the geoid signal can easily be 0.1 kilometer in size. Differencing the repeat track heights time series, i.e., point-by-point differences of corresponding sea-surface height observations collected along different satellite passes, removes most of the geoid signal. What is left after differencing the passes consists mostly of noise containing a residual geoid that results from the two passes not being exactly along the same ground track and from oceanography that results in the ocean surface varying from pass-to-pass. The height difference between two data sets varies by several meters due to these effects. To quantify how this noise varies as a function of spatial wave number, along-track-noise power spectral density functions must be computed. The power spectral density (PSD) of the differenced data will contain low frequency energy that is attributed to the residual geoid and to oceanography. High frequency energy is attributed to the altimeter itself.

More recently, investigations from Driscoll and Sailor [2001] have shown that since white noise dominates the Geosat Follow On (GFO) altimeter sea surface height time series at the shortest wavelengths, a noise measurement algorithm that works by high-pass filtering 1-Hz data to estimate white noise level is a good and simple alternative method. They have demonstrated the robust nature of this simplified, single-track analysis approach that avoids the need to compute the difference of repeat track height time series and power spectra. They used for this assessment 52 GFO track segments. The number of data along these segments ranges from approximately 180 to 830 samples. They also showed that the noise level is sensitive to significant wave height (SWH). The noise level increases linearly with increasing significant wave height.

Several issues will be discussed in the following. We will first apply this high-pass filter to quantify the white noise level of the TOPEX altimeter data. This assessment will be on a cycle-by-cycle basis. We will then compare these results with the operational range noise estimation of the TOPEX Ku altimeter. Finally, we will discuss the influence of the atmospheric corrections to the range in the noise level estimations.

4.2.2 Data and Routine

For details about the high-pass filter process, please refer to Driscoll and Sailor's report [2001]. TOPEX data are from IGDR files. We test the cycle-by-cycle noise level estimation routine over 3-cycles from cycle 295 through cycle 297. The different measurements used are 1-second averages. These altimeter data are limited in space between latitudes 60^{o}N and 60^{o}S. Rather stringent editing is applied to eliminate anomalous data. In addition to the use of TOPEX data flags, all cases with OffNadir > 0.12^{o} or with sigma0 > 16 dB, or SWH > 10 m are also discarded. The application of the editing procedure leads to gaps in the sea surface height (SSHgt) time series. In order to not remove too many track segments, we filled the small gaps between 2 and 5 seconds by a linear interpolation. The high-pass filter is a 5th-order Butterworth filter (to remove the geoid and all long-wavelength environmental signal) with a cutoff frequency of 0.30 Hz. It has been applied on track segments of 290-310 samples (~ 5 minutes) and 50-70 samples (~ 1 minute) respectively. Smaller segments in each case are not considered.

4.2.3 Results

Figure 4-8 on page 4-9 shows the results obtained for the cycle 295 for the 5-minute segments. The top panel shows the distribution of the track segments over the ocean. The left panel at the bottom of the Figure shows the high-pass filtering estimates of TOPEX RMS white noise level with respect to the significant wave height. Values of RMS noise level range from 1.0 to 5.0 cm. The straight line represents the linear least-square fit. As expected from Driscoll and Sailor's results [2001] for GFO altimeter, the noise level increases linearly with increasing significant wave height. The two others panels show respectively the distribution of the averaged significant wave height values and the 1-Hz noise level estimates. Due to the length of the segments, there is no data for averaged significant wave height values below 1 m and above 7 m. Table 4-1 on page 4-9 summarizes the statistical indicators from these different plots for the 3 cycles considered. The mean of the Ku SWH distribution is ~ 2.8-3.0 m, and the mean of the

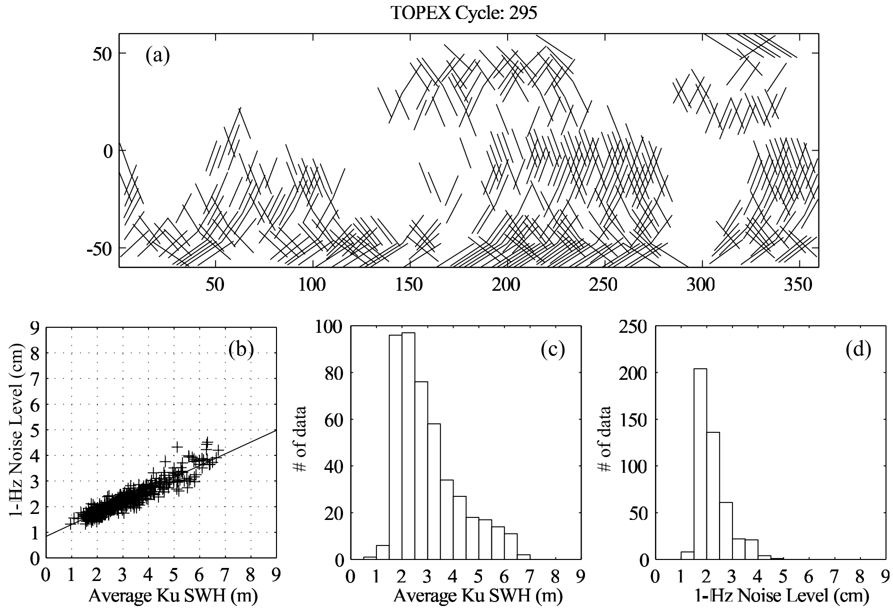

Figure 4-8 Plots for Cycle 295 and 5-minute Segments

noise level distribution is ~ 2.20-2.22 cm. The slope of the linear regression is ~ 0.43-0.46. This result shows that the TOPEX noise level is about 1.76-1.78 cm at SWH of 2 m.

Table 4-1 Statistical Indicators for Cycle 295 through Cycle 297 and 5-Minute Segments

Highpass Filter	5 min.	295	296	297
	nb of segments	457	438	494
Ku SWH (m)	**Mean** Std Skewness Kurtosis	**3.0** 1.221 1.048 3.381	**2.957** 1.186 1.035 3.372	**2.843** 1.126 0.988 3.253
Noise level (cm)	**Mean** Std Skewness Kurtosis	**2.222** 0.599 1.342 4.622	**2.204** 0.562 1.419 5.679	**2.152** 0.529 1.321 4.841
Noise level vs. Ku SWH	**Slope** Intercept R^2 **Noise Level at 2m SWH**	**0.460 +/- 0.016** 0.842 0.880 **1.762**	**0.442 +/- 0.016** 0.898 0.868 **1.781**	**0.437 +/-0.015** 0.907 0.865 **1.782**

In order to have a better representation of the noise level at low and high SWHs, we decreased the track segment size from 5-minute to 1-minute. Figure 4-9 on page 4-10 and Table 4-2 on page 4-12 show the results in this case. Figure 4-9 (b) and (c) show a bigger variability of the noise level with respect to the higher variability of the averaged significant wave height. Table 4-2 shows a decrease of the mean of the Ku SWH distribution up to 5%. The mean of the RMS noise level decreases up to 2.5% but the noise level value at 2 m SWH increases ~1.5%. The slope of the linear fit between the RMS noise level and the Ku significant wave height shows a decrease in average of 4.4%.

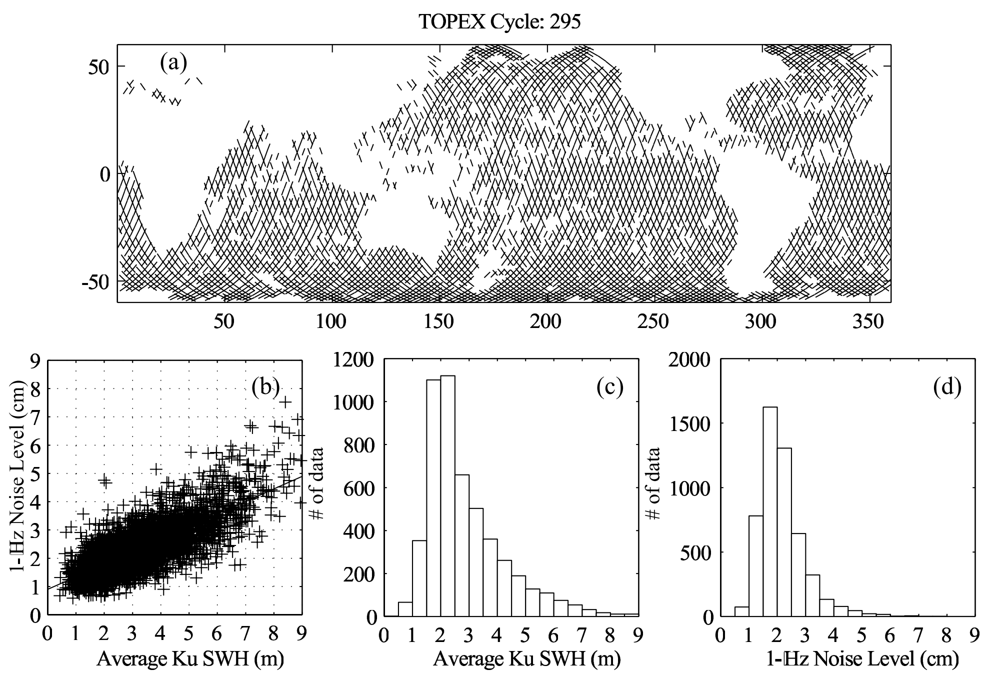

Figure 4-9 Plots for Cycle 295 and 1-minute Segments

We compared these 1-minute estimations of the RMS noise level with our operational estimation of the 1-minute averaged Ku range noise. Table 4-3 on page 4-11 presents the same statistical indicators as Table 4-2. Note that the mean of the Ku range noise level, the slope of the linear fit, and the noise level at 2 m SWH are all lower than for the high-pass filter by respectively ~14.2%, 32.4%, and 10.5%. The mean of the Ku range noise level is ~ 1.83-1.88 cm and the noise level at 2 m SWH is ~ 1.58-1.63 cm.

Table 4-2 Statistical Indicators for Cycle 295 through Cycle 297 and 1-Minute Segments

Highpass Filter	1 min.	295	296	297
	nb of segments	5053	5183	5290
Ku SWH (m)	**Mean** Std Skewness Kurtosis	**2.857** 1.377 1.357 4.878	**2.929** 1.350 1.201 4.312	**2.820** 1.296 1.200 4.522
Noise level (cm)	**Mean** Std Skewness Kurtosis	**2.167** 0.791 1.576 7.201	**2.195** 0.767 1.469 6.833	**2.140** 0.740 1.459 7.042
Noise level vs. Ku SWH	**Slope** Intercept R^2 **Noise Level at 2m SWH**	**0.444 +/- 0.010** 0.897 0.597 **1.786**	**0.417 +/- 0.010** 0.973 0.540 **1.807**	**0.419 +/- 0.010** 0.959 0.538 **1.797**

Table 4-3 Statistical indicators for Cycle 295 through Cycle 297 by Using TOPEX Ku-band Range RMS Method to Estimate the Altimeter Noise

Operational	1 min.	295	296	297
Ku SWH (m)	**Mean** Std Skewness Kurtosis	**2.848** 1.368 1.464 5.613	**2.940** 1.350 1.212 4.582	**2.823** 1.281 1.187 4.622
HgtKuRMS (cm)	**Mean** Std Skewness Kurtosis	**1.835** 0.458 1.408 6.215	**1.876** 0.473 1.693 9.802	**1.867** 0.515 2.752 22.708
HgtKuRMS vs. Ku SWH	**Slope** Intercept R^2 **Noise Level at 2m SWH**	**0.297 +/- 0.004** 0.982 0.80 **1.581**	**0.286 +/- 0.005** 1.033 0.67 **1.606**	**0.282 +/- 0.007** 1.072 0.49 **1.635**

In fact, it is expected that these two noise estimates are different because we did not apply these two methods on the same quantities. The high-pass filter is applied on the sea surface height while the operational method is based on the Ku range estimations. The sea surface height is computed as the difference between the satellite altitude and the altimeter range with propagation corrections. The propagation corrections correspond to the dry tropospheric correction (DryTropo), the ionospheric correction from the dual-frequency altimeter (IonoCorr), and the wet tropospheric correction (WetTropoRad). So any high frequency signal in those corrections would lead to an increase of the RMS noise level estimation by high-pass filtering the sea surface height time series.

In order to assess the influence of each correction on the RMS noise level, we first remove all three propagation corrections and then successively remove one of them from the sea surface height value before applying the high-pass filter. By the definition of the SSHgt, adding the range correction removes the correction in the SSHgt. Table 4-4 on page 4-14 and Table 4-5 on page 4-15 summarize the results for the 5-minute and 1-minute segments respectively. Note that removing the dry and wet tropospheric corrections have no influence on the RMS noise level, while removing the ionospheric correction estimated from the dual-frequency altimeter leads to a decrease of the noise level. The decrease of the mean value of the noise level is of ~ 13.2% leading to a value of ~ 1.86-1.93 cm for the 5-minute segments and a value of ~ 1.86-1.91 cm for the 1-minute segment. The RMS noise level at 2 m SWH decreases of ~14.3% to 1.50-1.52 cm for the 5-minute segments and 1.53-1.56 cm for the 1-minute segments, which is now more comparable in value to the Ku range noise level (Table 4-3).

Two things need to be pointed out here. (1) By employing range measurements from a second altimeter to obtain an ionosphere correction, one propagates the errors from both individual ranges into this correction. The dual-frequency estimate of the ionosphere range correction is then contaminated with the altimeter range measurement noises. This explains why removing this correction in the sea surface height value decreases the mean noise level. (2) Both the range noise which is correlated with SWH and the ionospheric electron content exhibit a latitudinal dependence. The relationship between the noise level estimates and SWH changes when we remove the ionosphere correction, leading to a change in the slope of the linear fit.

We next used the DORIS ionosphere correction provided by CNES on the MGDR files as an independent source of ionosphere data to verify that the white noise signal in the NASA dual-frequency ionospheric correction comes from the range noise. The advantage of the DORIS ionosphere correction over the NASA dual-frequency ionosphere correction is that it is independent of the altimeter range measurement although the DORIS ionosphere correction is less accurate.

Table 4-6 on page 4-16 and Table 4-7 on page 4-16 present results when we replace the ionospheric correction estimated by the TOPEX two-frequency algorithm by DORIS estimations. Note that the RMS noise level stays low as it was when we only remove TOPEX ionospheric correction from the sea surface height. The TOPEX ionospheric correction, computed from the difference in the delays of the Ku- and C-band radar pulses, to the range measurement introduces an additional high frequency signal which leads to an increase of the RMS noise level estimated by high-pass filtering the sea surface height time series.

Table 4-4 Statistical Indicators for Cycle 295 through Cycle 297 and 5-Minute Segments with Removal of the Atmospheric Corrections

Highpass Filter	5 min.	295	296	297
SSHgt + all atmospheric corrections	**Mean** Std Skewness Kurtosis	**1.926** 0.554 1.410 4.796	**1.912** 0.525 1.498 5.955	**1.862** 0.486 1.392 5.112
	Slope Intercept R^2 **Noise Level at 2m SWH**	**0.425 +/- 0.015** 0.652 0.876 **1.501**	**0.410 +/- 0.016** 0.700 0.858 **1.519**	**0.401 +/- 0.014** 0.721 0.862 **1.524**
SSHgt + DryTropo	**Mean** Std Skewness Kurtosis	**2.221** 0.599 1.342 4.620	**2.204** 0.563 1.415 5.660	**2.151** 0.529 1.321 4.840
	Slope Intercept R^2 **Noise Level at 2m SWH**	**0.460 +/- 0.016** 0.841 0.879 **1.761**	**0.442 +/- 0.016** 0.896 0.869 **1.781**	**0.437 +/- 0.015** 0.907 0.865 **1.782**
SSHgt + IonoCorr	**Mean** Std Skewness Kurtosis	**1.926** 0.554 1.414 4.820	**1.911** 0.524 1.505 5.994	**1.861** 0.486 1.394 5.131
	Slope Intercept R^2 **Noise Level at 2m SWH**	**0.425 +/- 0.015** 0.652 0.876 **1.501**	**0.409 +/- 0.016** 0.701 0.858 **1.519**	**0.400 +/- 0.014** 0.723 0.860 **1.524**
SSHgt + WetTropoRad	**Mean** Std Skewness Kurtosis	**2.221** 0.598 1.342 4.621	**2.205** 0.563 1.415 5.662	**2.152** 0.530 1.325 4.856
	Slope Intercept R^2 **Noise Level at 2m SWH**	**0.460 +/- 0.016** 0.842 0.879 **1.762**	**0.442 +/- 0.016** 0.897 0.869 **1.782**	**0.438 +/- 0.015** 0.906 0.866 **1.782**

Table 4-5 Statistical Indicators for Cycle 295 through Cycle 297 and 1-Minute Segments with Removal of the Atmospheric Corrections

Highpass Filter	1 min.	295	296	297
SSHgt + all atmospheric corrections	**Mean** Std Skewness Kurtosis	**1.882** 0.723 1.763 8.239	**1.914** 0.705 1.650 7.863	**1.858** 0.674 1.631 8.096
	Slope Intercept R^2 **Noise Level at 2m SWH**	**0.405 +/- 0.009** 0.725 0.594 **1.535**	**0.382 +/- 0.010** 0.794 0.537 **1.559**	**0. 382+/- 0.009** 0.779 0.541 **1.543**
SSHgt + DryTropo	**Mean** Std Skewness Kurtosis	**2.167** 0.791 1.576 7.202	**2.195** 0.767 1.469 6.828	**2.140** 0.740 1.459 7.040
	Slope Intercept R^2 **Noise Level at 2m SWH**	**0.444 +/- 0.010** 0.898 0.597 **1.786**	**0.417 +/- 0.010** 0.973 0.540 **1.807**	**0.419 +/- 0.010** 0.960 0.538 **1.797**
SSHgt + IonoCorr	**Mean** Std Skewness Kurtosis	**1.882** 0.723 1.767 8.258	**1.915** 0.705 1.650 7.881	**1.858** 0.674 1.631 8.093
	Slope Intercept R^2 **Noise Level at 2m SWH**	**0.405 +/- 0.009** 0.725 0.594 **1.535**	**0.382 +/- 0.010** 0.794 0.537 **1.560**	**0.383 +/- 0.009** 0.779 0.541 **1.544**
SSHgt + WetTropoRad	**Mean** Std Skewness Kurtosis	**2.167** 0.791 1.576 7.202	**2.195** 0.767 1.469 6.820	**2.139** 0.741 1.460 7.043
	Slope Intercept R^2 **Noise Level at 2m SWH**	**0.444 +/- 0.010** 0.898 0.598 **1.786**	**0.417 +/- 0.010** 0.972 0.540 **1.807**	**0.419+/-0.010** 0.956 0.539 **1.795**

Table 4-6 Statistical Indicators for Cycle 295 through Cycle 297 and 5-Minute Segments by Replacing TOPEX Ionospheric Correction with DORIS Estimation

Highpass Filter	5 min.	295	296	297
SSHgt + IonoCorr	**Mean** Std Skewness Kurtosis	**1.926** 0.556 1.431 4.887	**1.912** 0.524 1.502 5.985	**1.861** 0.486 1.393 5.127
	Slope Intercept R^2 **Noise Level at 2m SWH**	**0.426 +/- 0.015** 0.647 0.876 **1.500**	**0.409 +/- 0.016** 0.702 0.858 **1.520**	**0.401 +/- 0.014** 0.722 0.860 **1.523**

Table 4-7 Statistical Indicators for Cycle 295 through Cycle 297 and 1-Minute Segments by Replacing TOPEX Ionospheric Correction with DORIS Estimation

Highpass Filter	1 min.	295	296	297
SSHgt + IonoCorr - IonoDoris	**Mean** Std Skewness Kurtosis	**1.882** 0.723 1.768 8.260	**1.914** 0.705 1.650 7.877	**1.858** 0.674 1.631 8.092
	Slope Intercept R^2 **Noise Level at 2m SWH**	**0.405 +/- 0.009** 0.725 0.595 **1.535**	**0.382 +/- 0.010** 0.794 0.537 **1.559**	**0.383 +/- 0.009** 0.779 0.541 **1.544**

4.2.4 Conclusion

This noise estimation can be applied to single-frequency altimeter data as GFO and the French altimeter Poseidon as well as on dual-frequency altimeter data such as TOPEX. This new approach to estimating the altimeter noise give similar results with the noise spectra computed from repeating ground tracks [Driscoll and Sailor, 2001] and also is in good agreement with the TOPEX Ku-band noise estimation method after removing the dual-frequency ionospheric correction from the sea surface height value. This method allows comparison of the quality of the different altimeters in a straightforward manner.

4.3 Ancillary Performance Assessment Results

This report section introduces the use of differencing the Ku Band data and the C band data to detect any change in characteristics. We acknowledge science investigators Dr. P. David Cotton, Satellite Observing Systems, Godalming, Surrey, United Kingdom; Dr. Pierre Queffeulou, Department of Spatial Oceanography, IFREMER, Plouzane, France; and Dr. Graham D. Quartly, Southampton Oceanography Centre, Southampton, United Kingdom for pointing out this method for checking data consistency. In future reports, we expect to show only side B data in the updates to these plots, but in this report we show the entire time span from launch to the end of year 2000 for these new performance summary figures.

First, Figure 4-10 "Cycle-Average SWH Delta in Meters" plots cycle averages of the C-band minus Ku-band significant waveheight difference, from launch to the end of year 2000. In a recent change to a new Oracle-based GDR launch-to-date database, we added several data fields to those in our older FoxPro-based system, and the delta SWH (C- minus Ku-band) was one of the new fields. The figure shows clearly that Side A and Side B are two completely different altimeters with different SWH performance. The figure also shows the gradual change of slope in the delta SWH starting somewhere between cycles 100 and 150 and continuing through the end of the Side A operation, as the Side A point-target response (PTR) changed. We do not understand the downward drift of the delta SWH for the first 50 cycles or so. The entire range of the delta SWH is very small, however, only about 0.02 meters, and we expect to use the delta SWH cycle-averages as a continuing system health monitor rather than as a product having any particular science usefulness.

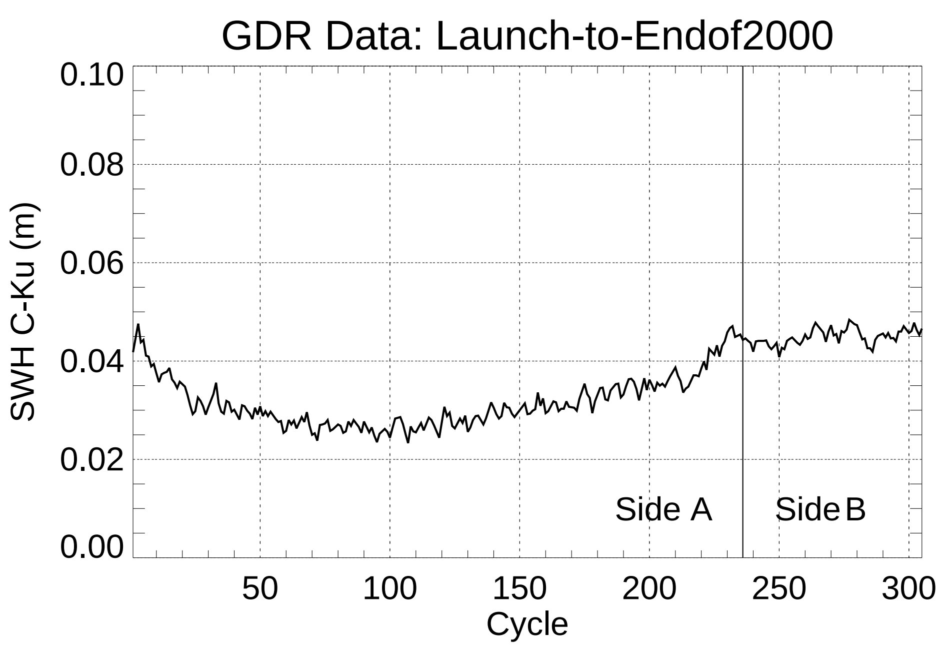

Figure 4-10 Cycle-Average SWH Delta in Meters

Second, Figure 4-11 "Cycle-Average Gate Index Delta" plots cycle averages of the gate index delta, the difference between the secondary (C-band) and the primary (Ku-band) gate index, from launch to the end of year 2000. Again, we see a small difference between the overall Side A and Side B behaviors, and we also see the change in the later Side A results as the PTR changed. In this figure, the later Side A change only becomes apparent somewhere after cycle 150. This figure is again a system health monitor.

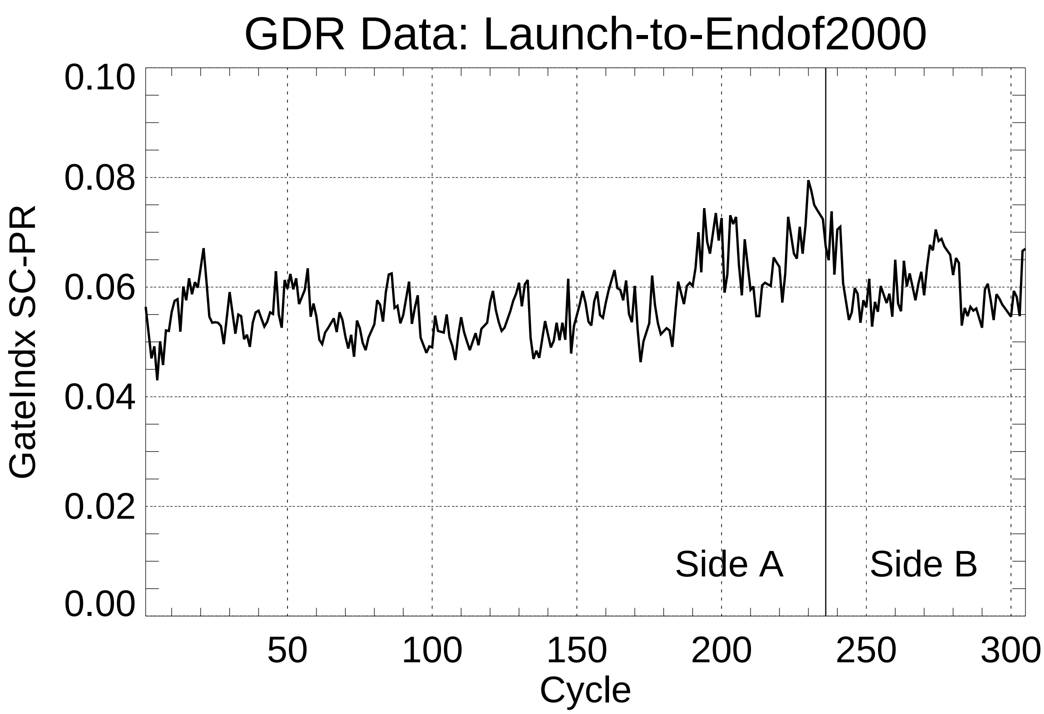

Figure 4-11 Cycle-Average Gate Index Delta

Third, Figure 4-12 "Cycle-Average Sigma0 Delta in dB" plots the sigma0 difference, C-band minus Ku-band, from launch to end of year 2000. This provides a quick indication that the sigma0 calibration has been maintained to within 0.25 dB. Unlike the previous two figures, this figure is not a pure indication of system health because both the Ku- and the C-band sigma0 calibrations have been adjusted manually at the beginning of a number of different cycles through the TOPEX history. For those few groups in the world trying to use the sigma0 difference, relating it to rainfall estimation for instance, we strongly recommend that our TOPEX web site (topex.wff.nasa.gov) be visited. At that web site, we have provided a history of the sigma0 calibration changes as well as a possible set of sigma0 calibration adjustments to be applied to the distributed GDR sigma0 values.

Some of the relatively abrupt changes in Figure 4-12 are the result of various manual tweaking and adjustment of the sigma0 CalTable through the TOPEX mission. Section 3.2 of this report discussed the TOPEX processing system's Cal Table which adjusts the sigma0 estimates for the effects of possible drifts or trends in the altime-

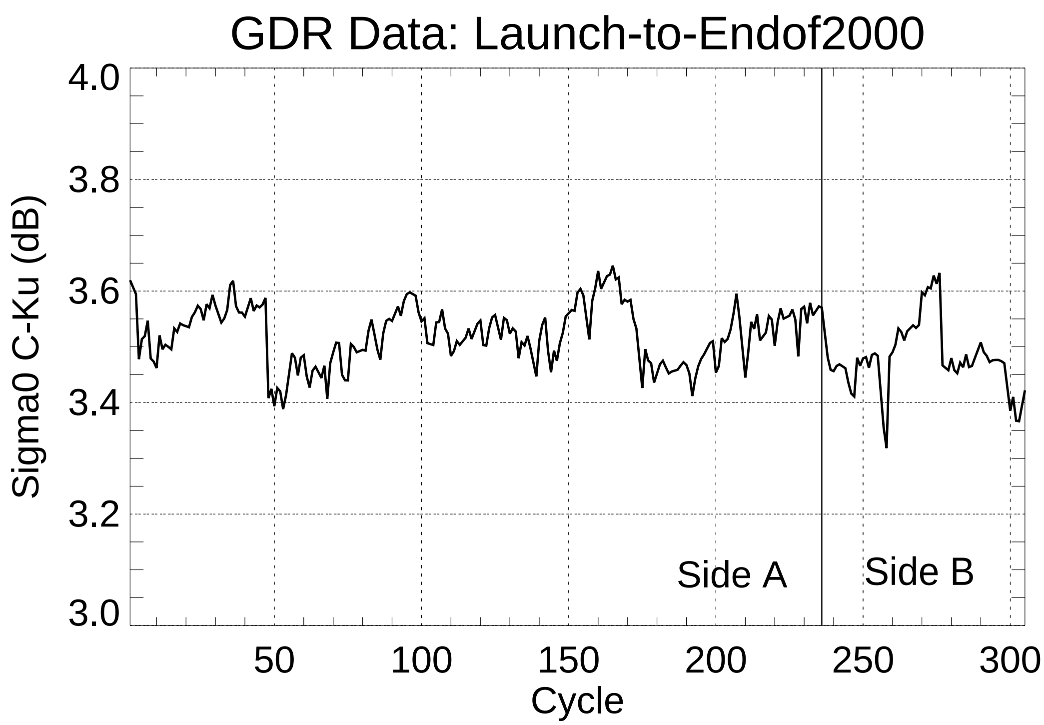

Figure 4-12 Cycle-Average Sigma0 Delta in dB

ter's power estimation. As discussed in Section 3.2.5, it is possible to reassess the trends and to produce an estimate of a "better guess" set of values that one might wish had been used instead of the actual Cal Table values in the GDR production. The Side A sigma0 calibration history and our current best estimate of Side A sigma0 adjustments is described in "TOPEX Sigma0 Calibration Table History for All Side A Data", by G.S. Hayne and D.W. Hancock III, July 27, 1999, available at our TOPEX documents web location http://topex.wff.nasa.gov/docs.html. An interim Side B calibration history and set of adjustments is available from "TOPEX Side B Sigma0 Calibration Table Adjustments: February 2001 Update", by G.S. Hayne and D.W. Hancock III, February 15, 2001, also available at http://topex.wff.nasa.gov/docs.html.

A set of cycle by cycle adjustments of the sigma0 difference (C- minus Ku-band) was obtained from the Side A and Side B calibration history documents just described, and these adjustments were applied to the sigma0 difference (as plotted in Figure 4-12) to produce the result shown in Figure 4-13. Figure 4-13 plots the sigma0 difference (C minus Ku) based on our best current guess at the values which should have been in the sigma0 Cal Table. Figure 4-13 appears somewhat smoother than Figure 4-12, smoothing out the step change just before cycle 50 for instance. Figure 4-13 does suggest a slightly different performance after the change from Side A to Side B, possibly the result of a small calibration error in either Ku-band or C-band (or both). The Figure 4-13 does not tell us if the calibration error is in Side A or Side B, only that there is an apparent difference.

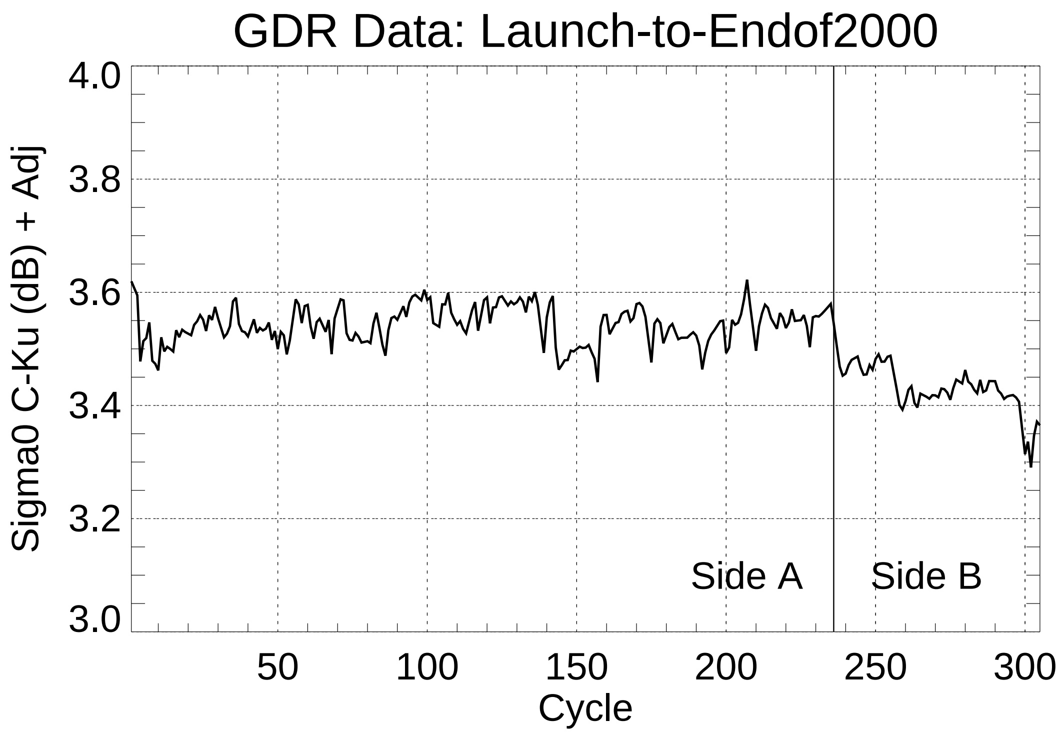

Figure 4-13 Cycle-Average Sigma0 Delta in dB with Cal Table Adjustment

Section 5

Engineering Assessment Synopsis

5.1 Performance Overview

Side B of the NASA Radar Altimeter was turned on, for the first time in space, on February 11, 1999. This followed six-and-a-half years of very successful on-orbit operations by Side A. Side A was turned off due to its Point Target Response having changed slightly over time, affecting measurement consistency. Side B is now the operational altimeter; however, Side A could be turned back on if needed.

Side A performance significantly surpassed all it pre-launch specifications, including its length of service. Based on our performance analysis and based on the reports of science investigators, Side B is performing as well as, or perhaps even better than, Side A.

We are continuing our NASA Radar Altimeter performance assessment of Side B on a daily basis. Our performance assessment techniques are relevant not only for the NASA Radar Altimeter, but are very applicable to other spaceborne altimeters as well.

Section 6
References

6.1 Supporting Documentation

Callahan,P.S., 1993, *GDR Users Handbook,* JPL Document 633-721.

Callahan,P.S., D.W. Hancock III, and G.S. Hayne, 1994, *New Sigma0 Calibration for the TOPEX Altimeter.* TOPEX / POSEIDON Research News, JPL 410-42, Issue 3, pp.28-32.

Driscoll, Mavis L. and Richard V. Sailor, *GFO On-Orbit Altimeter Noise Assessment*, NASA Technical Report: NASA / TM-2001-209984, Vol. 2.

Hancock, D.W., G.S. Hayne, C.L. Purdy, and R.L. Brooks, 1994, *TOPEX Radar Altimeter Engineering Assessment Report*. NASA / WFF TOPEX Report.

Hancock, D.W., G.S. Hayne, C.L. Purdy, and R.L. Brooks, 1995, *TOPEX Radar Altimeter Engineering Assessment Report - Update: Launch to January 1, 1995.* NASA / WFF TOPEX Report.

Hancock, D.W., R.L. Brooks, and J.E. Lee, 1995, *Passive Microwave Radiation Effects on the TOPEX Altimeter Cal-2 Measurements*. TOPEX / POSEIDON Research News, August 1995, pp. 4-8.

Hancock, D.W., and G.S. Hayne, 1996, *Error in TOPEX Oscillator Drift Correction*. NASA / WFF TOPEX Report.

Hancock, D.W., G.S. Hayne, C.L. Purdy, R.L. Brooks, J.E. Lee, and D.W. Lockwood, 1996, *TOPEX Radar Altimeter Engineering Assessment Report - Update: Launch to January 1, 1996.* NASA / WFF TOPEX Report.

Hancock, D.W., G.S. Hayne, R.L. Brooks, J.E. Lee, and D.W. Lockwood, 1997, *TOPEX Radar Altimeter Engineering Assessment Report - Update: Launch to January 1, 1997*. NASA / WFF TOPEX Report.

Hancock, D.W., G.S. Hayne, R.L. Brooks, J.E. Lee, and D.W. Lockwood, 1998, *TOPEX Radar Altimeter Engineering Assessment Report - Update: Launch to January 1, 1998*. NASA / WFF TOPEX Report.

Hancock, D.W., G.S. Hayne, R.L. Brooks, D.W. Lockwood, and J.E. Lee, 1999, *TOPEX Radar Altimeter Engineering Assessment Report - Update: From Launch to Turn-Off of Side A on February 10, 1999.* NASA / WFF TOPEX Report.

Hancock, D.W., G.S. Hayne, R.L. Brooks, D.W. Lockwood, and J.E. Lee, 2000, *TOPEX Radar Altimeter Engineering Assessment Report - Update: Side B Turn-On to January 1, 2000.* NASA / WFF TOPEX Report.

Hayne, G.S., D.W. Hancock III, and C.L. Purdy, 1994, *TOPEX Altimeter Range Stability Estimates from Calibration Mode Data.* TOPEX / POSEIDON Research News, JPL 410-42, Issue 3, pp.18-22.

Hayne, G.S., D.W. Hancock III, C.L. Purdy, and C.S. Callahan, 1994, *The Corrections for Significant Wave Height and Attitude Effects in the TOPEX Radar Altimetry*. Journal of Geophysical Research, v. 99, no. C12, pp. 24,941-24,955.

Hayne, G.S. and D.W. Hancock III, 1997, *TOPEX Sigma0 Calibration Table and its Updates*. NASA / WFF TOPEX Report, available on the Web at *http://topex.wff.nasa.gov/Sigma0Cal.html* or alternatively, as a PDF version at *http://topex.wff.nasa.gov/docs/Sigma0Cal.pdf*.

Hayne, G.S. and D.W. Hancock III, [Updated regularly on the Web], *TOPEX Sigma0 Calibration Table and its Updates*. (*http://topex.wff.nasa.gov/docs/docs.html)*

Hayne, G.S., [Updated regularly on the Web], *Latest Altimeter Range Stability Estimate Update*. (*http://topex.wff.nasa.gov/docs/docs.html)*

Hayne, G.S. and D.W. Hancock III, 1999, *TOPEX Sigma0 Calibration Table History for All Side A Data. http://topex.wff.nasa.gov/docs/Sigma0 Cal_A_All.pdf*

Jensen, J.R.,1998, *TOPEX Simulation Study October-November 1998*, Report SRO-98-14, Johns Hopkins Applied Physics Laboratory.

Sailor, R.V. and M.L. Driscoll, *Comparison of Noise Models and Resolution Capabilities for Satellite Radar Altimeters*, Proceedings Oceans 92 Conference, Newport, RI, Oct. 1992, pp. 249-253.

Sailor, R.V. and A.R. LeSchack, *Preliminary Determination of the Geosat Radar Altimeter Noise Spectrum*, Johns Hopkins APL Technical Digest, vol. 8, no. 2, 1987, pp. 182-183.

Zieger, A.R. and D.W. Hancock III, G.S. Hayne, and C.L. Purdy, 1991, *NASA Radar for the TOPEX/POSEIDON Project*. Proc. IEEE, v. 97, no. 6, pp. 810-826.

Appendix A
Accumulative Index of Studies

Side B Point Target Response - *TOPEX Radar Altimeter Engineering Assessment Report, Update: From Side B Turn-On to January 1, 2000*, September 2000.

Land-to-Water Acquisition Times - *TOPEX Radar Altimeter Engineering Assessment Report, Update: From Side B Turn-On to January 1, 2000*, September 2000.

Transition to Side B - *TOPEX Radar Altimeter Engineering Assessment Report, Update: From Side B Turn-On to January 1, 2000*, September 2000.

Side A Point Target Response Changes and Consequences - *TOPEX Radar Altimeter Engineering Assessment Report, Update: From Launch to Turn-Off of Side A on February 10, 1999*, August 1999.

Launch-to-Date Internal Calibrations - *TOPEX Radar Altimeter Engineering Assessment Report, Update: From Launch to Turn-Off of Side A on February 10, 1999*, August 1999.

Launch-to-Date Cycle Summaries - *TOPEX Radar Altimeter Engineering Assessment Report, Update: From Launch to Turn-Off of Side A on February 10, 1999*, August 1999.

Launch-to-Date Key Events - *TOPEX Radar Altimeter Engineering Assessment Report, Update: From Launch to Turn-Off of Side A on February 10, 1999*, August 1999.

Launch-to-Date Engineering Monitors - *TOPEX Radar Altimeter Engineering Assessment Report, Update: From Launch to Turn-Off of Side A on February 10, 1999*, August 1999.

Launch-to-Date Waveform Monitoring - *TOPEX Radar Altimeter Engineering Assessment Report, Update: From Launch to Turn-Off of Side A on February 10, 1999, August 1999*.

Oscillator Drift Algorithm Change (Update) - *TOPEX Radar Altimeter Engineering Assessment Report, Update: Launch to January 1, 1998*, June 1998.

AGC and Range Corrections During the 1997 ASTRA Event - *TOPEX Radar Altimeter Engineering Assessment Report, Update: Launch to January 1, 1998*, June 1998.

C-Band Power Drop - *TOPEX Radar Altimeter Engineering Assessment Report, Update: Launch to January 1, 1997*, March 1997.

Oscillator Drift Algorithm Change - *TOPEX Radar Altimeter Engineering Assessment Report, Update: Launch to January 1, 1997,* March 1997.

Seasonal Distribution of Sigma-0 Blooms - *TOPEX Radar Altimeter Engineering Assessment Report, Update: Launch to January 1, 1997*, March 1997.

Effects of Coastlines - *TOPEX Radar Altimeter Engineering Assessment Report, Update: Launch to January 1, 1997*, March 1997.

TOPEX Altimeter 1996d362t 12:55 Side B C MTU Transmit Anomaly - *TOPEX Radar Altimeter Engineering Assessment Report, Update: Launch to January 1, 1997*, March 1997.

TOPEX C Band Received Power Study Results - *TOPEX Radar Altimeter Engineering Assessment Report, Update: Launch to January 1, 1997*, March 1997.

Sea Surface Height Residuals as Indicators of Global Sea Level Change - *TOPEX Radar Altimeter Engineering Assessment Report, Update: Launch to January 1, 1996*, May 1996.

Over-Land Losses of Lock: Seasonal Variations - *TOPEX Radar Altimeter Engineering Assessment Report, Update: Launch to January 1, 1996*, May 1996.

Range Corrections for the Effects of Waveform Leakage - *TOPEX Radar Altimeter Engineering Assessment Report, Update: Launch to January 1, 1996*, May 1996.

Waveform Leakage Range Correction - *TOPEX Radar Altimeter Engineering Assessment Report, Update: Launch to January 1, 1996*, May 1996.

Sigma0 Error Effect on Range - *TOPEX Mission Radar Altimeter Engineering Assessment Report, Update: Launch to January 1, 1995*, March 1995.

Cal2 Differences Over Water and Land - *TOPEX Mission Radar Altimeter Engineering Assessment Report, Update: Launch to January 1, 1995*, March 1995.

Waveform Samples Assessment - *TOPEX Mission Radar Altimeter Engineering Assessment Report*, February 1994.